Progress in Particle and Nuclear Physics 142 (2025) 104163

Contents lists available at ScienceDirect

Progress in Particle and Nuclear Physics

journal homepage: www.elsevier.com/locate/ppnp

Review

Neutron sources for large scale user facilities: The potential of high current accelerator-driven neutron sources

P. Zakalek, T. Gutberlet, Th. Brückel *

JCNS-HBS, Forschungszentrum Jülich GmbH, 52425, Jülich, Germany

ARTICLE INFO

Keywords:
Neutron sources
Fission
Spallation
HiCANS
CANS

ABSTRACT

A review of neutron sources for large scale user facilities is provided, aimed at users of neutron sources who need to understand the characteristics and peculiarities of the different types of neutron sources in order to select the most suitable source for their needs and to optimize their experimental setups for their specific scientific requirements. To this end, we provide an overview of (i) the main nuclear processes used at user facilities to release neutrons from nuclei, namely fission, spallation, and low-energy nuclear reactions, (ii) the various possibilities to tailor the time structure and spectrum of free neutrons, from pulsing to moderation, (iii) the mechanisms to extract and transport neutron beams with desired properties in terms of flux, brilliance/brightness, spectrum, pulse shape, etc., (iii) the applications and related experimental requirements in major scientific fields, with emphasis on those with a larger user community, (iv) the technology and realization of research reactors and neutron spallation sources, and (v) the progress made in Compact Accelerator-driven Neutron Sources (CANS), but especially in High Current Accelerator-driven Neutron Sources (HiCANS).

HiCANS are the focus of the current review, as this entirely new type of facility could in the future play the role in the neutron ecosystem that national reactor-based sources have played in the past. As such, HiCANS do not aim for the highest neutron brightness, but rather for parameters such as resilience, reliability, flexibility, ease of access, minimization of radioactive waste, excellent signal-to-noise ratio and optimization of the price/performance ratio. These are key features needed to further expand the community of neutron users from science and industry to whom this review is addressed.

Contents

* Corresponding author.
E-mail address: t.brueckel@fz-juelich.de (T. Brückel).

https://doi.org/10.1016/j.ppnp.2025.104163

Available online 11 February 2025

1. Introduction

Free neutrons are a true gift of nature to science and industry. To name just a few of the most important applications:

- They are one of the most powerful microscopic probes in a wide variety of fields such as condensed matter physics, chemistry, materials science, engineering, geosciences, life sciences, cultural heritage and many more. They tell us “where the atoms are, how they move, how they interact, and how they are magnetic”, see the 1994 Nobel Lectures in Physics by Clifford Shull [1] and Bertram Brockhouse [2].
- They are also extremely interesting research objects in their own right. Precision experiments with ultracold neutrons are used to study elementary particles and their interactions. They allow, for example, stringent tests of the Standard Model of particle physics and give indications for physics beyond this model [3].
- They are important for medical applications, such as the production of radionuclides, e.g. for radiopharmaceutical treatment [4] or for Boron Neutron Capture Therapy [5] of malignant tumors. They are essential for the development of new medicine like in the case of mRNA vaccine [6,7].
- They are essential for industrial applications such as imaging, analysis in quality control and recycling or for neutron transmutation doping, e.g. of silicon [8].
- They are used in the petroleum and mining industries to locate and identify recoverable deposits.

While neutrons are abundant in nature, tightly bound in atomic nuclei, it is necessary to overcome the binding energies of neutrons to eject them from nuclei and ultimately produce beams of free neutrons. The MeV energy scale involved and the need for a high flux of neutrons for research and applications require large scale facilities serving a wide community of scientific and industrial users. In Europe, about 5000 scientists are regular users of the existing large scale neutron sources [9], most of them using neutrons as probes of condensed matter.

Historically, the first neutron beams were produced by fission reactions in nuclear reactors. Neutron diffraction techniques developed at the Clinton Pile Graphite Reactor at Oak Ridge National Laboratory (ORNL) were the first application of neutrons as probes of condensed matter and led to the Nobel Prize for Clifford Shull [1]. Many research reactors were realized in the 50s and 60s of the last century and provided neutron beams for many groundbreaking discoveries. Starting in the 1980s, additional facilities using the spallation reaction induced by high-energy proton beams striking a heavy metal target became available to

Table 2.1
Basic parameters of the neutron as a free particle.

Neutron mass	939.565360 ± 0.000081 MeV/c^2 [20] or 1.67492750056±0.00000000085× 10^{-27} kg [21] or 1.00866491560 ± 0.00000000055 Da [20]
Mean square charge radius	0.113 ± 0.005 fm^2 [22]
Electric charge	−0.4±1.1× 10^{-21} e [23]
Magnetic dipolar moment	−1.91304272±0.00000045 μ_N [24]
Mean lifetime	879.6 ± 0.8 s [25] (about 14 min, 40 s)

the scientific community. Today, fission and spallation are still the two processes at the basis of large-scale facilities for research with neutrons. However, many of the older research reactors have reached or are approaching the end of their lifetimes and are not being replaced by newer spallation sources due to their relatively high cost. Therefore, a new type of neutron facility has been proposed and is being developed mainly in Europe: the High-Current Accelerator-driven Neutron Sources (HiCANS), which use a low energy nuclear process [10]. Several European research centers are collaborating within the European Low Energy accelerator-based Neutron facilities Association (ELENA) [11] to realize this new type of neutron source, which is considered to become an important pillar in the neutron ecosystem in Europe and eventually worldwide.

This overview is primarily aimed at users of neutron sources who need to understand the characteristics and peculiarities of the different types of neutron sources in order to optimize their specific experimental requirements. It is not intended to give a comprehensive account of established source techniques, i.e. for fission or spallation neutron sources. This goes far beyond the scope of the present article. For both there are excellent overviews in textbooks ([12] is an excellent current reference) as well as handbooks with technical details, see e.g. [13,14] and references therein. In the present review, we instead give a simple introduction to fission and spallation and refer to some recent developments. These chapters serve as a reference for the main focus of this article: the presentation of ongoing projects for next-generation neutron sources, so-called *Hi*gh-*C*urrent *A*ccelerator-driven *N*eutron *S*ources (HiCANS). These do not aim at highest neutron brilliance, but rather at parameters such as resilience, reliability, flexibility, minimization of radioactive waste, price/performance ratio and ease of access, features that are needed to further expand the neutron community. HiCANS concepts are technologically very advanced, have been demonstrated experimentally, and are ready for realization as large scale facilities. They are considered by LENS (the League of advanced European Neutron Sources) as *"the only route for entirely new facilities with significant capacity, which could occupy the role played by national reactor-based sources in the past"* [9]. Therefore HiCANS are the focus of this review. Other ongoing developments, such as laser-driven sources, are mentioned in passing because they cover only some very specialized applications and require much more development to become facilities for a broader user community.

After introducing the basics of neutrons and neutron beams in Section 2, this review gives an overview of the different processes used to produce intense neutron beams at large facilities (Section 3), discusses how these beams can be tailored (Section 4) for specific applications (Section 5), describes how these neutron sources work, and gives examples of existing and planned facilities based on fission and spallation (Section 6). Section 7 is the focus of the review: a comprehensive overview over ongoing HiCANS projects, briefly touching *C*ompact *A*ccelerator-driven *N*eutron *S*ources (CANS) and laser-driven sources. Finally, conclusions and an outlook are given (Section 8).

2. Basic properties of neutrons and neutron beams

This chapter serves as a basic introduction, in which we define important terms in a non-exhaustive way, without going into details.

In 1920, Ernest Rutherford proposed that the atomic nucleus might consist of positive protons and further neutrally charged particles [15]. Similar suggestions were made at the same time by others. The American chemist W. D. Harkins first named this hypothetical particle a "neutron" merging the Latin root for neutralis (neuter) and the Greek suffix -on [16]. Based on some work by Walther Bothe and Herbert Becker [17] and Irène and Frédéric Joliot-Curie [18], James Chadwick performed a series of experiments in the early 1930s showing the presence of a new radiation consisting of uncharged particles of about the same mass as the proton which matched the properties of Rutherford's hypothesized neutron [19]. In 1935, the Nobel Prize in Physics was awarded to James Chadwick for the discovery of the neutron.

In the Standard Model for particle physics the neutron is described as of two down quarks with charge −1/3e and one up quark with charge +2/3e. As such, neutrons are composite particles that are hadrons. The quark substructure and internal charge distribution determine the neutron magnetic moment [20]. The basic parameters of the neutron are given in Table 2.1.

The kinetic energy of a neutron at room temperature is in the range of meV with $E = h^2/2m\lambda^2$, where λ is the wavelength of the neutron, m the neutron mass and h the Planck constant [26]. Based on the interaction potential $V(\underline{r})$ of a neutron with matter the cross section σ describes the interaction potential of the probe with the nucleus $V(\underline{r}) = 2\pi\hbar^2/mb\delta(\underline{r} - \underline{R})$ [27]. The total cross section of a given nucleus is $\sigma = 4\pi|b|^2$ with the scattering length b and varies in a seemingly random manner depending on the composition of the nucleus. For different isotopes of a given element b can be largely different and also for different spin states. It can be a positive value as most but also a negative value.

Table 2.2
Definition of neutron energy groups as given by the IAEA [33]. It should be noted that there is some overlap in the energy ranges, and that alternative definitions are also in use in the community.

Neutron group	Energy	Wavelength Å
Fast	>10 keV	≤0.03
Epithermal	0.5 eV–10 keV	0.4–0.03
Hot	0.1 eV–1 eV	0.3–0.9
Thermal	<0.5 eV	≥0.4
Cold	<5 meV	≥4
Very cold	0.3 μ eV–0.1 meV	28–50
Ultracold	≤0.3μ eV	≥500

The length and time scales that can be probed with neutrons span many orders of magnitude. In space they range from a few centimeters (even up to a meter for imaging) to interatomic distances of 10^{-10} m (0.1 nm = 1 Å) to nuclear dimensions of 10^{-15} m. In time they range from a few seconds to femtoseconds of 10^{-15} s. For a neutron with a kinetic energy of e.g. 25 meV the wavelength λ is about 0.18 nm, which fits well with interatomic distances. The energy also fits well with elementary excitations such as lattice vibrations (phonons) or spin waves (magnons). Thus, neutrons of such energies scattered in matter are ideal for probing the structure and dynamics of condensed matter systems. Since the energy of 25 meV corresponds to a temperature equivalent of about 300 K, i.e. lies in the ambient temperature range, such neutrons are called *thermal* neutrons.

If the scattering process is purely elastic scattering, i.e. scattered neutrons have the same energy as the incident neutrons, the scattering vector [12,26] is given by $\underline{Q} = \underline{k}' - \underline{k}$. The magnitude of the scattering wave vector can be calculated from the neutron wavelength and the scattering angle 2Θ between $\underline{k}$ and $\underline{k}'$ by $Q = 4\pi/\lambda \sin\Theta$.

If the neutron looses or gains energy by interacting with the atomic nuclei with a difference in the energy $\Delta E = E' - E$ of the incoming and outgoing wave, the scattering is said to be inelastic. The magnitude of the scattering vector $\underline{Q}$ now also depends on the energy transfer $\hbar\omega$ and is expressed as $Q = \sqrt{k^2 + k'^2 - 2kk'cos(2\Theta)}$.

Depending on the energy of the neutron it can also be absorbed when the neutron collides with the atomic nucleus and merges to form a heavier nucleus [28]. During the process a discrete and characteristic quantity of electromagnetic energy (gamma-ray photon) is emitted. This nuclear reaction is commonly termed as neutron capture [29].

Neutron beams can be polarized by scattering if there is a spin–orbit interaction between the incident particle and the scattering nucleus [30]. The interaction depends on the parallel or antiparallel alignment of the spin of the neutron and the nucleus. The application of a magnetic field $\underline{H}$ defines a quantization axis and the normalized mean of the neutron spin component along this axis defines the polarization. Resonance absorption of neutrons in certain filter materials can also be used to polarize neutron beams. In the case of resonance absorption of neutrons by ^{3}He isotopes in ^{3}He gas cells, nearly complete polarization can be obtained [31].

Typical velocities of thermal neutrons are in the range of a few meters per millisecond. When the neutron beam is given as a short pulse of neutrons with a certain energy spread and repetition frequency, neutrons of different energies will arrive at a detector at different times. From the recorded time-of-flight spectrum the scattering function $S(Q,\omega)$ can be derived [32]. Table 2.2 gives the definition of neutron energy groups following the IAEA [33].

The phase-space volume in a neutron scattering experiment is expressed by the brilliance which is commonly used for any radiation source (light sources, synchrotron radiation facilities etc.) [34,35]. The brilliance normalizes the number of emitted particles to the area from which they are emitted, the wavelength band, the time interval and the solid angle. Since this definition of the brilliance does not take into account the time-of-flight capabilities of an accelerator-driven neutron source, the repeatability of the neutron beam must be taken into account. This can be done by normalizing to the number of particles hitting the target as the neutrons are produced by nuclear reactions of light ions (e.g. protons) inside a suitable target material [35]. For more details we refer to Section 4.2.

3. Release of neutrons from nuclei: the basics

To release neutrons from nuclei, the binding energy due to the strong nuclear force binding neutrons and protons in the nucleus must be overcome. This typically requires high-energy processes and results in kinetic energies of the released neutrons in the MeV range. For this reason, neutron sources with a high source strength, i.e. the number of neutrons released per unit time interval, are large-scale facilities. This is in contrast to X-ray sources, which only need to overcome the binding energy of the electrons in the atom in the keV range and can be extremely powerful even on a laboratory scale, while of course large scale synchrotron radiation sources produce even brighter beams and are more versatile than laboratory based sources.

In this chapter we present the main processes that underlie powerful neutron sources for the applications mentioned in the introduction. We will not discuss exotic schemes like laser fusion [36] or Halo nuclei [37], which have been proposed but not realized. We also will not elaborate on spontaneous neutron emission from radioactive decay, which is not relevant for large-scale user facilities. However, it has to be mentioned that the isotope ^{252}Cf, which undergoes spontaneous fission, is used in special applications, e.g. as a source for portable neutron spectroscopy (Prompt Gamma Neutron Activation Analysis (PGNAA), also known as Neutron-induced Prompt Gamma-ray Analysis (PGA), see below in Section 5) or as a start-up source for nuclear reactors [38].

Major processes underlying powerful neutron sources are (the list number refer to the corresponding subsection):

1. Nuclear fusion, used in (portable) neutron generators, where compact linear accelerators are used to bombard a metal hydride target containing deuterium (D, ^{2}H) or tritium (T, ^{3}H) with the hydrogen isotopes D or T to induce the fusion reaction.
2. Nuclear fission as used in research reactors, where mainly the fission of (enriched) ^{235}U is used in a controlled chain reaction. The fission reaction is induced by neutron absorption. It results in two fission product nuclei and 2 to 3 ejected neutrons.
3. Nuclear spallation reaction, used in neutron spallation sources, in which a high-energy proton beam in the GeV range is shot at a heavy metal target, exciting the target nuclei, which subsequently eject up to 30 neutrons upon deexcitation.
4. Low energy nuclear reactions, used in Compact Accelerator-driven Neutron Sources (CANS) and proposed for so-called High-Current Accelerator-driven Neutron Sources (HiCANS) [10]. These reactions can be induced by ion- or electron-beams from particle accelerators or by powerful lasers. Electron beams hitting heavy metal targets produce high energy X-rays or gamma-rays which subsequently eject neutrons from target nuclei by the photonuclear reaction. Laser beams can use the photonuclear reaction, too, but mainly use a pitcher-catcher geometry, where a laser beam hitting a thin pitcher target generates an ion beam, which subsequently releases neutrons upon impact with the catcher target. CANS and HiCANS based on ion beams (mainly protons or deuterons) use particle energies below the spallation threshold in the range of some MeV for CANS and up to 100 MeV for HiCANS. Several different low energy processes are relevant and can be used for such a neutron source:

    - Elastic breakup, e.g. the dissociation of deuterons from an accelerator in the Coulomb potential of the target atom (usually Be for this reaction), producing a proton and a predominantly forward directed neutron.
    - Complete fusion of the impinging ion with a target nucleus, producing a short-lived excited compound nucleus, which decays by emission of a neutron.
    - Incomplete fusion where by inelastic scattering of the impinging ions neutrons are being knocked out from the target nuclei.
    - Photonuclear reaction when the photon energy exceeds the binding energy of a neutron and emits a neutron from a nucleus by evaporation.

3.1. Fusion: neutron generators

Fusion of heavy isotopes of hydrogen such as deuterium or tritium produces large numbers of neutrons. Small-scale fusion systems, often termed neutron generators, are used for research purposes at many universities and laboratories around the world. Neutron generators offer a high degree of versatility and, accordingly, can be used in a wide range of applications, from basic science to industry. Neutron generators are probably the most widely used neutron sources in industry, with several companies devoted to their manufacture and sale. The source strength is generally low, but these devices are small, less expensive, and easy to use for a variety of applications [39,40]. Although neutron generators are not the sources of large user facilities, their principle is mentioned here for completeness, as they are widely used.

In these devices the fusion reaction occurs by accelerating either deuterium, tritium, or a mixture of these two isotopes into a metal hydride target that also contains deuterium, tritium or a mixture of these isotopes. Fusion of deuterium atoms (D + D) results in the formation of a helium-3 ion and a neutron with a kinetic energy of approximately 2.5 MeV. Fusion of a deuterium and a tritium atom (D + T) results in the formation of a helium-4 ion and a neutron with a kinetic energy of approximately 14.1 MeV. The DT reaction is used more often than the DD reaction because the yield of the DT reaction is 50 to 100 times higher than that of the DD reaction.

$$D + T \rightarrow n + {}^{4}\mathrm{He} \qquad E_n = 14.1\ \mathrm{MeV} \tag{3.1}$$

$$D + D \rightarrow n + {}^{3}\mathrm{He} \qquad E_n = 2.5\ \mathrm{MeV} \tag{3.2}$$

Fusion neutrons are emitted nearly isotropically for DT and with moderate angular bias for DD in the forward (ion beam axis) direction [41].

Neutron generators consist of a particle accelerator as the central unit, sometimes called a neutron tube. Inside the neutron tube, an ion source, ion optical elements, and a beam target are placed in a vacuum-tight housing. High voltage insulation is provided between the ion optical elements by glass and/or ceramic insulators. The accelerator head is filled with a dielectric medium which is isolated from the high voltage elements of the tube and the operating area. External power supplies provide the high voltage [42]. Sealed designs are used in pulsed mode to be operated at different output levels, depending on the life time of the ion source and loaded targets.

The ion source has to provide a strong ion beam without consuming much of the gas [43]. Hydrogen isotopes are favored over molecular ions as atomic ions have higher neutron yield on collision. The ion source anode is at a positive potential, with respect to the source cathode. It is operated normally between 2 and 7 kV. A magnetic field is produced with a permanent magnet oriented parallel to the source axis. A plasma is formed along the axis of the anode which traps electrons which, in turn, ionize the gas in the source. Between the exit cathode and the accelerator electrode ions emerge from the exit cathode and are accelerated through the potential difference. 2–3 electrons per ion are produced by secondary emission when the ions strike the target.

Thin films of metals such as titanium, scandium, or zirconium loaded with hydrogen isotopes are used as targets in neutron generators. Those metals that form stable metal hydrides are selected as target materials. These metal hydrides consist of two hydrogen (deuterium or tritium) atoms per metal atom. Thus, the target achieves extremely high hydrogen densities to maximize the neutron yield of the neutron tube [44]. Typical systems can provide a wide range of neutron source strengths ranging from

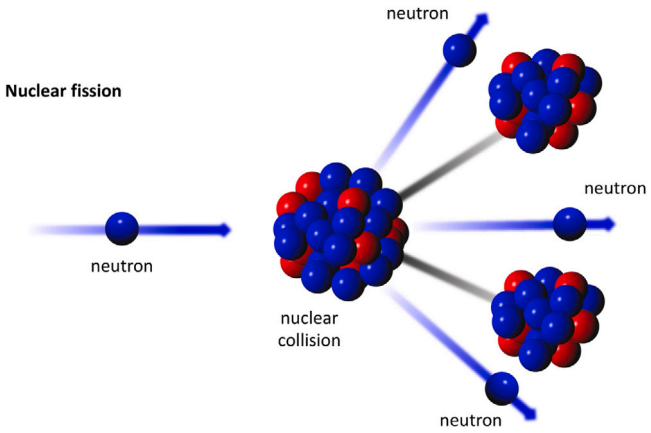

Fig. 3.1. Illustration of the fission nuclear reaction. When the neutron collides with the fissionable nucleus, an absorption process occurs, after which the nucleus splits into several (usually two) fragments, releasing neutrons in the process.
Source: Adapted from [52] with kind permission.

about 10^6 to 10^9 n/s for DD and DT generators. Up to 10^8 neutrons per second can be generated using a 1 mA ion beam accelerated at 200 kV onto a titanium–tritium target. Mostly the neutron yield is determined by the accelerating voltage and the ion current level [45]. Self-replenishing DT targets can be made with a deuterium–tritium gas mixture [46,47]. Here, the neutron yield is lower than that of tritium-saturated targets in deuteron beams, but they achieve a much longer lifetime and a constant level of neutron production. With higher ion beam current produced with a Cockcroft–Walton accelerator neutron yields of 10^{11} n/s for a DD and even 10^{13} n/s for a DT generator system have been demonstrated [41].

3.2. Nuclear fission

Nuclear fission, first observed in 1938 by Hahn and Strassmann [48,49] and explained by Meitner and Frisch [50], was the first process used to produce neutron beams for the study of materials on atomic length scales, leading e.g. to the experimental verification of the existence of antiferromagnetism [51]. Fission in research reactors is still the most widely used process to produce large quantities of free neutrons. High flux research reactors feature the highest time-averaged source strength, i.e. the number of neutrons released per unit of time (n/s).

Nuclear fission is the process by which a heavy nucleus splits into two (or sometimes more) fission nuclei of comparable mass. The fission process can be induced by the fusion of a nucleus with an incident particle, or it can even occur spontaneously for atoms with high mass numbers (important example: the isotope ^{252}Cf [38]). For research reactors, the most common process used to release neutrons is the fission of the uranium isotope ^{235}U (natural abundance 0.72%) induced by neutron capture. Binary fission, i.e. splitting into two fragments, is by far the most probable process. Therefore, we will focus on the binary fission of ^{235}U induced by neutron capture as the most relevant reaction occurring in research reactors. Fig. 3.1 shows a schematics of this fission reaction.

Fig. 3.2 shows the binding energy per nucleon as function of the atomic mass number A for all isotopes listed in the Atomic Mass Data Center [53–55]. From the figure one can deduce that nuclear energy can be released either through fusion of light nuclei or through fission of heavy nuclei, since in both cases the average binding energy E_B of a nucleon in the resulting nuclei is larger than in the initial nuclei. According to Einstein this leads to a mass defect $\Delta m = E_B/c^2$ compared to the simple sum of the masses of the protons m_p and neutrons m_n in the nucleus $Zm_p + Nm_n$ (where $A = Z + N$).

The simplest model to describe the fission process is the liquid drop model of the nucleus [56]. It assumes that due to the short range of the strong force (order 2×10^{-15} m) and the hard repulsion radius of a nucleon (order 0.5×10^{-15} m), a nucleon can only interact with its immediate neighbors, so that the binding energy of a nucleon inside the nucleus is approximately independent of the number of nucleons, except for the very light atoms. However, as in a liquid droplet, the binding energy of the nucleons at the surface is smaller than in the center because the surface nucleons interact with fewer neighbors. The short-range attractive force between the nucleons is opposed by the electrostatic Coulomb repulsion of the protons. Finally, in an extension of the liquid drop model quantum corrections from the shell model are taken into account. It is well beyond the scope of this article to review recent progress of experiment and theory in nuclear fission and we refer to literature, e.g. [57–59].

Now the phenomenon of nuclear fission can be understood by the interplay of the different terms in the droplet model: the surface energy acts to maintain the spherical shape of the nucleus, the electrostatic repulsion of the protons, expressed in the Coulomb energy term, favors fission. For small deformations of a nucleus, the surface term will tend to maintain the spherical shape and the nucleus will resist changing its shape. For larger elongations, a fission barrier height resulting from the addition of the surface and Coulomb energy contributions can be overcome, e.g. when a nucleus is deformed by excitation in a neutron capture event. At the scission point, the repulsion due to the long-range Coulomb force overcomes the short-range attractive force, eventually leading to fragmentation of the nucleus, as shown schematically in Fig. 3.3. The fission barrier height for ^{235}U is about 6 MeV.

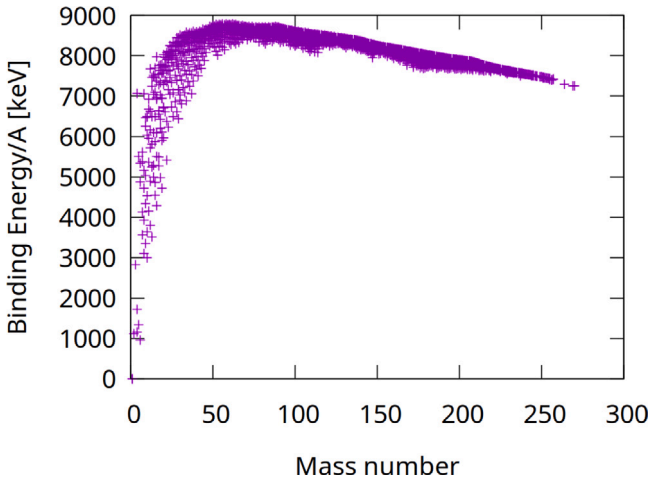

Fig. 3.2. Average binding energy per nucleon as function of atomic mass number A [53].

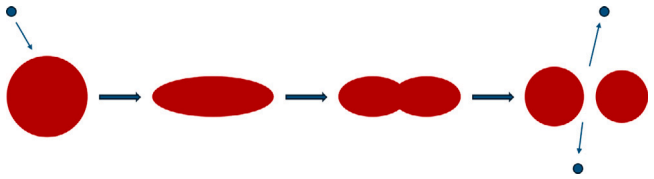

Fig. 3.3. Schematic of the time evolution of the deformation of a nucleus during the fission process within the liquid droplet model.

A typical fission reaction of ^{235}U induced by neutrons can be written as

$$^{235}_{92}\mathrm{U} + ^{1}_{0}n \longrightarrow ^{236}_{92}\mathrm{U} \longrightarrow ^{139}_{56}\mathrm{Ba} + ^{94}_{36}\mathrm{Kr} + 3^{1}_{0}n.$$

However, the fragmentation is not a deterministic process, but leads to a bimodal probabilistic distribution of fission products. The primary fission fragment yield distribution for the neutron induced nuclear fission of the isotope ^{235}U has two maxima at mass numbers of 94 and 139 with a half-width of the two distributions of about 16 [60].

It is beyond the scope of the present article to give a detailed account of the neutron induced fission reaction of ^{235}U. Instead we can cite a few characteristic features:

- Depending on the individual fission reaction, between 2 and 3 prompt fission neutrons (on average 2.47 neutrons) are released during the ^{235}U fission reaction.
- The total kinetic energy distribution of the post-neutron fission fragments for the ^{235}U(n, f) reaction is approximately a Gaussian function with the most probable value of 170 MeV when the reaction is induced by thermal neutrons [61].
- The prompt fission neutron spectra of the neutron induced fission of ^{235}U can be found e.g. in [62] and references therein. The energy distribution of these neutrons evaporating from the nucleus reflects the distribution of neutron energies in the nucleus and can be approximately described by a function

$$f(E) \propto \sqrt{E}\exp(-E/T), \tag{3.3}$$

with the energy equivalent of the characteristic temperature T $\approx$ 1.3 MeV or somewhat more accurate by [12]

$$f(E) \propto \exp(-1.036E)\sinh\sqrt{2.29E}. \tag{3.4}$$

In these Eqs. (3.3) and (3.4), E is expressed in MeV. Data [62] are represented as ratios to a Maxwellian with temperature 1.32 MeV. For the present purposes one may state that roughly speaking, prompt fission neutrons have an average energy of 2 MeV, but the spectrum extends to above 10 MeV (compare Fig. 3.9).
- In total, during one fission process about 190 MeV of energy is released in the form of kinetic energy of the fission products and the released neutrons, beta- and gamma-radiation and neutrinos (which escape and are not relevant for the heat deposited within the reactor fuel). This number is of practical importance for the reactor design (see Section 6) as removal of the heat deposited in the reactor core is in the end the limiting practical factor for the source strength of research reactors.
- The cross section for this important reaction ^{235}U(n, f) has become a neutron standard [63] and corrigendum [64]. With the hand-waving argument that the thermal neutron spends more time close to the uranium nucleus, the cross section is highest for thermal neutrons with resonances occurring at higher neutron energies [65].

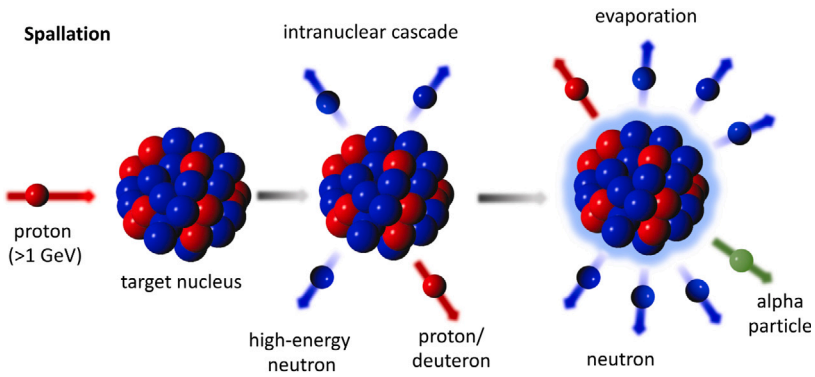

Fig. 3.4. Illustration of the spallation process, showing in a simplified way the sequence of reactions — from the intranuclear cascade to the evaporation. *Source:* Adapted from Brückel et al. [52] with kind permission.

- Finally, it should be noted that besides prompt neutrons, which appear within 10^{-14} s of the fission reaction, so called delayed neutrons are emitted after 0.1 s up to 30 s. These delayed neutrons are released, when unstable "precursor" fission fragments undergo radioactive beta decay, a process that may involve neutron emitting states from which neutrons are promptly ejected. In contrast to the continuous spectrum of prompt evaporation neutrons, these delayed neutrons are monoenergetic with energies between 0.1 and 1 MeV. While the fraction of delayed neutrons is very small (about 0.6% of all emitted neutrons), they are important for the steering of a nuclear reactor (see below, Section 6).

3.3. Nuclear spallation

High energy processes were discussed as early as 1947 [66] when Sullivan and Seaborg coined the term "spallation" [67]. The Intense Pulsed Spallation Source (IPNS) at Argonne National Laboratory, which became operational in 1981, was the first pulsed neutron source open to external users [68]. Today, MW-class high-power spallation sources have the largest neutron pulse height (see Section 6), which is particularly useful for time-of-flight experiments (see Section 5).

Nuclear spallation is a process initiated by the collision of a high-energy particle in the range of several 100 MeV to several GeV with a heavy nucleus, resulting in a complex series of reactions. In practice, at neutron sources, the incident particle is a proton from an accelerator colliding with a thick heavy metal target made of tantalum, tungsten, mercury, lead or uranium. The collision results in highly excited nuclei that emit high-energy protons, neutrons, and pions. These in turn collide with more nuclei. The excited nuclei shed energy by promptly evaporating more particles, mainly neutrons, but also protons, deuterons, tritons, α-particles. Finally, some excited states decay by emitting β-radiation, in which process delayed neutrons may be given off (compare nuclear fission). The sequence of reactions is shown schematically in Fig. 3.4.

Phenomenologically, the spallation process can be described by the so-called cascade model, which can be justified by the fact that protons at the typical energy scale for a spallation neutron source have energies around 1 GeV, where their de Broglie wavelength is of the order of 10^{-14} cm, significantly smaller than the diameter of a heavy nucleus. The sequence of reactions can then be described as follows:

1. Intranuclear cascade: The small wavelength of the incident proton justifies the description of the initial process as billiard-like collisions of the proton with single nucleons. During the approximately 10^{-22} s it takes for the incident proton to pass through the nucleus, a series of collisions with individual nucleons occurs inside the nucleus — the intranuclear cascade. The energy of the incoming proton is transferred to some individual nucleons.
2. Internuclear cascade: Energetic particles (protons, neutrons, pions) from this process may leave the nucleus and induce further spallation reactions in other nuclei — the internuclear cascade.
3. Transition stage: In a transition state of about 10^{-18} s, the high kinetic energy of the excited nucleons from the intranuclear cascades spreads throughout the nucleus by further collisions, during which some more nucleons may be ejected.
4. Evaporation: Now the nucleus remains in a highly excited state, from which the nucleons evaporate in a manner similar to the fission process, i.e. their spectrum can also be described by a Maxwellian, similar to the fission neutrons, but typically with a slightly higher Maxwell temperature.
5. Delayed decay processes: Finally, a small fraction of delayed neutrons can accompany beta decay processes, similar to the fission case. Delayed neutrons can also be produced by photoneutron reactions (see Section 3.4.1) from high-energy gamma radiation in nearby deuterium moderators or beryllium reflectors.

Again, it is beyond the scope of the present article to give a detailed account of the proton induced spallation process. Instead we refer to textbooks and review articles (e.g. [12,69,70]) and only cite a few characteristic features:

- In contrast to fission and fusion, spallation is an endothermal process which cannot be used per se for thermal energy generation. Instead, an energetic beam of particles is needed to sustain a spallation reaction. In this review of neutron sources we do not consider the case of fissionable target materials, which is of technological interest for driven reactors for energy supply or spallation facilities for treatment of nuclear waste by transmutation.
- It is a very efficient process to release neutrons from nuclei. While one fission reaction in research reactors typically results on the average in only one free neutron for experiments (one other neutron is needed to sustain the chain reaction and some neutrons are lost in the shielding), some 10 to 30 neutrons are released during a spallation reaction, depending on the energy of the incident particle and the target material.
- A time structure can be imposed on the neutron flux by the filling pattern of the driving proton accelerator. This allows one to use the peak flux instead of the average flux for the same deposited power in the target, a main limiting factor for the source strength. The peak flux of spallation sources can be significantly higher than the average flux of research reactors, a very useful feature for time-of-flight experimental methods (see Section 5).
- The spallation neutron spectra can be described as consisting of mainly three components (compare Fig. 3.9): the evaporation and transition state neutrons follow a Maxwellian similar to the case of fission neutrons with an average energy of around 2 MeV, while cascade neutrons have energies of several 100 MeV distributed continuously all the way up to the energy of the incident proton. A nice comparison between the spectrum of fission neutrons and spallation in a tungsten target can be found in [71]. In accordance with our phenomenological cascade model, the neutron spectra can be described by three components [70], where again, E is expressed in MeV:

$$f(E) = A_1 E^{1/2} \exp(-E/E_{T1}) + A_2 E \exp(-E/E_{T2}) + A_3 E \exp(-E/E_{T3}) \tag{3.5}$$

  The three terms correspond to the three stages discussed above: evaporation, transition and cascade neutrons with the energy equivalents of their characteristic temperatures $E_{Ti} = k_B T_i$. Evaporation (first term) and transition (second term) contribute about 90% of all emitted neutrons, with characteristic energies comparable to fission neutrons (about 2 MeV) for thin spallation targets. For more realistic thicker targets, the neutrons lose energy through collisions before leaving the target material, and the spectrum shifts and becomes softer as a function of target thickness. Cascade neutrons, however, can reach energies up to the incident proton energy for thin targets. They are extremely difficult to shield and lead to the heavy shielding of spallation sources compared to research reactors.
- While evaporation and transition neutrons have an essentially isotropic angular distribution, cascade neutrons are preferentially emitted in the forward direction, but will take on a wider angular distribution for thicker targets.
- The spallation neutron yield for thick targets (e.g. where the proton beam loses all its energy and is stopped in the target) has been determined experimentally by Fraser at al. in 1965 [72]. Over a wide range, it can reasonably well be described for non-fissionable materials by the following function [12], where E_{GeV} denotes the numerical value of the incident proton energy in units of GeV:

$$Y(E_{\mathrm{GeV}}, A) = 0.1(E_{\mathrm{GeV}} - 0.12)(A + 20) \tag{3.6}$$

  The Eq. (3.6) indicates that there is an apparent threshold energy for the spallation process [12]. This is not a true threshold, as some neutrons can be released below this energy. But from 0.12 GeV to energies of about 1 GeV (extending with slight deviations to around 1.5 GeV), the neutron yield is approximately linear in proton energy and atomic mass number A of the target material. To give an example: A 1 GeV proton hitting a lead target will produce an average of 20 spallation neutrons. It should be noted that the number of usable neutrons for beam experiments can be significantly smaller, depending on the type and geometry of the surrounding reflector and the arrangement of the moderators, see Section 6.

3.4. Low energy reactions

There are a large plethora of other processes that can release neutrons; here we present only those that are currently of foreseeable interest to user facilities. A comparison of the neutron yield of the different processes can be found in [73].

3.4.1. Photonuclear reactions

Neutron production based on the photonuclear reaction of electron bremsstrahlung has played an important role in the development of accelerator-driven sources [74,75]. Energetic electrons striking high-mass targets slow down to emit bremsstrahlung (e, γ) photons, which then interact with target nuclei to produce (γ, n) photoneutrons. Most of the electron energy is dissipated as heat, which must be removed from the target, severely limiting the power on the target; consequently the process is limited in neutron yield and relatively inefficient.

Photoneutron yields depend on the target material and on the photoneutron source: its spectrum, strength and geometry. For a reasonable production of epithermal neutron fluxes from a photonuclear reaction, the appropriate choice of the photoneutron target materials (on the basis of its photodisintegration threshold), its photoneutron cross section, geometry and physical dimensions are important [76]. The cross section of the photonuclear effect is characterized by the Giant Dipole Resonance (GDR) most pronounced in materials with high-Z [77]. An exception to this rule is found in the γ–n cross section of ^{13}C where the cross section increases almost linearly [78].

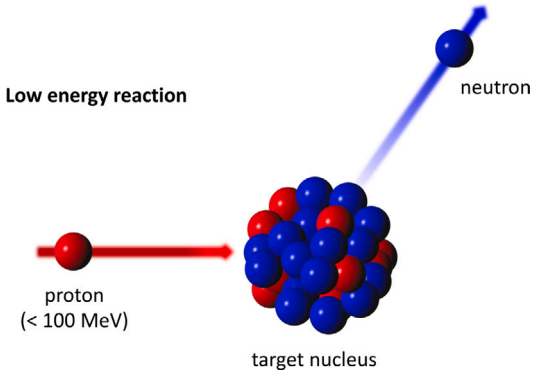

Fig. 3.5. The illustration depicts a low-energy nuclear reaction, initiated by an impinging proton, which results in the release of a neutron from a metal nucleus (see text for details).
Source: Adapted from Brückel et al. [52] with kind permission.

3.4.2. Ion induced low energy reactions

This subsection discusses nuclear reactions induced by ions at energies well below the spallation threshold (see Eq. (3.6)). These energies typically range from a few MeV to about 100 MeV. We define this range as the range for low energy reactions. The bombardment of metallic targets with low-energy ions from accelerators to induce neutron-releasing reactions is the most commonly used technique in so-called Compact Accelerator-driven Neutron Sources (CANS), see Section 7.1, and is the method of choice for High Current Accelerator-driven Neutron Sources HiCANS, Section 7.2. It eliminates the high gamma background typical of the photonuclear reaction path used in electron accelerator-driven neutron sources. Fig. 3.5 shows a schematic of such a nuclear reaction for the case of an incident low energy proton. By inelastic scattering of the incident proton, a neutron is ejected from the target nucleus in an incomplete fusion reaction. The process can also involve complete fusion of the impinging ion with the target nucleus. This produces a short-lived excited compound nucleus that decays by emitting a neutron.

When deuterons (D^+) are used as incident ions, the most relevant reactions are stripping and elastic breakup [79]. In the stripping reaction, one nucleon of the incident deuteron combines with the target nucleus, while the other nucleon mostly continues in the forward direction. In the breakup reaction, deuterons from an accelerator dissociate in the Coulomb and nuclear potential of the target nucleus (usually beryllium (Be) for this reaction), producing a proton and a neutron. D^+ as the incident ion is of particular interest for this reaction because of the weakly bound neutron that can be released at relatively low energies. Of particular interest for the application of this reaction in a neutron source is its directional property: the neutron is predominantly forward directed. Due to its importance for low energy neutron sources, the integrated neutron yield, the (continuous) neutron energy spectrum and the (anisotropic) angular distribution of the ^{9}Be(d, xn) reaction have been calculated in great detail and compared with experimental data [80,81]. Fig. 3.6 shows the different reaction channels for a deuteron striking a Be target nucleus. For comparison, the figure also shows the reaction channels for a proton hitting a Be target nucleus.

It is obvious that the stripping reaction ^{9}Be(d, n) requires extremely low energies due to the low binding energy of the neutron in the deuteron. It has a narrow peak in energy but a large peak cross section, which is favorable for the realization of a CANS with a low energy accelerator. At higher energies, other reaction pathways become possible, such as ^{9}Be$(d, n + \alpha)$ or ^{9}Be$(d, n + p)$. In comparison, the ^{9}Be(p, n) reaction has a gap at low energies due to the Coulomb barrier and is much broader in energy, but has a significantly smaller peak cross section.

An important reaction, e.g. for the preparation of keV neutrons for nuclear astrophysics or Boron Neutron Capture Therapy (BNCT), see Section 5, is the reaction ^{7}Li$(p, n)^7$Be. The reaction sets in at a threshold energy for the incident protons of 1.88 MeV and has two resonances, a narrow one between a proton energy of 2.2–2.3 MeV and a broad one around 5 MeV [82]. Near the threshold, the neutron energy spectrum peaks around 30 keV and is mainly forward directed [83]. The low threshold energy, the significant neutron yield and the favorable neutron spectrum with an attractive average neutron energy make this reaction interesting for this kind of applications [84,85].

Since the incident ion loses energy during collisions with the target atoms, the total neutron yield for a thick solid target is given by the sum of all processes releasing neutrons from zero energy up to the energy of the incident particle. The energy and material dependence of the neutron yield for incident protons and deuterons [86] is shown in Figs. 3.7 and 3.8, respectively. The values were determined for cross sections calculated with the TALYS nuclear code and stopping powers calculated with the SRIM toolkit. Elements with atomic numbers 43 (Tc) and 61 (Pm) do not occur naturally, and all of their isotopes are radioactive. Therefore, the corresponding data are missing. The (p, n) reactions are endothermic, since the Coulomb barrier must be overcome, which is why the neutron yield disappears at low energies. It is obvious that the neutron yield increases with increasing proton energy and atomic number. The simulations show that for low energy processes, up to an energy of about 20 MeV, light elements, in particular beryllium, have the highest neutron yield. After a transition region, the neutron yield of heavy elements such as tantalum exceeds that of light elements above about 45 MeV [86]. This behavior was verified experimentally for proton induced neutron release from Be, V and Ta targets in the energy range 22–42 MeV by means of prompt gamma neutron activation analysis [87]. The choice of

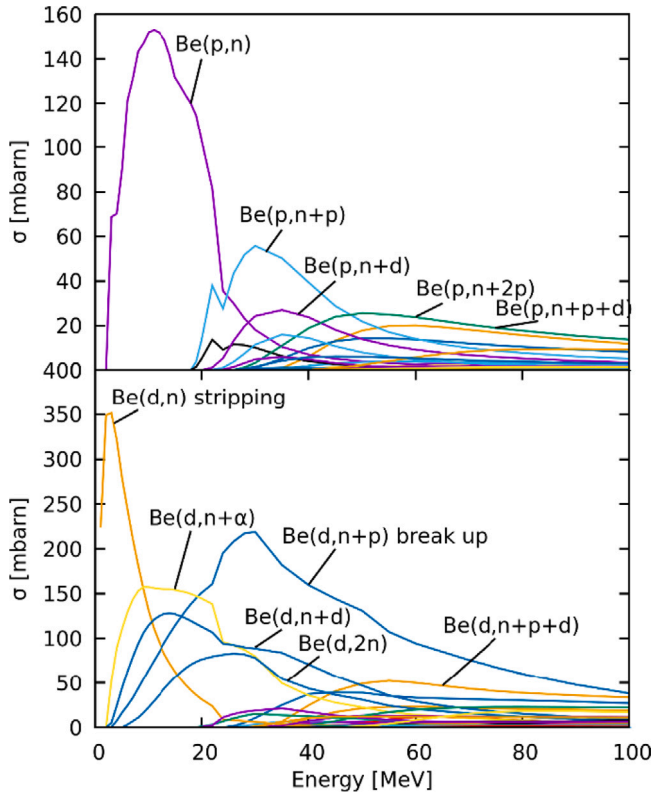

Fig. 3.6. Cross sections for different reaction paths for the ^{9}Be(p, xn) reaction (top) and the ^{9}Be(d, xn) reaction (bottom) as a function of incident energy according to the TALYS nuclear code.
Source: Reproduced from [86], under the terms of the Creative Commons Attribution License 4.0.

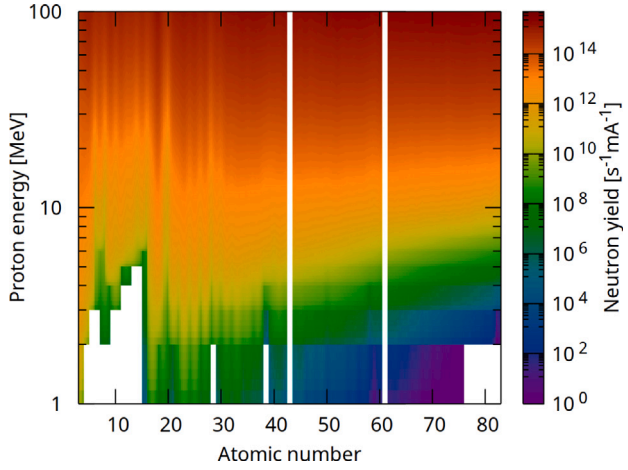

Fig. 3.7. The proton-induced neutron yield per mA proton current as a function of incident proton energy for different target materials. Please note that the white lines at atomic numbers 43 and 61 result from the fact that these elements do not have stable isotopes. In addition, the white regions below a few MeV show that in these regions neutrons are not released due to the Coulomb barrier.
Source: Reproduced from [86], under the terms of the Creative Commons Attribution License 4.0.

projectile energy and target material is discussed in more detail in Sections 7.1 and 7, since other factors must be considered besides maximizing the neutron yield.

In comparison to fission and spallation, the energy spectrum of the released neutrons is somewhat softer for typical proton energies and target materials. Fig. 3.9 illustrates the energy spectra of released neutrons for the case of protons with energies of 2.5 MeV, 7 MeV and 70 MeV hitting the typical CANS and HiCANS targets Li, Be and Ta, respectively. The spectra were produced

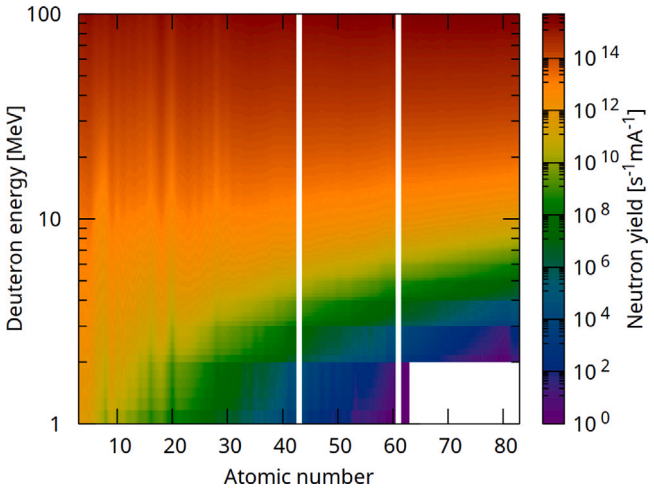

Fig. 3.8. The deuteron-induced neutron yield per mA deuteron current as a function of incident deuteron energy for different target materials. Please note that the white lines at atomic numbers 43 and 61 result from the fact that these elements do not have stable isotopes. In addition, the white regions below a few MeV show that in these regions neutrons are not released due to the Coulomb barrier.
Source: Reproduced from [86], under the terms of the Creative Commons Attribution License 4.0.

Table 3.1
The characteristic energies (mean value, energy where the peak in neutron yield occurs, and maximum energy of neutrons in the spectra) for the calculated spectra for Li, Be and Ta using PHITS with the JENDL-5.0/HE database. The calculated values for fission and spallation are based on the spectra published in [70].

Reaction	Mean energy [MeV]	Peak energy [MeV]	Max energy [MeV]
Li(p, nx) @ 2.5 MeV	0.13	0.12	0.79
Be(p, nx) @ 7 MeV	0.59	0.43	5.2
Ta(p, nx) @ 70 MeV	0.65	0.47	65
Fission	1.88	1.72	~20
Spallation @ 800 MeV	17.5	2.2	~800

using PHITS with the JENDL-5.0/HE database. The illustration demonstrates the significantly enhanced neutron yield that can be achieved through the use of high Z material (Ta) and high incident proton energy (70 MeV) in comparison to the conventional CANS approach. For purposes of comparison, the normalized spectra for fission and spallation are also presented. These data have been extracted from the publication [70]. The relevant energies for neutron sources like mean energy, peak energy and maximum energy are presented in Table 3.1. While the proton energy in the $Ta(p, nx)$ reaction is the highest compared to the Li and Be reactions, the peak and mean energies are similar to the others. This is due to the higher proton energy being distributed to many particles as a result of significant $(p, 2n)$, $(p, 3n)$, and $(p, 4n)$ reactions. While there are higher energy neutrons present, the probability of such neutrons occurring is low. In fact, the probability of a neutron with higher energy occurring is less than 1/100 at 10 MeV and less than 1/1000 at 50 MeV compared to the yield at the peak energy. Similarly, spallation follows this pattern, but with the highest neutron peak energy, mean energy, and a more pronounced shoulder at higher energies due to the high incident proton energy. For accelerator-based neutron sources, the highest neutron energy is more or less the energy of the impinging proton, slightly reduced by the Coulomb barrier. The required shielding therefore increases significantly if going from a low energy nuclear reaction to the spallation reaction. The fission spectrum shows higher mean and peak energies but compared to spallation a relatively low maximum energy.

The lower neutron energies of a CANS or a HiCANS, resulting from the low-energy nuclear reactions, offer a distinct advantage in terms of shielding. The use of a thinner shielding allows for the placement of optical elements in closer proximity to the moderator surface, thereby enhancing the performance of the instruments.

3.5. Neutron yields

After discussing the various processes used to release neutrons from nuclei, the question arises as to which processes are best suited for a source of free neutrons. Many aspects have to be considered for a practical realization of a neutron source, see Sections 6 and 7. However, two criteria seem obvious: (i) the neutron yield per process, and (ii) the energy released per neutron during the process, since most of this energy will appear as heat that has to be removed. Table 3.2 lists some of the processes mentioned along with the values for these two main criteria. Spallation has the highest neutron yield per process combined with the lowest heat release per neutron, followed by nuclear fission. Thus, it is obvious that these two processes are favorable for the realization of a neutron source if the source strength is the main criterion. However, as we will see in Section 7, a neutron source can be very competitive for certain applications if it is based on one of the other less efficient processes.

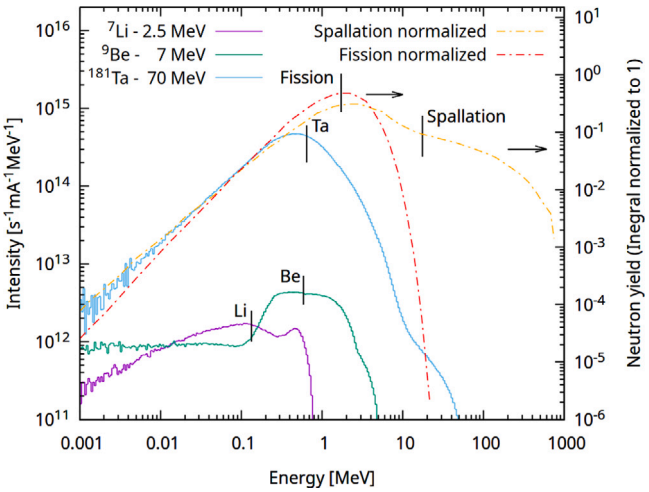

Fig. 3.9. Primary neutron energy spectrum for protons of 2.5 MeV, 7 MeV and 70 MeV energy impacting a bare lithium, beryllium and tantalum target, respectively. Mean energies are indicated with vertical lines. Spectra for Li, Be and Ta have been calculated using PHITS with the JENDL-5.0/HE database. The spectra for fission and spallation have been extracted from [70]. Note that the latter spectra are normalized and therefore not directly comparable to those for the low energy processes.

Table 3.2
Compilation of different nuclear processes to release neutrons from atomic nuclei with examples for the corresponding neutron yield and facilities using the respective processes. The table is updated, based on Ref. [88].

Nuclear process	Example	Primary Neutron yield	Heat release [MeV/n]	Facilities (examples)
D-T in solid target	400 keV d on T in Ti	4×10^{-5} n/d	10 000	Neutron generators
Deuteron stripping	40 MeV d on liq. Li	1.6×10^{-1} n/d	2500	SARAF [89]
Nuclear photo effect	32 MeV e- on W/Pb	8×10^{-3} n/e-	4000	HUNS [90]
^{9}Be$(d,n)^{10}$Be	15 MeV d on Be	1.5×10^{-2} n/d	1000	
^{9}Be$(p,n)^{10}$Be	7 MeV p on Be	1.6×10^{-3} n/p	4500	RANS [91]
Ta(p,n)	70 MeV p on Ta	1.4×10^{-1} n/p	500	HBS [86]
Fission	Fission of ^{235}U by thermal neutrons	2.5 n/fission[a]	180	ILL, MLZ
Spallation	2000 MeV p on W	≈20 n/p[a]	100	SNS, J-PARC, ESS

[a] Note that for fission sources only about one neutron per fission process can be used for experiments, since another one is needed to maintain the fission process and about 0.5 neutrons are lost. Also for spallation, only a fraction of the neutrons are available for beamline experiments due to losses. For spallation, this number varies greatly depending on the moderator–reflector geometry and the means of adjusting the time structure (see Section 4.3): between a few percent and less than 50% of the primary released neutrons can typically be used for experiments.

4. Tailoring of the spectrum

The free neutrons released in the processes described in Section 3 all have in common that they have kinetic energies in the MeV range and mostly do not exhibit strong directional properties. However, most neutron research applications require neutrons in the meV to eV range (“cold”, “thermal”, “hot” or “epithermal” neutrons, see Section 2) and highly directed neutron beams. Depending on the experimental technique used, a pulsed beam or a steady, continuous stream of neutrons may be preferable. Therefore, this chapter briefly discusses how to tailor a neutron energy spectrum, how to impose a desired time structure, how to extract neutrons, and how to transport them to the experiment. Other manipulations necessary for specific experiments, which are not directly related to the neutron source itself, such as the polarization of a neutron beam, are not discussed here and are referred to in the specialized literature, e.g. in the textbooks [12,26,92–95].

4.1. Basics of the moderation process

Moderation describes the daunting task of reducing the kinetic energy of neutrons by typically 6 to 10 orders of magnitude to move from the MeV energy range of neutrons released from nuclei to an energy regime most useful for fundamental and condensed matter research with neutrons. Electric or magnetic fields can only act on the tiny nuclear moment of the neutron and are therefore unsuitable for this task. Instead, inelastic collisions within a suitable medium, known as a moderator material, are used. It is beyond the scope of this article to discuss the diffusion and slowing-down theories, which are discussed in detail in textbooks [12,73]. Instead, the practical aspects relevant to the design of a neutron source are presented.

Roughly, for moderation of neutrons two regimes can be distinguished:

Table 4.1
Parameters for some typical thermal moderators: "Material" denotes the moderator material, "Fraction" rounded values of the average fraction of energy loss during each collision in %, "N Collision" rounded values of the average number of collisions for moderation from 2 MeV to 1 eV, "Absorption" the absorption cross section per atom (H, D, Be, C) for thermal neutrons (velocity 2200 m/s) in barn, and "Lambda" the mean free path between collisions in cm.

Material	Fraction [%] energy loss per collision	N Collision from 2 MeV to 1 eV	Absorption [barn] per nucleus H, D, Be, C	Lambda [cm] mean free path
H_2O	50	16	0.3326	0.67
D_2O	40	29	0.0005	2.86
Be	19	70	0.0076	1.32
C	15	92	0.0035	1.82

- Slowing down regime: When the neutron scatters from the nuclei of the moderator material at very high neutron energies, the chemical bonding and thermal motion of the atoms can be neglected because the binding energy and the kinetic energy of the atomic motion are much smaller than the kinetic energy of the neutron. The scattering can be considered to occur from free atoms that are initially at rest. The collisions of the neutrons with the nuclei of the moderator can be regarded as "billiard-like" elastic collisions in the center-of-mass frame; these collisions appear to be inelastic in the laboratory frame, i.e. the neutron loses energy during diffusion in the moderator ("down-scattering"). The processes just described provide a good approximate description of the moderation of neutrons into the hot to thermal energy range.
- Thermal scattering regime: As the neutron energy approaches the energy scale of chemical bonds, i.e. the eV range, the excitation spectra of the moderator material must be considered. Typically, these can be translational, rotational, vibrational, librational motions of molecules in molecular moderator materials or elementary excitations such as phonons or magnons in solid moderator materials. This regime is essential for further moderating the thermal neutrons into the cold or very cold energy regime. It requires a high density of states of low energy levels of the moderator material, which the neutron can excite during the scattering process, thus losing kinetic energy.

The Boltzmann equation is the fundamental equation describing the neutron transport process. A detailed analytical description based on the diffusion equation can be found in [96]. However, analytical calculations cannot deal with the detailed complex geometry of a realistic neutron source. Therefore, nowadays numerical simulations based on Monte Carlo codes, such as the "Monte Carlo N Particle" code (MCNP) [97], the "Particle and Heavy Ion Transport code System" code (PHITS) [98], the "FLUktuierende KAskade" code (FLUKA) [99,100] or "GEometry ANd Tracking" code (GEANT4) [101], are used to solve the integral form of the Boltzmann equation.

Let us first discuss moderation in the slowing down regime. The choice of moderator material in the slowing down regime is rather obvious already from classical mechanics: Down scattering is most effective when the neutron is scattered by a particle of equal or nearly equal mass, i.e. the proton. Neglecting the tiny mass difference, in a head-on collision of a neutron with a proton, the neutron can lose all its kinetic energy, and the minimum energy after a collision is zero. From this point of view, materials with a high hydrogen density are ideal thermal moderators. Light water (H_2O) or polyethylene are examples of such moderator materials. However, hydrogen has a rather high absorption cross section for neutrons, which leads to an undesired decrease of the neutron flux in the moderator. The next best choices are heavy water (D_2O) or beryllium (Be). Large volumes of these materials surrounding the primary neutron source also act as reflectors, i.e. they reduce the probability of neutrons leaking out of the moderator or, in the case of fission sources, increase the probability of neutrons backscattering into the core and having a second chance to cause a fission. While such large volume moderators are desirable for continuous sources, they can degrade the time structure of pulsed sources, see subsection below.

The fraction of energy lost during each collision is independent of the initial energy, i.e. E_1/E_2 is a constant. The logarithm of this constant $\xi = ln(E_1/E_2)$, the logarithmic energy decrement, is given by [70,96]:

$$\xi = ln(E_1/E_2) = 1 \quad (A = 1) \tag{4.1}$$

$$\approx 2/(A + 2/3) \quad (A > 1), \tag{4.2}$$

where A is the atomic mass number. ξ allows one to calculate the average number of collisions X required to slow down a neutron from its initial energy E_0 to the final energy E_f:

$$X = \ln(E_0/E_f)/\xi \tag{4.3}$$

Another relevant parameter is the average distance a neutron travels between subsequent collisions. This mean free path Λ is inversely proportional to the macroscopic cross-section, which is the sum of the free atom microscopic cross sections σ_{fr}, times the volume number density n.

$$\Lambda = \frac{1}{n \sum \sigma_{fr}} \tag{4.4}$$

Λ being constant means that the time between collisions is inversely proportional to the neutron velocity. This allows one to calculate the slowing down time relevant for short pulse primary neutron sources, see [70].

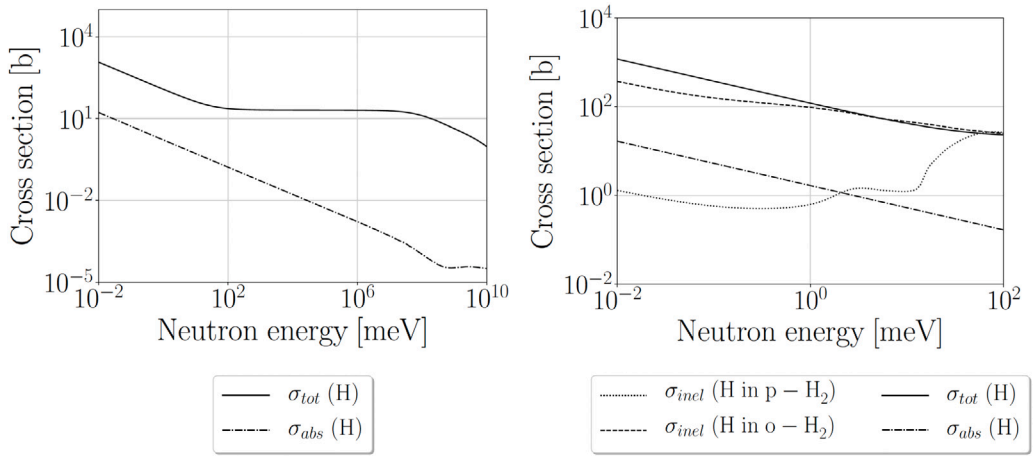

Fig. 4.1. Total and absorption cross section of hydrogen (^{1}H) (left) as well as inelastic scattering cross sections of hydrogen in para- and ortho-H_2 (right) vs. incident neutron energy.
Source: Reproduced from [103].

Table 4.1 lists some characteristic parameters for common thermal moderator materials [12,102]. As mentioned in the introduction, it is not our aim to provide a comprehensive overview of well-established properties for known source types, but rather to highlight new developments. Therefore, we refer to [70] for more detailed parameter lists for additional moderator materials with additional physical parameters. However, such tables can guide one to chose the optimal moderator material depending on the design goal to be met [70]:

- In order to achieve a high neutron flux within the moderator, it is usually desirable to avoid a large spread of the "neutron cloud"; this requirement translates directly into a small value of the mean free path or a large value of the macroscopic cross section. In this respect, among the choices presented in the Table 4.1, a light water moderator (H_2O) is the most suitable. It should be noted that some hydrocarbons, such as polyethylene, have a higher hydrogen number density than water, but a high radiation field or thermal heating effects limit their applicability.
- However, for a high time-averaged flux, a long storage time in the moderator is desirable, i.e. neutron absorption must be minimized. While the total absorption cross section for thermal neutrons in light water is 0.665 barn (2 H atoms, absorption of O can be neglected), the same value for a heavy water moderator is 0.001 barn. In this respect, a heavy water moderator (D_2O) is advantageous to achieve a high average neutron flux for a continuous source.

This discussion shows that a light water moderator could be a good choice for a short pulse source if combined with an appropriate reflector that does not deteriorate the time structure (see following subsections). On the other hand, a heavy water moderator tank is often used for continuous sources, such as high flux research reactors, where the D_2O tank can serve as both thermal moderator and reflector due to its low neutron absorption. Carbon (C) plays an important role in research reactors as a "hot source", enabling the production of a neutron spectrum in the hot neutron regime. The hot source consists of a block of graphite, heated by gamma-radiation from the fission processes to a temperature of 2300 K.

Having discussed moderation in the slowing down regime, let us turn to moderation in the thermal scattering regime. Here one can no longer use the approximation of neutrons colliding with free atoms at rest, but have to take into account the chemical bonding of the atoms, i.e. the solid or molecular structure of the moderator material and the respective excitations. This regime is particularly important for slowing down the neutrons into the cold or very cold regime. Typically, this is done by a two-step process: first, the neutrons are moderated into the thermal regime by a thermal moderator. A "cold source" is embedded in the thermal pre-moderator and receives neutrons in the thermal energy range. Thus, the moderation in the cold source can be described solely by the thermal scattering regime.

A very instructive example of the effect of chemical bonding is provided by a cold source of liquid hydrogen (LH_2), usually at temperatures around 20 K. Molecular hydrogen (H_2) exists in two nuclear spin isomeric forms: a triplet state in which the two nuclear spins of the H atoms are parallel (total spin $S = 1$), called orthohydrogen (o-H_2), and a singlet state in which they are antiparallel ($S = 0$), called parahydrogen (p-H_2). In thermal equilibrium at room temperature, hydrogen consists of 75% of orthohydrogen and 25% of parahydrogen, due to the three S_z states ($S_z = 1, 0, -1$) for $S = 1$ versus one S_z state ($S_z = 0$) for $S = 0$. The energy difference between the two states is 14.7 meV, equivalent to about 170 K. Parahydrogen is the ground state and in a cold source, at a temperature of 20 K, well below the temperature equivalent of the excitation energy for orthohydrogen, the equilibrium distribution approaches 100% parahydrogen. In practice, the metastability of orthohydrogen makes it necessary to use iron-oxide catalysts to achieve this desired state within a reasonable time frame.

Since neutrons and protons can exchange spin during the scattering process with hydrogen molecules, the scattering cross sections for the two isomers are very different at low neutron energies. Fig. 4.1 on the left shows the total and absorption cross sections of

Table 4.2
Parameters for some possible cold moderators: "Material" denotes the moderator material, "Formula" the chemical formula, "T_B" the boiling point in Kelvin, "T_M" the melting point in Kelvin, and "Phase" the phase (liquid/solid) commonly used for a cold moderator.

Material	Formula	T_B [K]	T_M [K]	Phase
Hydrogen	H_2	20.27	13.99	Liquid
Deuterium	D_2	23.64	18.72	Liquid
Methane	CH_4	111.6	90.7	Solid
Ethane	C_2H_6	184.7	90.4	Solid
Mesitylene	C_9H_{12}	437.8	228.3	Solid

a hydrogen atom. While the absorption cross section increases with decreasing neutron energy, the total cross section for scattering plus absorption remains constant over a wide range of incident neutron energies. On the right side of Fig. 4.1 the inelastic scattering cross sections for para- and ortho-hydrogen are plotted. While these are practically identical for neutron energies greater than 0.1 eV, the parahydrogen scattering cross section decreases sharply below this value, while for orthohydrogen it continues to increase. This behavior is very useful for a cold source: thermal neutrons entering the p-H_2 cold source have a high probability of being downscattered into the cold neutron regime. Once at energies of a few meV (cold neutron regime), they have a much lower probability of being scattered, i.e. a much higher mean free path, and can leave the cold moderator without further scattering events. This feature is used for so-called low-dimensional cold moderators, as will be discussed in more detail in Section 7.

The Table 4.2 lists some characteristic parameters for possible cold moderator materials [33,103–106]. Due to the low absorption cross section of deuterium (D = ^{2}H), liquid deuterium (LD_2) sources with volumes in the range of 10 l to 20 l are usually used for continuous fission based neutron sources. Practical aspects are being discussed in the classical paper by Ageron [107]. In order to minimize the effect of absorption in the cold source, particularly for LH_2 as moderator material, the cold source geometry has been adapted by introducing a cavity from which the neutrons can emerge, see e.g. [108]. For pulsed sources, liquid hydrogen LH_2 or hydrocarbons are mainly used. While hydrocarbons can achieve high hydrogen densities and offer many possible transitions between energy levels that can scatter neutrons into the cold neutron regime, there is a danger of radiolysis producing hydrogen that can freeze in the solid matrix, exert pressure on the moderator walls, and eventually release energy as "blurbs" that can even destroy the cold source. Advantages of so-called low dimensional moderators have been discussed by Mezei et al. [109] and Zanini et al. [110]. Practical aspects for "one-dimensional" liquid hydrogen moderators for pulsed sources are discussed in [111]. For pulsed sources, techniques have been developed to adapt the pulse spectrum of such moderators to the instrumental requirements, such as the so-called decoupling or poisoning of the moderator. These aspects will be discussed in one of the following subsections.

When full thermal equilibrium is reached in a moderator material in the thermal scattering regime, the energy spectrum of the neutron density emitted from the moderator should follow a Maxwellian distribution:

$$N(E) = 2\pi N \frac{\sqrt{E}}{(\pi k_B T_{eff})^{3/2}} \exp\left(-E/(k_B T_{eff})\right) \tag{4.5}$$

Note that for the important case of a p-H_2 cold source, a Maxwellian does not correctly describe the energy spectrum, since neutrons can leave the moderator after one scattering event when full thermalization has not been achieved.

However, in reality the spectra often contain several components, e.g. if the cold source is undermoderated, or if neutrons are extracted from thermal and cold moderators simultaneously (so-called bi-spectral beam extraction, see below). And more realistically, there remains a high-energy component of neutrons from the slowing-down regime. A modified Westcott function [113] provides a good description of the spectra as product of energy E times flux per unit energy $I(E)$:

$$EI(E) = I_{th} \frac{E^2}{E_{T_{eff}}^2} \exp\left(-E/E_{T_{eff}}\right) + I_{epi} \left(\frac{E}{E_{ref}}\right)^{\alpha} \frac{1}{[1-(E/E_{co})^s]} \tag{4.6}$$

The first term is the storage term which follows the Maxwellian distribution (4.5), while the second term is the slowing down term which describes the neutrons emitted by the moderator during slowing down. Parameters of the function are determined by fitting to experimental data: I_{th} and I_{epi} are the contributions of the two components, $E_{T_{eff}}$ the mean thermal energy, usually larger than $k_B T$ where T is the temperature of the moderator (compare (4.5) where also an effective temperature was used instead of the physical temperature), α is the leakage exponent, describing the leakage of neutrons from the slowing-down regime out of the moderator, E_{ref} and E_{co} are the reference and cutoff energies, respectively, and s is the cutoff exponent.

We conclude this section with an example of the arrangement of secondary sources at the research reactor FRM II in Germany, one of the most modern continuous neutron sources. Neutrons from the various secondary sources are extracted through evacuated beam tubes pointing toward the respective secondary source. Fig. 4.2 shows a horizontal section through the FRM II reactor pool. It shows the arrangement of the thermal, cold and hot sources and the evacuated beam tubes through which the neutrons are extracted through the biological shielding of the reactor. The wavelength spectra of the three sources are shown in Fig. 4.3. The thermal source has a near Maxwellian spectrum with a tail to higher energies (shorter wavelength) from the slowing-down regime. The hot source shifts the spectrum to shorter wavelengths. Clearly, the cold source is undermoderated: while the spectrum is shifted to longer wavelengths, there remains a strong second component of thermal neutrons.

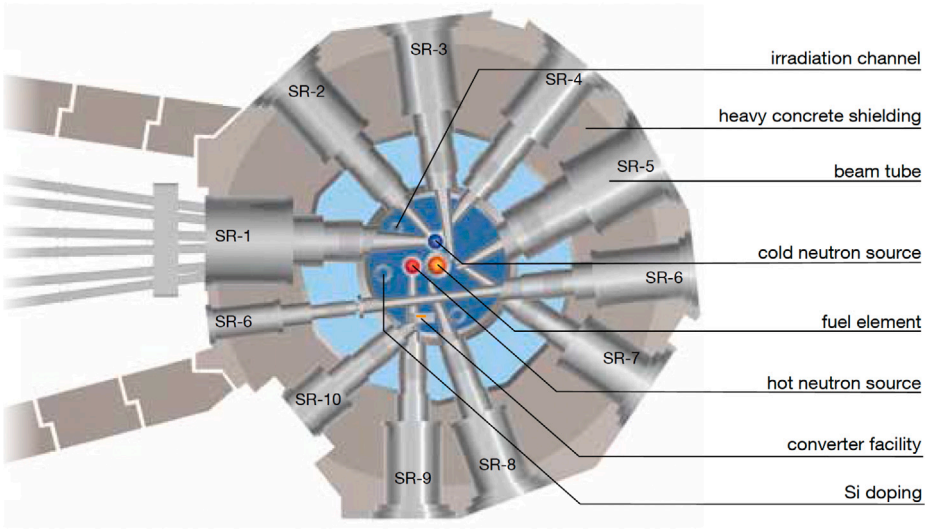

Fig. 4.2. Horizontal section of the FRM II reactor pool showing the arrangement of the beam tubes, the fuel element, and the cold and hot neutron sources. The thermal D_2O moderator tank surrounding the fuel element is shown in dark blue, the H_2O water tank surrounding the thermal moderator tank is shown in light blue. Copyright Heinz Maier-Leibnitz Zentrum (MLZ), reproduced from [112] with kind permission from MLZ.

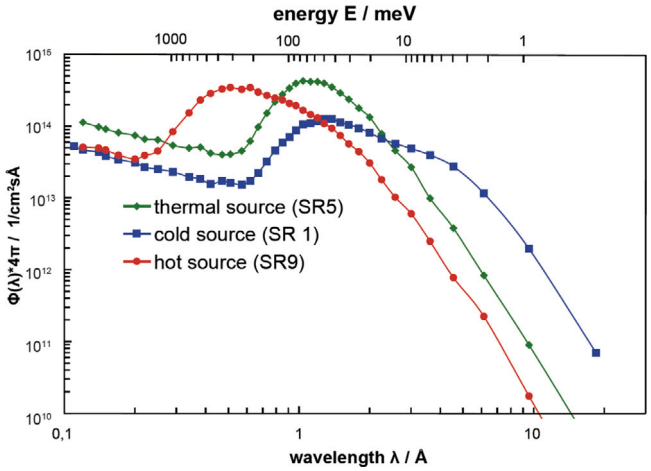

Fig. 4.3. Neutron wavelength spectra from the cold, thermal and hot sources at FRM II for a reactor power of 20 MW at the entrance to the beamtubes. Copyright Heinz Maier-Leibnitz Zentrum (MLZ), reproduced from [112] with kind permission from MLZ.

4.2. Moderator geometries and emission characteristics

In addition to the characteristics of the moderator material, such as absorption cross section, scattering cross section, and density, the geometry of the neutron moderator is also a significant factor affecting the emission characteristics. In order to optimize the instrument and assess its performance, it is essential to ascertain the characteristics of the emitted neutrons, including their wavelength, position, and direction. In this regard, the concept of brilliance, as previously mentioned in Section 2, is particularly useful as it provides a comprehensive characterization of both the moderators and the emitted neutrons.

The terms "brilliance" or "brightness" can be defined in several ways with respect to accelerator-driven neutron sources. Different definitions exist in different scientific communities and in different contexts. Here we refer to [35], where brilliance is defined as the number of neutrons emitted per unit time from the source area into a solid angle element, normalized by the relative wavelength interval and the number of incident particles or current times time interval. Accordingly, it has the unit

$$[B] = 1/(scm^2 sr(1\%\Delta\lambda/\lambda)(mAs)). \tag{4.7}$$

In literature the following definition is frequently employed:

$$[B] = 1/(scm^2 sr\ \text{Å}) \tag{4.8}$$

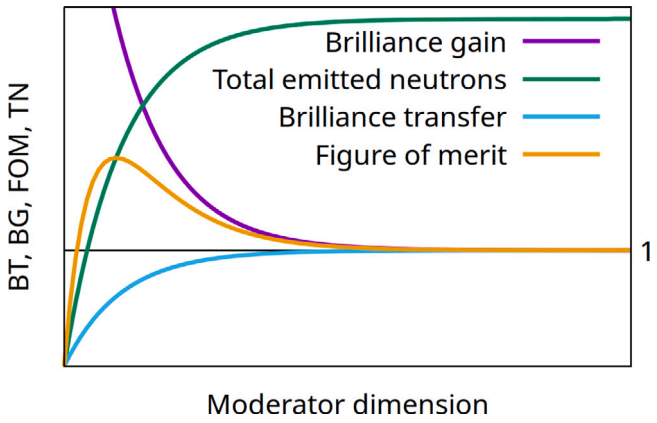

Fig. 4.4. Brilliance gain (BG) for a low dimensional moderator together with the total number of emitted neutrons (TN), the brilliance transfer (BT) and the resulting figure of merit (FOM). BG is the ratio between the brilliance emitted by a reference volume moderator and the brilliance emitted by the modified moderator. BT is defined as the ratio between the phase space density at the moderator surface and the transported phase space density. FOM is the product of BG and BT. Figure is inspired by [110,114].

It describes the number of neutrons emitted per time interval from an area of the moderator into a solid angle with a given wavelength, thereby fully characterizing the neutron beam with respect to position and momentum. By integrating over the accepted wavelengths and the solid angle, the flux F can be calculated:

$$F = \int_{\Delta\lambda} \int_{\Omega} B. \tag{4.9}$$

In order to achieve high brightness, it is essential to ensure that the neutrons are emitted within a narrow parameter space. This is the case for the low-dimensional moderators [109] where the neutrons are emitted from a small moderator surface area. For a low-dimensional LH_2 moderator with its different mean free paths for thermal and cold neutrons, resulting in a thin but long moderator, the moderator in itself acts as collimator just by its geometry. The neutron emission by a low-dimensional moderator is, therefore, in comparison to that of a volume moderator with isotropic emission, rather directed. This lower divergence further increases the brightness. Conversely, a high flux can be achieved if samples with sizes comparable to the moderator size are investigated. It is important to note that a reduction in moderator dimensions results in a decrease in the total number of neutrons emitted from the moderator, while the brightness increases. This phenomenon is illustrated in Fig. 4.4.

The necessity for different moderators is contingent upon the specifications of the instrument and the sample that is to be investigated. For instance, in the case of irradiation, imaging, and PGNAA with relatively large samples, the use of a volume moderator with a large number of totally emitted neutrons is crucial for achieving a high flux at the sample position. In the context of scattering experiments, the need for a high-brilliance neutron beam is becoming increasingly apparent, especially in the light of the continuing desirable reduction in sample size.

An additional crucial element influencing the instrument's performance is the impact of neutron guide filling and the subsequent brilliance transfer. The different experiments require specific beam properties at the sample position in terms of beam dimensions, divergence and wavelength. The guide filling of neutrons with these properties depend on the moderator dimensions, the guide dimensions and the distance between the guide entrance and the moderator surface. The whole topic is beyond the scope of this review article and we refer the interested reader to excellent literature [115] and its application [114,116]. We would just like to emphasize that two different states of a neutron guide filling can be distinguished depending on the moderator dimension. For small or low-dimensional moderators, the guide cannot be filled with the required divergence and thus shows a linear dependence. For volume moderators, the entire phase space required by the sample can be filled into the neutron guide and thus shows saturation.

The brightness filled into the neutron guide can be transported almost without loss with modern neutron optics resulting in a brightness transfer (BT) of $BT \sim 1$ which is the limit according to Liouville's theorem [117]. The brightness transfer from the moderator to the sample is thus dominated by the neutron guide filling, resulting in the dependence as shown in Fig. 4.4. Together with the brightness gain for low-dimensional moderators a Figure of Merit (FOM) can be constructed showing an optimal brightness transfer for a given moderator dimension. It should be emphasized that this optimal moderator dimension depends on the experimental requirements, e.g. the sample dimensions and the distance of the neutron optics from the moderator surface, since this influences the possible guide filling and thus the brilliance transfer. The optimal moderator dimension will therefore be different for the different source types and for different neutron instruments.

4.3. Time structure

In terms of time structure, accelerator-driven neutron sources offer great flexibility to produce neutron pulses of different peak length, shape, peak height and repetition rate, compared to steady-state neutron sources where the main figure of merit is the

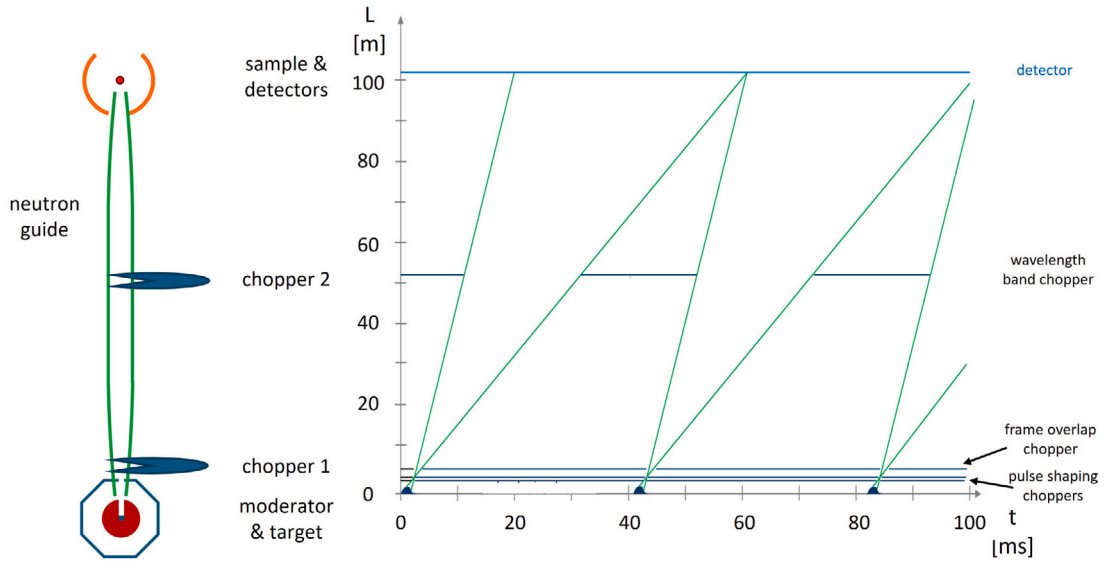

Fig. 4.5. Distance-time diagram (right side) for a simple diffractometer at a pulsed source, which is shown schematically on the left [119].

neutron flux in the thermal moderator. The required time scales depend largely on the desired application, see Section 5. Accelerators accelerate particles in micropulses at frequencies of a few 100 MHz. The repetition rate of these micropulses is too high to be relevant for neutron sources; they appear as a continuum, but are grouped into macropulses which provide the flexibility mentioned above. Characteristic time scales for pulse lengths and pulse distances can be illustrated on a simple but typical instrument.

For pulsed sources, time-of-flight (tof) methods are the techniques of choice because they can use the peak flux, which is much larger than the average flux. Fig. 4.5 illustrates the tof technique for the example of a very simple diffractometer at a pulsed source. A pulse is generated in the target–moderator–reflector assembly housed in the biological shielding. The source pulse can be used as is, or with further pulse shaping by a pulse shaping chopper system, see Section 4.4. A chopper is a device that periodically opens and closes the beam path [118]. Chopper 1 in Fig. 4.5 is a so-called frame overlap chopper that ensures that only neutrons from one pulse arrive at the detector at any given time. The neutrons are transported to the detector by a neutron guide, see Section 4.4. Chopper 2 is used to define the wavelength band used for the experiment. Finally, for a diffractometer, the neutrons are elastically scattered and detected in a position sensitive detector surrounding the sample. The time elapsed from the release of the neutrons in the pulse to their detection is a measure of the wavelength, and the scattering angle for that wavelength, together with the recorded intensity, gives the desired structural information.

The wavelength band of a pulsed source is determined by the source period T_{src} and the total instrument length L. In order to avoid frame-overlap, the maximum bandwidth $\Delta\lambda$ that can be used at the detector has a time-of-flight range ΔT equal to the source period T_{src}:

$$\Delta\lambda = \frac{h}{m_n}\frac{T_{src}}{L} \approx 3956\ \text{mÅ/s}\frac{T_{src}}{L} \tag{4.10}$$

For long pulse sources, which require pulse shaping to improve the time-of-flight resolution, the position L_1 of the pulse shaping device constraints the accessible bandwidth. Together with the duty cycle of the source, this defines a 'natural' instrument length

$$L_{\text{nat}} = \frac{L_1}{\text{duty cycle}}, \tag{4.11}$$

That is the reason, why the high resolution instruments at a long pulse spallation source like the ESS (see Section 6) are all placed at a distance of approximately 160 m [120]. Typical CANS and HiCANS instruments are much shorter [121].

For a diffractometer, one is interested in the d-spacing resolution, i.e. how accurately can the distances d between reciprocal lattice planes be determined? There are three independent contributions: uncertainties in the wavelength, the path length, and the scattering angle: The total resolution is then given by

$$\frac{\delta d}{d} = \sqrt{\left(\frac{\delta\lambda}{\lambda}\right)^2 + \left(\frac{\delta L}{L}\right)^2 + \left(\cot\theta\frac{\delta\theta}{\theta}\right)^2} \tag{4.12}$$

The wavelength spread is given by the uncertainty in the time of flight T caused by the neutron pulse length τ_{pls}:

$$\frac{\delta\lambda}{\lambda} = \frac{\tau_{pls}}{T} = \frac{\tau_{pls}h/m_n}{L\lambda} \tag{4.13}$$

Eq. (4.13) shows that the wavelength resolution increases, i.e. $\frac{\delta\lambda}{\lambda}$ decreases, with decreasing pulse length τ_{pls} and increasing distance source–detector L. To achieve the desired resolution $\frac{\delta d}{d}$ of 0.01–0.1, such instruments typically have a length of the order

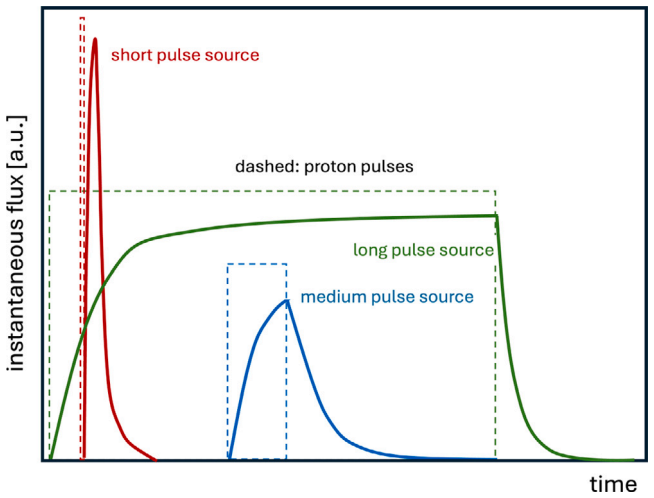

Fig. 4.6. Schematic illustration of the pulse shapes for neutrons of a certain wavelength (please note that the pulse shapes for different wavelengths differ) from the moderator for a short-, medium-, and long-pulse length source. The neutron pulses are represented by solid lines, while the corresponding proton pulses are shown as dashed lines. The figure is not to scale, neither for the intensity axis nor for the time axis. The typical length of the proton pulses is less than 1 μs, a few hundred microseconds, and a few milliseconds for short, medium, and long pulse sources, respectively.

of 100 m. According to Eq. (4.13) the desired resolution can be achieved with this instrument length with pulse lengths on the order of a few 10 μs and according to Eq. (4.10) repetition rates on the order of some 100 Hz are required. For instruments working with cold neutrons, the pulse length can be correspondingly longer, say on the order of 100 μs, and the repetition rates smaller.

It should be noted that the above estimates are valid for a simple diffractometer. For such an instrument, long pulse sources have a higher fluence in the pulse, but according to Eqs. (4.11) and (4.13) need longer flight paths to achieve the same resolution. This increases the cost of the instrument significantly. The solution is multiplexing: more sophisticated instrument designs and other instrument types may include pulse shaping by additional choppers and elaborate multi-wavelength data acquisition schemes such as "wavelength frame multiplication" or "repetition rate multiplication", which overcome some of the constraints between instrument length, resolution and repetition rate. However, a discussion of these techniques is beyond the scope of the present neutron source review and we refer to the appropriate literature [120,122–124]. The main aspect of the above discussion is to obtain the required timescales for the different neutron energy ranges: The required pulse lengths range from about 1 μs for eV neutrons, a few times 10 μs for thermal neutrons, to over 100 μs for cold neutrons, while the appropriate pulse frequencies range from a few 100 Hz for thermal neutrons to 10 Hz for cold neutrons. These estimates guide the design of the neutron moderator and determine the macro pulse length provided by the accelerator, while long pulse sources use the multiplexing schemes mentioned above [120].

Preferably high density hydrogenous moderators are being used for pulsed sources. They minimize the spreading out of the pulse due to the small mean free path, see Table 4.1. Still there remains the conflict between the desired high time averaged flux and the short pulse lengths. Roughly speaking, one can distinguish the following cases, see Fig. 4.6:

- Short pulse length sources, where the macro pulse length of the accelerator is shorter than the average storage time of the neutrons in the moderator–reflector assembly. This is typical for short pulse spallation sources with proton pulse lengths below 1 μs, see Section 6. For short pulse sources, it is the moderator–reflector assembly that determines the shape and intensity of the neutron pulse as a function of energy. For short pulse sources, pulse shaping is difficult and the asymmetric pulse shape can cause problems for certain applications. However, an advantage of short pulse sources is the intrinsically better resolution (see Eq. (4.13)) that can be achieved without additional means. To produce truly short neutron pulses and better pulse shapes, special measures must be taken, such as decoupling the moderator from the reflector and poisoning the moderator [12], see below.
- Medium pulse length sources, where the macro pulse length of the accelerator is comparable to the average storage time of the neutrons in the moderator–reflector assembly, typically in the range of a few hundred microseconds for cold neutrons. The pulse shape essentially consists of a rising edge as the moderator fills with neutrons from the target in the slowing down regime and a decay edge when the target pulse has passed. Medium pulse length sources are typically sources with lower source strength such as HiCANS, see Section 7.2. Matching the pulse length from the accelerator to the neutron storage time in the moderator–reflector assembly increases the neutron fluence in the pulse, since the moderator is continuously filled with fast neutrons. The moderator–reflector assembly, together with pulse shaping choppers, can be designed to produce a nearly symmetric pulse, which is advantageous for most applications.
- Long pulse length sources, where the pulse length is essentially determined by the macro pulse length of the accelerator. Typical pulse lengths are in the range of a few milliseconds, which is significantly longer than the time needed to slow the neutrons down in the moderator–reflector assembly. This is typical for long pulse spallation sources, see Section 6. Neutron

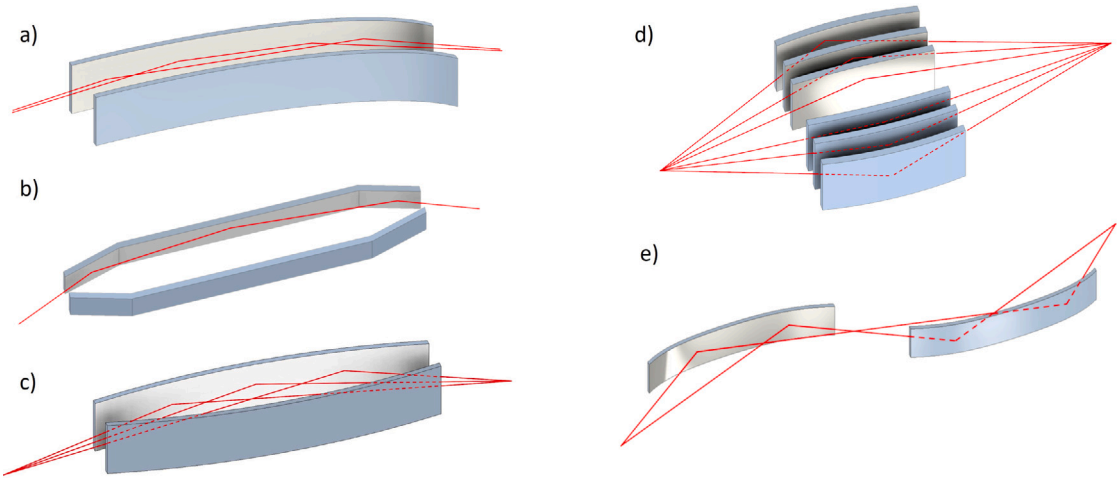

Fig. 4.7. Schematic drawing of various guide geometries. From top to bottom: (a) curved neutron guide to avoid direct line of sight to the source; (b) ballistic neutron guide to transport long wavelength neutrons over long distances; (c) elliptical neutron guide to image the source onto the sample position; (d) nested mirror optics to achieve similar imaging; (e) SELENE optics to produce a small, virtually background free neutron beam footprint by avoiding the coma-aberration of a simple elliptical neutron guide. The thin red lines represent possible neutron trajectories.

pulses from the moderator have a rising edge as the pulse from the target fills the moderator and a decay edge when the pulse from the target has passed. At the trailing/decay edge, absorption and leakage through the surface determine the decay of the flux in the moderator. In between, the moderator–reflector behaves as in the steady state case, and the pulse from the moderator has a (nearly) flat top. Using pulse shaping schemes with choppers, one can select this flat top region to generate a pulse for the instrument and produce a Gaussian pulse shape, which is advantageous for many applications.

Much of the trailing edge of the neutron pulse is due to neutrons that have left the moderator, become thermalized in the reflector, and are backscattered into the moderator. This contribution can be suppressed by simply decoupling the moderator for thermal neutrons from the reflector while allowing fast neutrons to pass [125]. This can be achieved by a layer of a neutron absorbing material that has resonant absorption for thermal neutrons. Examples are cadmium (Cd) and gadolinium (Gd), which decouple at 0.5 eV and 0.1 eV, respectively. On the other hand, absorbers without resonances have an absorption cross section proportional to the wavelength or inversely proportional to the velocity v. An example is boron (B). Due to the less abrupt energy dependence of the neutron absorption cross section, such 1/v absorbers are less suitable because they also absorb epithermal neutrons.

While decoupling is used to suppress the trailing edge of the pulse, the pulse width can be controlled by poisoning the moderator [126]. Again, resonance absorbers are used, which have a high absorption cross section for thermal or cold neutrons, but a low absorption cross section for high energy neutrons, again typically Cd and Gd. In the heterogeneous poison scheme, a layer of neutron absorbing material is introduced into the moderator, but outside the direct view of the instrument. In effect, the moderator appears large for fast neutrons, which can pass through the absorber, and small for thermal neutrons. This limits the time slow neutrons spend during diffusion in the moderator and narrows the pulse for low energy neutrons while maintaining a high probability of thermalization of fast neutrons. Obviously, poisoning comes at the expense of intensity. If poisoning and decoupling can be avoided, almost an order of magnitude of flux can be gained if the extra pulse length can be accepted from a resolution standpoint; see [127] for a detailed discussion of the interplay between pulse intensity and pulse length for various geometries.

4.4. Neutron transport and optics

For beam experiments, the neutrons released and moderated in the primary neutron source must be extracted and transported to the experiment. This offers another way of modifying the neutron spectrum and its time structure to suit the needs of the experiment. Details are far beyond the scope of this review and would require a separate review article. For the sake of completeness, a very cursory overview of the techniques used is given here, again omitting specialized topics such as neutron beam polarization. For an introduction we refer to the textbooks [12,92,95] and recommend [120] and references therein for a fairly complete and recent overview of modern techniques used to tailor neutron beams — from moderation to beam extraction and beam transport to pulse shaping for various types of beamline applications for the instruments designed for the European Spallation Source (ESS).

In short, the neutrons are extracted from the primary source through evacuated beam tubes. They are transported over long distances of up to more than 100 m through neutron guides. These evacuated glass tubes are often rectangular in cross-section. Neutrons are transported by total reflection from the polished glass surface or a thin low roughness metal layer on the glass surface. In its simplest form this can be a thin film of ^{58}Ni, but nowadays supermirror coatings are used to increase the transported neutron divergence by Bragg reflection from a gradient multilayer. Gamma radiation from the primary source can be suppressed by curved

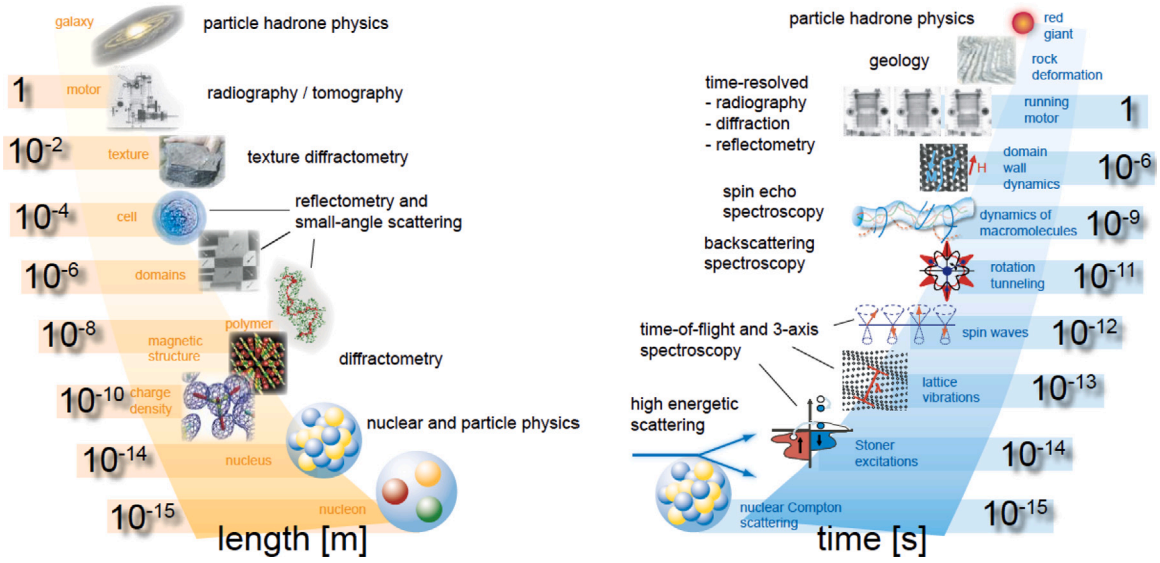

Fig. 5.1. Length- and timescales covered by research with neutrons. Typical applications and the corresponding techniques used are indicated [135].
Source: Adapted from a strategy paper of the German Committee Research with Neutrons (KFN) [135].

guides that avoid direct line of sight between the instrument and the neutron source. The transmission properties of neutron guides can be used to suppress short wavelength neutrons while transporting long wavelength neutrons over long distances with very little loss, e.g. in so-called ballistic neutron guides [128]. Neutron guides may include focusing optics to image the source to a sample position on the instrument. This can be done by elliptical neutron guides [129], special double-bounce so-called SELENE optics [130,131], or by a nested mirror arrangement [132], see Fig. 4.7.

Neutron beam filters are used to clean or modify the spectrum or as elements of instrumentation. They are based on either resonance absorption or scattering using the Bragg cutoff. Examples include: (i) bismuth (Bi) single crystals absorb gamma radiation from the source while being transparent to neutrons when properly oriented; (ii) cadmium (Cd) is a strong neutron absorber in the thermal and cold energy range while being transparent to hot neutrons; (iii) polycrystalline beryllium (Be) has a cutoff wavelength of 0.392 nm, blocking shorter wavelength neutrons by Bragg scattering out of the transmitted beam. Neutrons with wavelengths beyond the Bragg cutoff ($\lambda > 0.4$ nm or $E < 5$ meV) pass through the filter with little attenuation when the filter is operated at liquid nitrogen temperature (77 K) to suppress phonon scattering.

Another approach to tailor the spectrum of a neutron beam and to modify its pulse time structure is the time-of-flight method. Neutron choppers are used for this purpose [118]. Fast rotating neutron absorbing disks with openings to let the beam pass only for a short time are called “disk choppers”. Double disk choppers, consisting of two counter-rotating disks, are often used to produce shorter neutron pulses. Another approach is to use cylinders of neutron-absorbing materials that rotate around the cylinder axes and have a slit that allows neutrons to pass only when the slit is in the direction of the incoming beam, called Fermi choppers. Modern instrument concepts use clever combinations of focusing guides with pulse shaping choppers, e.g. in an eye-of-the needle arrangement [133].

5. Main application of neutrons in large scale facilities

Large neutron user facilities serve a broad range of important applications: (i) free neutrons are used in beamline instruments as probes of condensed matter on a wide range of length and time scales; (ii) neutrons are used in materials research, quality control, and industry for high sensitivity elemental analysis through the technique of Prompt Gamma Neutron Activation Analysis (PGNAA); (iii) beams of free neutrons are used to produce images or tomograms of various objects revealing their internal structure; (iv) neutrons are themselves objects of study in high precision particle physics experiments; (v) neutrons are used to produce radioisotopes for various purposes, e.g., radionuclides for medical applications; (vi) neutrons are used to induce transmutation, e.g. for homogeneous doping of Si single crystals for electronics applications; (vii) neutrons are used to treat cancer by irradiation, e.g. in Boron Neutron Capture Therapy (BNCT); (viii) high intensity neutron sources are key for the development of fusion reactors [134]; and of course (ix) there are many other applications, too numerous to list here. By far the largest community served uses classical scattering methods as outlined in the next section.

Fig. 5.1 shows the length and time scales covered by neutron research. It gives a rough overview of the techniques used and shows some major applications. The very extremes of length scales – below 10^{-12} m – are the domain of nuclear and particle physics, at the other extreme intimately connected to cosmology. Neutrons as probes for condensed matter research cover a range in the phase space from picometers (pm) to meters and femtoseconds (fs) to hours, an extremely impressive range! The majority of users

come from the study of materials and material systems in many research fields: condensed matter physics, chemistry, materials science, magnetism and soft matter research, engineering, life sciences, geosciences, medicine, food science, and many more. Cold, thermal and hot neutrons are ideally suited for these uses because their wavelengths match the relevant length scales and their energies match the typical excitation energies in the respective materials. Ultracold neutrons, on the other hand, are the subject of particle physics research. In this chapter we give a very brief overview of the main applications of neutrons in large scale facilities and mention briefly the techniques used. From their requirements general specifications that neutron sources should fulfill to serve the respective purposes can be deduced.

5.1. Scattering

The majority of users of large-scale facilities for research with neutrons utilize neutron scattering as their preferred technique. The efficacy of this technique is contingent upon the distinctive properties of neutrons:

- As neutral particles, neutrons have large penetration depths in most materials, allowing, for example, operando studies of entire devices.
  Diffraction from large objects has important applications in many areas. Stress and strain diffractometers are used to probe strain and texture in materials and for engineering applications [136]. Effects of the production process of engineering materials are investigated by texture analysis, e.g. the ordering of the crystalline structure in steel grains due to industrial rolling processes [137]. The method is also effective for acquiring knowledge about the production process of historical artifacts [138,139] or the history of geological samples that have undergone multiple transformations and subduction during the evolution of the Earth, including plate tectonics and volcanism [140].
- Neutrons interact with atomic nuclei, which means that their interaction is isotope specific and allows the labeling of specific functional groups by isotope exchange, a very important technique in soft matter or life science studies [141,142] by H–D exchange.
  Diffraction from larger (many nm) size objects requires specialized techniques. Small angle neutron scattering (SANS) is strongly applied to study polymers, colloids and complex fluids (i.e. the classical soft matter), membranes, proteins and protein complexes, but also for many other applications [143–145]. To detect a lateral surface or interface roughness, lateral correlations, sizes and shapes of objects such as particles positioned on top of the surface or in a surface near region off-specular scattering is required. Grazing incidence small-angle scattering (GISAS) enables access to this desired structural information [146–148].
- The nuclear interaction of neutrons with matter leads to a high sensitivity for light elements and the possible discrimination of neighboring elements in the periodic table.
  The sensitivity to light elements is an essential feature for the study of biomolecules [141,142] and energy materials, where light atoms, such as hydrogen, lithium, or sodium, are the atoms responsible for functionality [149–152].
- Neutrons are a gentle, non-destructive probe, which is particularly important for life sciences [141,142].
- Through the nuclear moment, neutrons are sensitive to the magnetic fields inside samples and are therefore the most important probe to study magnetic structures and dynamics [153].
  Magnetic SANS is employed to study structures on the nm length scale such as skyrmions or flux line lattices [154]. Reflectometry [155,156] is used to investigate layered systems, e.g. for spintronic devices. Monochromatic neutron reflectometers [157] as well as many time-of-flight instruments [158–160] are employed to study a wide variety of layered systems, from soft matter and biological systems through engineering materials to magnetic multilayers.
- Thermal neutrons have wavelengths comparable to interatomic distances, which allows one to solve the atomic structure.
  Single crystal and powder diffractometers are available at any neutron facility. They operate in either constant wavelength (CW) or time-of-flight (TOF) mode, depending on the neutron source [161,162]. These instruments enable the determination of the atomic structure of crystalline materials and the investigation of correlations on the length scale of a few nm of the local structure in amorphous materials and liquids [163]. For studies of the local crystal structure of materials, where the information is buried underneath strong Bragg peaks in the form of a weak diffuse scattering, pair-distribution-function (PDF) measurements are used [164]. PDF studies are particularly helpful for nanocrystalline materials where atoms with a reduced coordination number often determine structural and magnetic properties of nanoparticles and are key for enabling real-life applications of nanoscale materials [165].
- Thermal neutrons have energies comparable to the excitation energies in materials, allowing the study of microscopic (atomic, molecular) dynamics.
  Neutron spectroscopy provides unique information about the dynamic properties of condensed matter. Computer modeling of inelastic neutron scattering cross sections allows one to obtain parameters of model Hamiltonians, such as interatomic forces or exchange constants, which allow one to predict the macroscopic response of a material and thus lead to a microscopic understanding of the relationship between structure and function. Neutron spectroscopy provides direct access in absolute units to self-, pair- and spin-correlation functions, which are the fundamental quantities derived by modern ab-initio theories. Thus, the simplicity of the neutron cross sections and the fact that they can be measured on an absolute scale allow benchmarking of ab-initio theories and computer modeling with huge impact in many different scientific fields [166]. Quasielastic neutron scattering (QENS) allows measurement of the molecular displacements and probes dynamics from fast vibrational modes down to slow diffusive motion [167]. The instruments best suited to performing high-energy-resolution neutron spectroscopy are spin-echo spectrometers and backscattering spectrometers [168].

Neutron scattering utilizes the spectral range from hot to cold neutrons, and highly sophisticated and efficient techniques have been developed for both continuous and pulsed sources, as detailed in the cited literature and textbooks such as [12].

5.2. Imaging

As the neutron can penetrate matter deeper than most other microscopic probes it can be used to image large objects, for example running engines or large geological specimen. Uniquely, the neutron can also image the magnetism in these objects. On a scale from some micrometers up to a meter, neutron imaging is applied for non-destructive investigation or quality control of complex devices.

Neutron imaging is a real-space technique. It resolves structures on length scales above the pixel size of the detector system in use which can go down to some μm [169,170]. A divergent neutron beam originating from a small source point impinges on the sample and the undisturbed, transmitted beam is recorded by a 2D position sensitive detector. In simple neutron radiography, the contrasts evident in the recorded image show all structures inside the sample that have attenuated the neutron beam. A series of neutron images, taken together with a rotation of the specimen inside the beam, allows for the reconstruction of the three-dimensional structure, a process known as neutron tomography [171].

The phenomenon of attenuation can be attributed to either absorption or scattering. The absorption contrast is important for elements like B, Li, or Cd, while scattering is a very important process for H containing materials and for every crystalline matter especially for wavelengths slightly below a Bragg edge [172]. For this reason, neutron imaging is technologically relevant to detect organic materials embedded in a metallic environment, e.g. lubricants inside a motor or water induced corrosion inside a steel construction. Nevertheless, the scientific cases encompass a plethora of disciplines, including, but not limited to, geology, construction materials, porous materials, engineering materials, liquid metals, plant sciences, magnetism, and cultural heritage [173,174].

Depending on the size of the structure under investigation the energy of the neutron beam can be chosen to have a penetration depth appropriate to the attenuation power of the entire sample. Fast neutrons (energy > 10 keV) are used to image entire machines up to 1 m in size, while thermal (energy < 0.5 eV) or cold (energy < 5 meV) neutrons are used to image materials and devices with dimensions of centimeters or less. Neutron imaging has been applied in the determination of liquid water in operating polymer electrolyte fuel cells (PEFCs) to resolve the water distribution in different layers of the fuel cell structure [175]. The high visibility of neutrons for light-Z elements, in particular hydrogen and lithium, enables the direct observation of lithium diffusion, electrolyte consumption, and gas formation in lithium batteries [176].

Resolution of the neutron wavelength in the cold neutron regime around the Bragg edges of the material under investigation allows one to image regions with different crystalline structures. This is of interest e.g. in the steel production, where the mixture and order of martensitic and austenitic phases determines important mechanical properties of the material [177].

The utilization of polarized neutrons in imaging allows the visualization of magnetic structures and fields. Imaging with polarized neutrons involves extended polarized neutron beams with well-defined collimation and the use of imaging detectors [178].

The application and utilization of neutron imaging have witnessed a notable expansion over the past few decades, with the establishment of numerous experimental facilities for neutron imaging and the announcement of further planned constructions [179–181].

5.3. Precision physics, particle and nuclear physics

While in materials research the neutron is used as a probe on atomic length and time scales, in particle physics the neutron becomes the object of research itself. Precision experiments with cold and ultracold neutrons allow rigorous tests of the Standard Model of particle physics and tests of new physics beyond the Standard Model [182–184]. This “precision frontier” complements research at the “energy frontier” at large accelerator facilities such as CERN or Fermilab [185,186]. In addition to resolving shortcomings of the Standard Model, neutron research can address a number of fundamental questions relevant to cosmology and our understanding of the universe, such as the much debated nature of dark matter and dark energy, quantum gravity, or the asymmetry between the abundance of matter and antimatter in the universe. Major experimental efforts are underway in the following areas: (i) Precision experiments to determine the electric dipole moment of the neutron [187]. In an attempt to understand the observed baryon asymmetry of the universe, these experiments probe the physics that violates time reversal invariance and, through the CPT theorem, the combined symmetry of charge conjugation and parity (CP). (ii) Precision measurements of the neutron beta decay lifetime. They allow one to obtain numerical values of the free parameters of the Standard Model (SM) and to search for new physics [188]. (iii) Neutron interferometry as a test of quantum mechanics and quantum gravity [189].

Such precision experiments often require a high density of ultracold neutrons, which can be stored in (magnetic) “neutron bottles” for e.g. neutron lifetime measurements or to search for an electric dipole moment of the neutron. Major efforts are underway to optimize ultracold neutron (UCN) sources at the major neutron research facilities. As the “precision frontier” is intertwined with the “intensity frontier”, MW spallation sources such as the future European Spallation Source ESS promise to open up new unexplored territory [3].

5.4. Radioisotope production

Molecular imaging of molecules, biochemical processes, and physiological activity within the human body is one of the most powerful tools for diagnosis and staging of disease. Common tools for molecular imaging to tag specific biologically active molecules (biomolecules) are medical isotopes. They are used worldwide for broad spectra of purposes [190] including nuclear diagnostic imaging, gamma imaging, positron emission tomography, bone density measurement, gastric ulcer detection, radioimmunoassay and therapeutic techniques, palliative care, radiotherapy, brachytherapy and irradiation of blood for transfusion.

Medical isotopes are produced using nuclear reactions at either nuclear reactors or accelerator facilities [191,192]. The basic setup involves exposing a target to a high flux of particles, either from a neutron source or from an accelerator. Nuclear (as opposed to chemical) reactions within the target then create the medical-isotopes from the nuclei of the target material. Neutron rich isotopes are produced in reactors by thermal neutron irradiation and neutron-deficient isotopes by using proton, deuteron or alpha accelerators. The production of radioisotopes may be achieved also using a compact accelerator neutron source with a dedicated target station furnished with sample irradiation positions [193].

The technetium isotope ^{99m}Tc has become the most prevalent radioisotope utilized for the diagnosis of pathological conditions. ^{99m}Tc (half-life 6 h) is generated from the molybdenum isotope ^{99}Mo (half-life 66 h). It accounts for approximately 80% of all nuclear medicine procedures, representing around 30 million examinations worldwide every year, of which about one quarter is located in Europe. ^{99}Mo is generally produced by fission of ^{235}U with thermal neutrons irradiating ^{235}U enriched uranium targets in a high neutron flux reactor. The production of ^{99}Mo in this way is very effective due to the high fission cross section of ^{235}U of 585 barn for thermal neutrons and the high cumulative fission yield of ^{99}Mo (6.1%). At current about 26.000 6-day Ci per week of ^{99}Mo are shipped out worldwide by about 11 reactors [194].

Accelerator based neutron sources represent an alternative to reactor sources in particular for the production of ^{99m}Tc via its precursor ^{99}Mo [195,196]. Here ^{99}Mo is produced based on the neutron capture reaction $^{98}\mathrm{Mo}(n,\gamma)^{99}\mathrm{Mo}$ by irradiating natural (the isotopic abundance of ^{98}Mo is 24.2%) or ^{98}Mo enriched molybdenum samples. In this process, highest epithermal neutron flux at the position of irradiation of the sample is required to achieve a usable ^{99}Mo activity. Compared to the uranium fission approach, the neutron capture method has the advantage to simplify the processing scheme and reduce the waste stream.

Another increasingly used medical radioisotope used in targeted radionuclide therapy for treating neuroendocrine tumors and prostate cancer is ^{177}Lu. ^{177}Lu can be produced either directly by irradiation of ^{176}Lu or indirectly by irradiation of ^{176}Yb. The irradiation of ^{176}Lu leads directly to ^{177}Lu, while irradiation of ^{176}Yb will lead to the production of the short-lived intermediate radioisotope ^{177}Yb, which decays to ^{177}Lu. It has a half-life of 6.7 days and is compatible with various targeting agents, ranging from short peptides to large biomolecules. Mainly produced in reactor facilities it is currently the most commonly used isotope for targeted radionuclide therapy.

Radioisotopes are also used in a wide range of industrial applications as on-line analytic with ^{241}Am, ^{252}Cf and ^{63}Ni, pollution measurement, home-land security, smoke detectors, irradiation and radiation processing with ^{60}Co for sterilization of medical supplies, pharmaceuticals or food packages, radioactive tracers and non destructive testing.

Radioisotope production usually requires relatively large volumes of high thermal neutron flux, such as those found in the thermal moderators of research reactors.

5.5. Irradiation

Radiation tolerance is strategic for many applications of electronics [197]: Space applications [198], aircrafts [199], High Energy Physics (HEP) [200], nuclear reactors [201], nuclear medicine [202]. The need to test commercial industrial products against neutrons is a growing issue that goes far beyond applications in extreme environments. This applies to avionics as well as commercial electronics used in everyday applications, as the terrestrial environment is far from radiation-free [203].

Radiobiological effects are of paramount importance for determining the impact of radiation on living organisms and for the development of effective radiation protection strategies [204]. The relevant data are derived either directly from dedicated measurements of biological samples subjected to neutron irradiation or from the effects observed in the human population following the atomic bombs detonated at Hiroshima and Nagasaki. The response to high-energy neutrons can be a valuable means of acquiring insight into the mechanism of DNA mutations. Advanced techniques have been developed for the observation of DNA damage and repair mechanisms [205]. Also the irradiation of cells and embryo for determining the Relative Biological Effectiveness (RBE) of high energy neutrons has been done [206] or for radiobiological studies at a cold neutron beam [207]. The impact of neutron irradiation of food resources is a significant consideration for astronauts at the International Space Station (ISS), as well as for those engaged in potential future space travel to the Moon or Mars. It is also a crucial factor in the development of neutron scanning techniques for security applications. The process of neutron capture has the potential to cause food activation or a modification of the oxidation state of proteins and lipids, which could subsequently alter the food intake and its compatibility for the human body [208–210].

Dedicated target station have been realized at CANS facilities where it has been shown that with the proper choice of target material combinations, the spectrum of high energy neutrons from cosmic ray air showers can be closely approximated [211].

Another important application of irradiation with neutrons is Neutron Transmutation Doping (NTD) of e.g. pure silicon. Due to neutron capture and a following β^- decay of the neutron rich silicon into phosphorus, n-type bulk doping can be achieved. Such highly doped silicon is then used for high-power electronics as well as for semiconductor detectors. NTD, in comparison to other methods, has the advantage of a highly homogeneous and uniform doping [212]. Typically, the NTD is done at research reactors close to the reactor core where a high neutron flux is present [8,213].

5.6. Boron neutron capture therapy

In the late 1930s Boron Neutron Capture Therapy (BNCT) was proposed as a potential method for cancer therapy. Based on the property of the isotope ^{10}B to capture thermal neutrons with high probability (high effective cross-section: 3835 barn), decaying into a He and a Li nucleus by the capture reaction $^{10}B(n,\alpha)^{7}Li$, BNCT is a precise targeted therapy concept. The $^{10}B(n,\alpha)^{7}Li$ reaction produces two particles with high biological effectiveness in killing cells and with a short range in tissues (about the diameter of a cell). If such reactions can be selectively triggered in tumor cells, a "cell-surgery" results: single tumor cells invading normal tissues are destroyed without damaging surrounding healthy structures [214]. BNCT has the potential to overcome radiation resistance in certain tumors or to re-irradiate local recurrences after high-dose radiotherapy.

Initially BNCT was evaluated clinically in the 1950s, and since significant progress has been made through a wide range of clinical and non-clinical research efforts [215]. Despite the potential, BNCT has not become a standard method for radiotherapy yet, mainly because BNCT required a research reactor for the supply with neutrons, which is mostly located far from a hospital and not always available for patient care. Recently this situation is changing with the advent of accelerator-based neutron sources [216]. First projects have started at hospitals in Japan [217] and Finland [215]; similar projects are underway in other countries [218].

5.7. Activation analysis

Prompt Gamma Neutron Activation Analysis (PGNAA), also called Neutron-induced Prompt Gamma-ray Analysis (PGA), is a non-destructive analytical tool that can be used to determine the elemental composition of samples or items of diverse origins. The technique is based on the detection of isotope-specific prompt gamma rays, which are induced by the capture of cold or thermal neutrons by atomic nuclei ((n, γ)-reaction). PGNAA allows a panoramic analysis, since all elements, excepted helium, emit prompt gamma rays. It is particularly useful for the accurate detection of light elements, for which only few nondestructive analytical techniques are available. PGNAA is an unique method to determine hydrogen in any kind of samples with a detection limit at ppm level or below and, at the same time, to provide the elemental content of the investigated sample. PGNAA may be used for in-situ investigation of chemical processes like catalytic reactions. Large objects may be investigated to some extent by PGNAA using cold or thermal neutron beams. However, due to their high penetration depth, fast neutrons are a better choice for the bulk analysis of large and thick objects. Pulsed sources offer the possibility of depth-resolved determination of elemental composition. Development is underway to combine activation analysis with imaging techniques, which could lead to efficient element-specific neutron tomography. Applications of PGNAA cover a wide range of disciplines [219,220] such as nuclear physics, material science, geochemistry, mineralogy, petrology, chemistry, environmental science, agriculture, food analysis, biology, medicine, forensic, archaeology, cultural heritage, cosmochemistry and other areas including specific industrial issues.

6. Large scale facilities for research with neutrons based on fission and spallation

While the main nuclear processes for neutron release from nuclei and essential aspects of the techniques used to tailor spectra and time structure have been discussed in Sections 3 and 4, we now turn to the actual technical realization of neutron sources, taking into account the specifications derived from the applications presented in Section 5. In the present chapter, as mentioned in the introduction, we will only sketch the known technologies of research reactors and spallation neutron sources and give a brief overview of existing and planned facilities. The following Section 7 is dedicated to a novel approach for future facilities, which is the main focus of this review.

6.1. Research reactors

6.1.1. Basics and realization

Fig. 6.1 shows a schematic cross section through the pool of the FRM II research reactor in Garching, close to Munich, Germany. The FRM II [221,222] became critical in 2004 and is one of the most powerful and advanced research reactors worldwide with a high thermal neutron flux of 8×10^{14} n/cm^2 s. The figure shows the main components of such a facility. We take the example of FRM II to explain the function of the various components in general terms.

- Fuel element: This is the core of the neutron source, where the fission process takes place. While most research reactors feature an arrangement of several fuel elements, the high flux sources like FRM II, or the High Flux Reactor (HFR) of the Institute Laue-Langevin (ILL) in Grenoble, France, have just one fuel element. Thus they are examples of "compact core reactors". The challenge is to dissipate the heat produced during the fission process in the fuel element. The thermal power amounts to 20 MW and 58.3 MW for the FRM II and HFR, respectively. The fuel element of these high flux sources consists of two coaxial cylindrical tubes with a length of more than 1 m (70 cm active zone for FRM II), between which fuel plates are arranged. The outer diameter of the FRM II fuel element is only 24 cm. Both mentioned reactors use highly enriched (>90%) uranium ^{235}U (8 kg for the FRM II) in the form of U_3Si_2, but are in the process of converting to lower enrichment [223].
- Cooling circuits: For cooling, light water is pumped through the central core channel, which separates the light water of the primary cooling circuit (down flow) from the surrounding pool water and the heavy water moderator tank. The cooling water flows through the fuel element at high velocity (several 100 l/s). For the FRM II, the water flow rate of 300 l/s (17.5 m/s) ensures that its temperature only rises from 36 °C to a maximum of approximately 51 °C. In total, there are three hydraulically

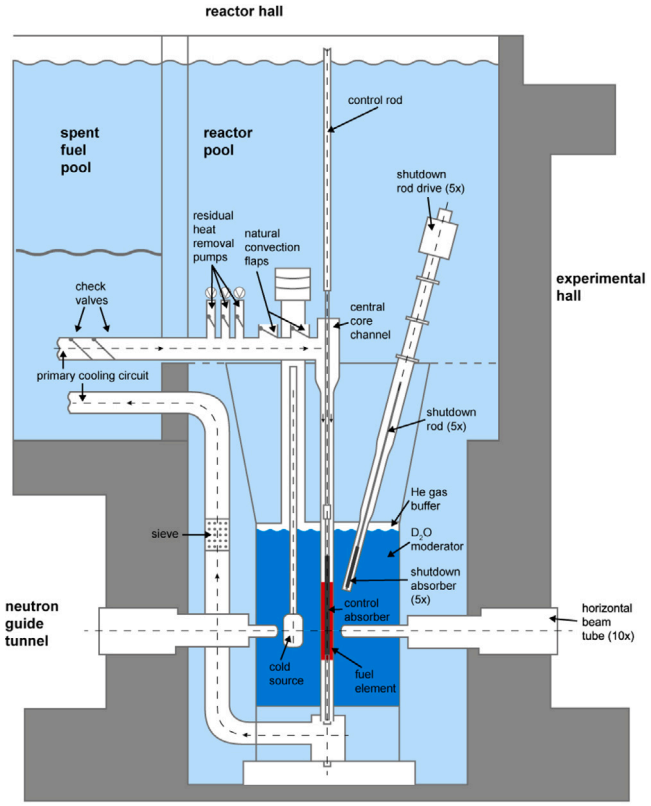

Fig. 6.1. Section of the reactor and spent fuel pool of the FRM II reactor in Garching, Germany. Copyright: FRM II/TUM. *Source:* Reproduced from [221] with kind permission.

separated cooling circuits in FRM II. They are thermally connected by heat exchangers. The primary cooling circuit pumps water through the fuel element and is equipped with several pumps (4 in the case of FRM II). The secondary cooling circuit connects the primary and ternary cooling circuits. In the latter, heat is dissipated to the environment by evaporation through cooling towers.

- Control rod: The chain reaction is characterized by the neutron multiplication factor k, which is defined as the ratio of the number of neutrons in one generation to the number in the preceding generation. Under normal operation conditions, the reactions proceed at a steady rate and the reactor is said to be critical, i.e. k is exactly unity and a nuclear chain reaction is self-sustaining with zero reactivity. A rod made of neutron absorbing material, so-called "neutron poison", which can mechanically be moved, is used to control k and the reactor power. Such mechanical control is made possible through the existence of delayed neutrons, which are emitted after the actual fission process on a timescale comparable to the times needed for the mechanical movement of the rod. In the FRM II reactor a single hafnium (Hf) rod, which moves within the inner tube of the fuel element, is used as control rod. The control rod is also able to shut down the reactor.
- Shutdown drive: Additional neutron-absorbing rods (five Hf rods for FRM II), which can serve as an additional shutdown system, are arranged around the fuel element or fuel element assemblies. Under normal operating conditions, they are completely withdrawn from the reactor core, but can be rapidly brought close to the fuel elements to suppress the chain reaction and shut down the reactor.
- Thermal moderator: The fuel element is located in the central core channel in the center of the thermal moderator. The moderator tank of FRM II has a cylindrical shape with a diameter of 2.5 m and a height of 2.5 m. It is filled with heavy water (D_2O), which also serves as a reflector of thermal neutrons back into the fuel element to sustain the chain reaction. Compared to light water H_2O, D_2O as a thermal moderator has the advantage of being less neutron absorbing, see Table 4.1. Thus a high steady flux of thermal neutrons can build up in a large volume, which is advantageous for the installation of irradiation facilities and secondary sources. Within the thermal moderator and the central core channel, the neutron flux is not homogeneous, but has a distribution due to the different installations with a maximum flux of 8×10^{14} n/cm^2 s [223,224].
- Secondary sources: In order to shift the spectrum to longer or shorter wavelength, cold and hot sources are located within the thermal moderator [225,226]. At FRM II the cold source is located close to the thermal flux maximum. It is filled with about 12 l of liquid D_2 at 25 K. The power of 4.5 kW developed by the nuclear heating is evacuated by a two-phase thermal siphon. A refrigerator outside the reactor pool provides the cooling power to maintain the required low temperature. The hot source

Table 6.1
Main parameters of major neutron facilities based on fission and spallation. While reactors are typically continuous sources, the majority of spallation sources are operated in pulsed mode. Notable exceptions to this are the pulsed reactor IBR-2 and the continuous spallation source SINQ.

Facility	Location	Start operation	Thermal power [MW]	Thermal Flux n/cm^2/s	Instruments	Reference
Reactor sources						
NPI	Řež (CZ)	1957	10	1×10^{14}	8	[230]
BNC	Budapest (HU)	1959	10	2.1×10^{14}	15	[230]
RID	Delft (NL)	1962	2	3×10^{12}	9	[230]
ATI	Vienna (AT)	1962	0.25	5×10^{12}	5	[230]
JRR-3	Tokai (JP)	1962	20	2×10^{14}	22	[231]
HFIR	Oak Ridge (US)	1965	85	2.3×10^{15}	12	[232]
NCNR	Gaithersburg (US)	1967	20	5×10^{14}	30	[233]
ILL	Grenoble (FR)	1971	58	1.5×10^{15}	42	[230]
MARIA	Swierk (PL)	1974	30	1×10^{14}	6	[230]
IBR-2	Dubna (RU)	1984	2	1×10^{16}[a]	14	[229]
MLZ	Munich (DE)	2005	20	8×10^{14}	35	[230]
CARR	Beijing (CN)	2005	60	8×10^{14}	8	[234]
ANSTO	Sydney (AU)	2007	20	4×10^{14}	15	[235]
Spallation sources						
ISIS	Didcot (GB)	1985	0.16	4.5×10^{15}[a]	35	[230]
SINQ	Villingen (CH)	1996	1	4.1×10^{14}	17	[230]
SNS	Oak Ridge (US)	2006	1.4	2.1×10^{16}[a]	20	[236]
J-PARC	Tokai (JP)	2008	1	1.5×10^{17}[a]	13	[237]
CSNS	Dongguan (CN)	2018	0.14	2×10^{16}[a]	3	[238]
ESS	Lund (SE)	2026	5	4×10^{16}[a]	22	[239]

[a] For pulsed sources, the peak flux is given.

consists of a thermally insulated graphite block, heated by gamma radiation from the reactor to a temperature of 2000 °C. The cold, thermal and hot neutron spectra of FRM II are plotted in Fig. 4.3.

- Reactor pool and spend fuel pool: The reactor core, moderator and other installations are immersed in an open pool, which in the case of FRM II is filled with 700 cubic meters of highly purified light water. The water acts as an additional reflector, moderator and coolant, but mainly as a radiation shield that allows technicians to work from above. Adjacent to the reactor pool is a pool for spend fuel elements, where they can be stored until they cool down.
- Biological shielding and beam tubes: A biological shielding made of heavy concrete surrounds the neutron source. At FRM II, the outer concrete wall is 1.8 m thick and protects the reactor against conceivable impacts from outside, including an airplane crash. Neutrons are being extracted through evacuated beam tubes pointing toward the respective secondary source, see Fig. 4.2, and guided to the instruments in neutron guide systems, see Fig. 4.7.

The FRM II was used as an example because it is a state-of-the-art research reactor with a compact core. Most research reactors are open pool reactors and have similar components, but often have an array of fuel assemblies instead of a single compact fuel element and correspondingly multiple control rods. Different reflectors and moderators are also used, but the principle remains the same. It is beyond the scope of this review to give an overview of all existing realizations and we refer to the Research Reactor Database of the International Atomic Energy Agency IAEA [227]. Well-known user facilities are presented in the next section of this chapter. However, while the example of FRM II provides a good overview of components and installations for steady-state research reactors, it must be mentioned that there are also pulsed reactors, such as the so-called TRIGA reactor type. TRIGA is an acronym for "Training, Research, Isotopes, General Atomics". It is a swimming pool reactor that uses uranium zirconium hydride (UZrH) fuel. This fuel has a large, prompt negative fuel temperature coefficient of reactivity, so that reactivity decreases rapidly as the core temperature increases. This inherent safety feature allows pulsed operation with automatic shutdown up to a power of 22,000 MW [228]. Another approach to pulsed reactor operation is realized at the IBR-2 reactor of the Frank Laboratory of Neutron Physics in Dubna, Russia [229]. It is based on mechanical reactivity modulation by a movable reflector.

6.1.2. Existing facilities and projects

The majority of research reactors have been constructed decades ago (Table 6.1). Of those still in operation in Europe the HFR reactor at the ILL in Grenoble, France, build in the late 1960s, serves the flagship facility for neutron science in Europe and indeed has been the leading neutron facility in the world until today [240,241]. Neutrons were first produced in 1971 and the facility, with almost 40 instruments in operation, is supported by 14 member countries.

In the late 1990s the only new research reactor in Europe, the FRM II reactor at the Heinz Maier-Leibnitz Zentrum in Garching, close to Munich, Germany, replaced the small FRM I facility and since 2004 is the second most powerful reactor based neutron source in Europe with nearly 30 instrument in operation [242].

Other national reactor-based neutron facilities in Europe that are currently operational include the Budapest Neutron Centre (BNC) in Hungary [243] and the Nuclear Physics Laboratory (NPL) in the Czech Republic [244]. They operate, respectively, 12 and seven instruments that are available to neutron users in Europe. The reactor at the National Centre for Nuclear Research (MARIA) in

Poland [245] and the reactor at the Reactor Institute Delft (RID) in The Netherlands, the TRIGA reactors at the Johannes Gutenberg-Universität Mainz (TRIGA JGU) in Germany [246], at the TU Wien Atominstitut (ATI) in Austria [247], and at the Jožef Stefan Institute (JSI) in Ljubljana, Slovenia [248], complete the ecosystem and complement the instruments available to neutron users in Europe.

Both flagship and large national facilities also exist in the United States. The Oak Ridge National Laboratory (ORNL) hosts the High Flux Isotope Reactor (HFIR) [249], the most powerful reactor-based source of neutrons in the US. A range of world-class capabilities are provided at the National Institute of Standards and Technology's (NIST) reactor-based source, the NIST Center for Neutron Research (NCNR) [250]. Both facilities started operation in the 1960s. The NIST Center for Neutron Research has a project on the level of a pre-conceptual design for a reactor, the NIST Neutron Source (NNS), to replace the National Bureau of Standards Reactor (NBSR) [108].

In Asia, Japan hosts the Japan Research Reactor (JRR-3) [251]. Since 1995 South Korea has operated a multi-purpose research reactor, HANARO at Daejeon [252], equipped with 15 instruments for neutron science. In China neutron research, supported by significant investment, is now increasing accordingly. Capacity is provided using the research reactor by the China Advanced Research Reactor (CARR) in Beijing [253] which started operation in 2004 [254] and the China Mianyang Research Reactor (CMRR) [255]. The Australian Nuclear Science and Technology Organization (ANSTO) hosts the Open Pool Australian Lightwater (OPAL) reactor, a large national facility operational since 2007 [256].

In Russia, neutron research is supported by two national facilities: the IBR-2 pulsed reactor in operation at the Joint Institute for Nuclear Research (JINR) [257], recently refurbished [258], and the PIK reactor at the St Petersburg Nuclear Physics Institute [259]. A few smaller reactor facilities exist further as the IR-8 research reactor in Moscow [260].

A new neutron multi-purpose research reactor is currently under construction in Argentina [261].

6.2. Spallation neutron sources

6.2.1. Basics and realization

As in the case of research reactors, we will discuss the basic elements of spallation neutron sources using the example of modern, powerful and advanced facilities. Worldwide, there are three user facilities with pulsed spallation neutron sources in the MW power class: The Spallation Neutron Source (SNS) in Oak Ridge, USA [262,263], the Japan Spallation Neutron Source (JSNS) at J-PARC, Japan [237,264,265], and the European Spallation Source (ESS) in Lund, Sweden [120,266]. The ESS is under construction and about to become operational. The SNS was completed in 2006. A second target station for the SNS is currently under development at the Oak Ridge National Laboratory (ORNL) [267]. In this section, the ESS and SNS will serve as examples for state-of-the-art long-pulse and short pulse spallation sources, respectively. The technology of such MW-class spallation neutron sources is extremely demanding. However, details of the design are beyond the scope of this article, and only a very general overview of the main components will be presented, as was done for the research reactors. Design details can be found in the bi-annual proceedings of the International Collaboration on Advanced Neutron Sources (ICANS). The following Section 6.2.2 gives an overview of existing user facilities and projects.

Conceptually, a spallation neutron source consists of the following main components, see Fig. 6.2:

- Ion source and LEBT: The ion source provides a high ion current (e.g. about 70 mA at 75 keV for ESS) with a low emittance that is compatible with the Low Energy Beam Transport (LEBT). The LEBT provides beam matching from the ion source to the Radio Frequency Quadrupole (RFQ) and contains diagnostic systems. Typically, hydrogen ions are used, either negatively charged H^- or positively charged $p = H^+$ ions, while other charge states are filtered out. H^- ions are used at short pulse sources to feed the proton accumulator ring (see below), while long pulse sources start directly with protons $p = H^+$. A chopper system determines the pulse length delivered to the LINAC. The SNS as a short pulse source has a pulse length of about 1 μs (650 ns flat top) at a repetition rate of 60 Hz, while the ESS as a typical long pulse source has a pulse length of about 3 ms (2.86 ms flat top) at a repetition rate of 14 Hz.
- LINAC: The LINear ACcelerator provides the acceleration of the ion beam to the desired energy above the spallation threshold. For shielding purposes, it is typically located in a tunnel underground with a klystron gallery above providing the required electrical power. The LINAC consists of a Radio Frequency Quadrupole (RFQ) providing the acceleration up to a beam energy of a few MeV followed by a Medium Energy Beam Transport (MEBT) section that steers the beam into the normal-conducting accelerator Drift-Tube Linac (DTL) structures that accelerate the beam to about 200 MeV. Above this energy it is advantageous to use superconducting cavities to reach the final energy of 1 to 2 GeV. Superconducting niobium cavities are used, cooled with liquid helium to an operating temperature of 2 K. Finally, the beam is transported to the proton accumulator ring or directly to the target, for SNS and ESS, respectively, by a High Energy Beam Transport section (HEBT). The final component of the HEBT is a beam rastering system that spreads the beam to a quasi-rectangular profile before hitting the target.
- Proton accumulator ring: This component is typical for short pulse spallation sources. It bunches and intensifies the ion beam for delivery onto the target. The H^- pulse from LINAC is injected into the ring through a stripper foil, which strips electrons from the negatively charged hydrogen ions. The H^- ions bend in the opposite direction to the H^+ ions in the magnetic field, allowing the protons H^+ to circulate in the ring and the charge to accumulate over typically more than 1000 revolutions. Sharp bunches of protons are kicked-out of the ring and directed to the target by the HEBT.

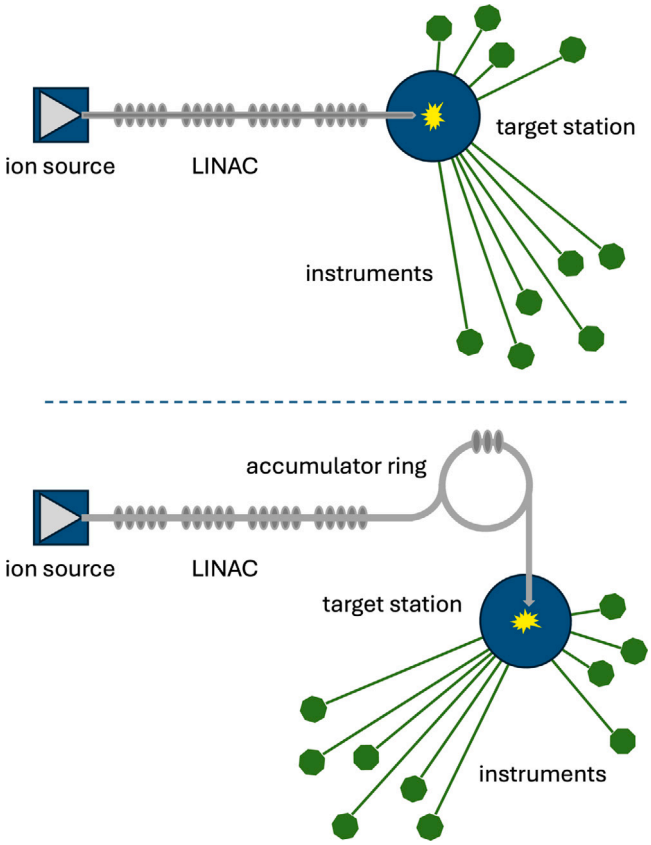

Fig. 6.2. Schematics of a long pulse (top) and short pulse spallation (bottom) neutron source based on linear accelerators.

- Target and target station: The target is the heart of the spallation source, where intense neutron pulses are produced by the nuclear spallation process when high-energy protons collide with heavy metal targets. The challenge for the target design is to remove the high thermal load deposited by the proton beam in a small volume (order of 10^{-3} m^3). The SNS operates with an average proton beam power of 1.4 MW, which is currently being upgraded to 2.8 MW. The ESS is designed for an average power of 5 MW, but will initially operate at 2 MW. Some of the proton beam power goes into the release of the neutrons, but most of the beam power is deposited as heat in the target and surrounding structures. The target design differs significantly for short pulse and long pulse MW spallation sources.
  SNS [268] and JSNS [269] use a mercury target: at SNS, approximately 50 tons of liquid mercury circulates in a steel structure containing the mercury process loop and having a long "nose" of rectangular cross-section facing the proton beam channel. Cooling is provided by a mercury/water heat exchanger located in the mercury process loop at a distance from the target. Embrittlement due to radiation damage at the proton beam entrance window and possible cavitation due to pressure waves during pulses are design challenges and limit the lifetime of the target, which has to be replaced periodically. Therefore, the target monolith is designed so that the target can be replaced without removing the moderator–reflector assemblies.
  The ESS [270] as a long pulse source uses a target wheel inside the target monolith. The monolith is a large structure of about 3000 tons of steel shielding. The target wheel has a diameter of 2.5 m and rotates at 0.5 Hz to distribute the heat generated by the incoming protons. It consists of 36 sectors containing tungsten (W) bricks cooled by a stream of pressurized helium (He) gas. The W bricks rest on the rotating steel cassette and are distributed in a cross-flow configuration. An advantage of this design over the liquid mercury target of the SNS or JSNS is that it does not need to be replaced as often, with an estimated lifetime at full power of 5 years.
- Moderator and reflector: Moderators can be placed above and below the spallation target. Again, specifications are very different for short pulse and long pulse sources:
  SNS [271] uses heavy water cooled reflector plugs, made of beryllium inside stainless steel housing. The steel has a dual function, as a reflector and as shielding. The reflectors have the function of scattering neutrons that have bypassed or escaped the moderator back into the moderators, giving them another chance to be redirected to the extraction channels. Four moderator vessels are embedded in the moderator plugs, two above and two below the target: one ambient decoupled and poisoned light water moderator, two coupled supercritical hydrogen (H_2) moderators, and one decoupled and poisoned supercritical hydrogen moderator. The H_2 moderators are operated at 20 K. In order to maintain the short pulse characteristics

of the source, the moderator can be decoupled from the reflector by cadmium sheets, which absorb the long tail of low energy neutrons while allowing the higher energy neutrons to pass. Gadolinium (Gd) plates are used as a poison to further shorten the pulse.

ESS [110,272] as a long pulse source uses a completely different approach for reflectors and moderators. For the long ms pulses, the neutron storage time in the reflector and moderator in the order of 100 μs is not important. Therefore, beryllium with its rather long neutron storage times is the material of choice for the reflector and there is no need for decoupling. At the moment, only one moderator above the target is planned for the ESS, which serves all the initial instruments. This leaves attractive possibilities for future developments. The configuration above the target consists of a thin light water pre-moderator, followed by the butterfly-shaped moderator to which all instruments are pointed, followed by a Be-reflector above. The pre-moderator is thin enough so that light water as highly efficient thermal moderator can be used despite its neutron absorption. The flat butterfly moderator with a height of 3 cm follows the idea of a low dimensional moderator to maximize moderator brilliance [109]. The cold moderator uses para-hydrogen at an average temperature of 18.5 K. It is surrounded by thermal light water channels to provide both cold and thermal and even bispectral beam extraction capabilities.

- Beam extraction and transport system: The beam extraction must be optimized so that each instrument extracts the optimal amount of phase space and the beam transport to the instruments is optimized using Liouville's theorem, which states that for conservative lossless optics the phase space density along the trajectories of the system is constant. With modern neutron guide systems, a brilliance transfer of more than 80% for cold neutrons is achievable even over long distances. For the ESS, a detailed study of the beam extraction system, taking into account the initial instrumentation, has been performed [114]. A compromise was found taking into account that (i) for space reasons the instruments are 6° apart; (ii) the butterfly moderator allows each instrument to extract the appropriate spectrum of neutrons by pointing either at the thermal or cold part of the moderator, or even to receive neutrons from the cold and thermal parts simultaneously, the so-called bispectral beam extraction (iii) while the butterfly moderator has a high brilliance, the beam extraction efficiency suffers when the source is reduced to a size similar to or smaller than the opening of the neutron guide, and (iv) in order to minimize the technical risks associated with the thermal load and radiation damage to the beam optics, the neutron guides start at a distance of 2 m from the moderator center.

  A challenge in the beam transport system is the fact that during the spallation process very high energetic particles up to the incident proton energy are produced, which can lead to a high background. So-called T0 choppers, heavy rotating shielding drums that are closed during the initial proton pulse, are used at short pulse sources to suppress this background, while at ESS neutron guide systems are usually used that deviate the beam path twice from the line of sight. Nevertheless, heavy concrete shielding, much thicker than in research reactors, is required along the entire beam transport system.
- Instrument performance: While spallation is a very efficient process for releasing neutrons from nuclei, the ability to remove heat from the target is the limiting factor for the performance of the source, as is core cooling in the case of fission neutron sources. Today's technology makes it possible to build neutron spallation sources in the MW power range, with average fluxes similar to those of high flux research reactors. However, for pulsed spallation sources, the neutron flux pulse height can be several decades higher than the average neutron flux. When comparing the performance of similar optimally designed instruments between these types of sources, the gain factor for instruments at spallation sources is given by the ratio of pulse height to average flux, as long as the instrument is able to fully exploit the time-of-flight method at neutron spallation sources [273].

6.2.2. Existing facilities and projects

First accelerator based spallation neutron sources were developed in the US and in Japan in the late 1970s (Table 6.1). The first project was the Intense Pulse Neutron Source (IPNS) at Argonne National Laboratory [274] followed by the KEK pulsed neutron source in Japan [69,275]. Both facilities are no longer in operation due to the construction of more powerful neutron spallation sources in both countries.

In England and in Switzerland decommissioned research reactors have been replaced by accelerator driven spallation neutron sources. The spallation source ISIS in the UK came into operation in 1984 with the first target station and 20 beam lines and an additional muon source [276]. The Swiss Spallation Neutron Source (SINQ) [277,278] was established in the late 1990s at the Paul Scherrer Institut. It operates more as 20 instruments, a dedicated ultra cold neutron source and a muon source. Each of these facilities have a significant international user base and are major contributors to neutron science, not just in their countries but across Europe and beyond.

The Spallation Neutron Source (SNS) at Oak Ridge in the US is currently the most intense accelerator-based source in the world [262]. It started operation in 2006 and hosts currently 20 instruments. It is planned to build a second target station within the next decade to increase the scientific capabilities further [263].

The Japan Proton Accelerator Research Complex (J-PARC) is one of the pioneers in accelerator-based neutron sources [237,264] and J-PARC, when operating at full design power, will be the neutron source with the brightest neutron beams in the world currently.

Recently the China Spallation Neutron Source (CSNS) started operation in 2018 in Dongguan, Guangdong province [238,279] with an instrument suite that is rapidly expanding.

The most ambitious project is the European Spallation Source (ESS) currently under construction in Lund, Sweden, and scheduled to begin operation in 2026 [120,280]. ESS will be the future international flagship facility in Europe with the potential to become a leading neutron facility in the world.

7. Low energy accelerator-driven neutron sources

Research reactors are very efficient neutron sources in terms of source strength: high flux reactors have a source strength of the order of 10^{17} to 10^{18} n/s, i.e. 10^{17} to 10^{18} neutrons are released per second in the reactor core. This leads to high neutron fluxes on the order of 10^{15} n/cm^2 s in large volume thermal moderators. Many important applications benefit from such high fluxes and the available space, such as the production of certain radioisotopes for medicine and technology, or irradiation studies.

MW spallation sources can reach similarly high levels of source strength. However, they do not have as large a volume of moderators and are therefore less suitable for irradiation, but are excellent for applications where the high peak fluxes can be fully exploited.

However, as detailed in Section 5, some of the most widely used applications of free neutrons, especially in research, are scattering, imaging and analytical experiments at beamlines. After adjusting the spectrum, collimation and time structure, see Section 4, typical scattering instruments at these facilities have a neutron flux of some 10^6 n/cm^2 s to 10^{10} n/cm^2 s at the sample position, i.e. by far most of the neutrons end up in the biological shielding and produce background radiation. This is a particular problem for spallation neutron sources, which produce very high energy particles that are difficult to shield. It is therefore reasonable to ask whether fission and spallation neutron sources could not be complemented for the applications mentioned above by sources with lower source strength but higher efficiency in the use of the neutrons produced. Such sources would obviously result in lower installation and operation costs for the same performance and have certain advantages, e.g. in terms of background levels, ease of operation, generation of activated materials, etc. As discussed in Section 4, for beam applications, the brightness of the source is a decisive quality criterion, and not only the flux in the moderator.

In Europe, many research reactors, which have been the basis of the neutron ecosystem since the 1960s, have been permanently shut down in recent years. This fact, together with the arguments presented above, has triggered the search for more efficient neutron sources. If brightness is chosen as the parameter to be maximized and the latest developments in accelerator, target, moderator and beam extraction technologies are applied, simulations show that a new type of neutron facility becomes very competitive for beam line applications, the so-called High Current Accelerator-driven Neutron Sources (HiCANS). These are developed in a joint effort of several European neutron centers and universities within the European Low Energy accelerator-based Neutron facilities Association (ELENA) [11]. To achieve high brightness, these sources (i) use accelerators with very high proton currents, (ii) minimize the neutron loss around the target by maximizing the solid angle covered by the moderator in a compact arrangement, (iii) use highly efficient low-dimensional moderators, and (iv) employ state-of-the-art neutron beam extraction and beam transport schemes. In effect, the source becomes an integral part of every single instrument, avoiding compromises.

In this chapter we review the ongoing projects for HiCANS in Europe. This is done in a similar way as for fission and spallation sources in the Section 6. While none of the pulsed HiCANS has reached the status of an operational facility, the High Brilliance neutron Source (HBS) project in Germany is the most ambitious and advanced. Its Conceptual [119] and Technical Design Report [281–285], has been published, the summary can be found in [285]. Therefore, we will explain the general concept of HiCANS using this facility as an example, and then review the other ongoing projects in Europe.

However, since HiCANS are related to the so-called Compact Accelerator-driven Neutron Sources (CANS), as they use similar basic processes, this chapter starts with a review of existing and planned CANS, in particular the RANS facility at RIKEN in Japan. Although CANS are small neutron sources with limited local and regional impact, they are very important for specialized applications, method development, and user education and training.

The distinction between a CANS and a HiCANS is not entirely clear-cut; however, a useful distinction can be made based on the average power on target. This number incorporates the proton beam current, the duty cycle, and the beam energy. According to this definition, a low-energy accelerator-driven neutron source is classified as a CANS if the average power on target is below 10 kW, and it is designated as a HiCANS if the average power on target is above 10 kW.

7.1. Compact Accelerator-driven Neutron Sources (CANS)

7.1.1. Basics and realization

Compact Accelerator-driven Neutron Sources (CANS) are utilizing low energy nuclear reactions for neutron release as described in Section 3.4. Typical components for CANS include an accelerator system, the target for neutron emission, a moderator/reflector system surrounding the target, as well as the shielding and the instrumentation. Different realizations and projects can be found, including an electron accelerator with a lead target [286], a proton accelerator with a Be target [287–289] and a proton accelerator with a Li target [290]. CANS are operated at a range of power levels, from a few watts to several kilowatts, below the threshold of the average power required for a HiCANS, which is 10 kW. In the following, the individual components of a CANS will be described on the example of one of the leading facilities, the RIKEN Accelerator-driven compact Neutron Source (RANS) [291].

Fig. 7.1 shows the RANS source at RIKEN in Wako near Tokio, Japan, which started operation in 2013 [292]. It uses a 7 MeV proton accelerator for neutron release from a Be target resulting in a source strength of 10^{12} s^{-1}. The principal elements of this source are as follows:

- Ion source: The ion source is responsible for providing the charged particles that are subsequently accelerated. At RANS, a duo-plasma ion source is employed, whereby a plasma is generated through the interaction of an inserted gas, such as hydrogen, with free electrons released from a cathode filament. Subsequently, the ionized hydrogen atoms are accelerated with a series of extraction electrodes, which also trap the electrons. Another frequently utilized ion source is the electron cyclotron resonance (ECR), which functions without a cathode and thus exhibits a superior lifetime.

Fig. 7.1. RANS facility showing relevant components for a CANS: Accelerator, target station, instrumentation.
Source: Copied from [291], under the terms of the Creative Commons Attribution License 4.0.

- LINAC: The proton linear accelerator increases the particle energy to a value of a few MeV. A Radio Frequency Quadrupole (RFQ) accelerates the protons to an energy of around 2.5–3.5 MeV. The final energy can be afterwards adjusted by adding additional Drift Tube Linac (DTL) segments. RANS uses a RFQ as the first accelerating element to an energy of 3.5 MeV and a DTL as the second accelerating element to a final energy of 7 MeV. The accelerator and the target limit the maximum duty cycle to 1.3% and the average current to 100 μA. Following these boundary conditions, the pulse width and the repetition rate can be chosen between 10 μs–180 μs and 20–180 Hz, respectively.
- LEBT and MEBT: Low Energy Beam Transport (LEBT) is required to transport the beam from the ion source to the RFQ at energies around a few keV. Similarly, the Medium Energy Beam Transport (MEBT) transports the beam between the accelerating structures above a few MeV. These sections are also necessary to match the beam properties to the acceptance of the next accelerating structures. The beam is mostly manipulated with quadrupole magnets for focusing and defocusing and dipole magnets for bending. Diagnostic elements such as Beam Position Monitors (BPM) and Fast Current Transformers (FCT) for current measurements are included in these sections.
- RF power supply: The accelerating structures require power supplies that operate at specific radio frequencies. In the case of RANS, the LINAC requires an operating frequency of 425 MHz, which is provided by electron vacuum tubes.
- Target: The release of neutrons from a suitable target by the bombardment of a charged particle beam due to nuclear reactions is energy dependent. A lithium target is typically used at low energies of around 2.5 MeV whereas a beryllium target is used at higher energies. RANS uses a beryllium target with a thickness of about 0.3 mm brazed to a 4.5 mm thick vanadium backing plate [293]. The thicknesses of the beryllium and the vanadium layers are chosen so that most of the protons are deposited in the vanadium layer, reducing blistering [293]. The target of a CANS is relatively thin compared to a spallation target and thus results mostly in a slab geometry for its moderators rather than a wing geometry. In a slab geometry the moderator is placed in direction of the proton beam directly behind the target whereas for a wing geometry the moderator is placed at the side of the target tangential to the proton beam direction [294].
- Moderator/Reflector: RANS uses the slab geometry for its thermal and cryogenic moderators [290]. The thermal moderator is a 2, 4, or 6 cm thick polyethylene (PE) slab. In addition, a decoupled 2 cm thick PE slab covered with 1 cm thick B_4C rubber can be used. After the thin PE slab, a mesitylene moderator can be placed to further reduce the neutron energy to a few meV. The moderators are surrounded by a reflector that scatters escaping fast neutrons back into the moderators. At RANS a graphite reflector is used. Other possibilities are Pb or Be.
- Shielding: Due to the low energy compared to spallation, the shielding around the target and the moderators is very compact. RANS uses layers of lead, borated polyethylene and iron with a total shielding structure size of $1.8 \times 1.8 \times 1.8$ m^3, resulting in approximately 90 cm of effective shielding.
- Beam extraction: Extraction ducts are placed through the shielding structure to allow the neutrons to escape from the inner core. RANS has a main extraction duct with a size of 40×40 cm^2 looking at the thermal PE moderator or the cryogenic mesithylene moderator. Inserts with different hole sizes can be placed in the extraction duct to act as collimators.

RANS was chosen as an example because it uses all relevant components of a CANS, mainly the accelerator for charged particle beam delivery and the target station for neutron release. The biggest difference in the CANS realizations is the particle type, ranging from electrons [90,286], to protons [91,288], to deuterons [295], as this directly influences the accelerator and the target. An overview of various CANS installations is provided in the following section.

7.1.2. Existing facilities and projects

Early CANS facilities became operational in the 1970s (Table 7.1), for example at the Bariloche Atomic Center in Argentina [304] or at Hokkaido University in Japan [286]. These facilities used electron accelerators with reasonable electron energies of 25 MeV and 32.8 MeV and low average beam currents of about 30 μA. Both used water-cooled lead targets for the production of neutrons. The facility at Hokkaido University was used to measure cold neutron spectra of ice, ethane, solid methane, and liquid hydrogen, to evaluate equipment (e.g., scintillation detectors, magnetic lenses) and neutron scattering instrumentation (e.g., small-angle neutron scattering (SANS), imaging) [286]. In recent years, the CANS at Hokkaido University has been upgraded, improving performance

Table 7.1
Main parameters of neutron facilities based on low energy nuclear reactions. A comprehensive overview on most CANS facilities is given in the review article by Andersen et al. [292].

Facility	Location	Start operation	Accelerator power [kW]	Thermal power [kW]	Neutron yield [n/s]	Target stations	Instruments	Reference
CANS								
HUNS	Japan	1973	3.2	3.2	5×10^{12}	2	2	[90]
LENS	USA	2005	32	4	2×10^{13}	2	4	[296,297]
RANS	Japan	2013	0.7	0.7	1×10^{12}	1	1	[91]
FRANZ	Germany	2025	16		1×10^{11}	2		[292]
CPHS	China	2016		2		2		[298]
CPHS upgrade	China	Project status		16	5×10^{13}	2		[299]
HiCANS								
SARAF	Israel	2025	200	200	1.35×10^{15}		3	[300]
ICONE	France	Project status	150	50/100	?	2	10	[301]
ARGITU	Spain	Project status	190	46	2.7×10^{14}	1	3	[302]
HBS	Germany	Project status	1750	100	1×10^{15}	3	25	[303]

by increasing the average current to 100 μA [90]. At the Bariloche facility, intensive work has been done on the determination of the total cross sections of materials as a function of neutron energy by transmission experiments with thermal and subthermal neutrons [304].

In the 1980s, low-energy proton accelerators were introduced for neutron production at CANS. These sources have much better background conditions compared to electron beam driven facilities, which produce massive amounts of bremsstrahlung gamma rays. The Low Energy Neutron Source (LENS) at Indiana University in the USA became operational in 2005, using a 13 MeV proton linac with a peak current of 25 mA and a water-cooled beryllium target. With a maximum power of up to 4 kW on target, the LENS facility was the most powerful CANS until recently [288]. At LENS, a small number of neutron scattering instruments for the study of large scale structure by SANS and SESAME (Spin-Echo Scattering Angle Measurement) are fed by a cryogenic methane moderator. A moderator imaging station has been implemented for moderator studies and testing of various neutron detectors, and a neutron radiation effects facility is also available [296].

At RIKEN in Japan, the RIKEN Accelerator-driven Neutron Source (RANS) specialized for the characterization of industrial products was established in 2013. Using a 7 Mev pulsed proton beam with an average current of maximum 100 μA, thermal and cold neutrons are produced with a water-cooled beryllium target [287]. The mission of the RANS facility is neutron interrogation of manufacturing treatments of metallic and light-element component materials. In addition RANS conducts R&D in fast neutron imaging, detectors, visualization and analysis techniques of nondestructive inspection [290]. In recent years, a second accelerator-driven CANS has been in operation at RIKEN, using a 2.5 MeV proton accelerator with an average current of 100 μA and a solid water-cooled lithium target.

In Japan, in addition to the university and research institution-based CANS, there are also a number of projects in industry for applied research and development such as irradiation of electronic devices or in hospitals for treatment of cancer patients using BNCT. The Japan Collaboration on Accelerator-driven Neutron Sources (JCANS) supports the development of these neutron sources in the country.

A multipurpose CANS has been established at Tsinghua University in Beijing, China for education, instrumentation development, and industrial applications [298]. The Compact Pulsed Hadron Source (CPHS) uses a 3 MeV pulse proton accelerator with a 50 mA ion source.

In recent years, projects for CANS facilities have also started in Europe. In Hungary, the company Mirrotron is building a small 2.5 MeV driven source with a water-cooled lithium target and a 30 mA ion source. The Helmholtz Zentrum Dresden Rossendorf in Dresden, Germany is building a small CANS as an extension of the existing HZDR ion beam center.

A growing number of CANS for Boron Neutron Capture Therapy are under construction, particularly in Asian countries such as Japan, Korea and China. Some projects are also under development in England, Finland and Italy. Other countries, such as Canada, are also developing CANS projects, some of which combine different applications, such as beamline instrumentation for condensed matter research, radioisotope production, and a development station for BNCT.

The Union of Compact Accelerator base Neutron Sources (UCANS) provides regular meetings and conferences for the growing community and provides opportunities for exchange and discussions [305].

7.2. High-Current Accelerator-driven Neutron Sources (HiCANS)

7.2.1. Basics and realization

The concept of a HiCANS is rather new: no pulsed HiCANS facility exists worldwide, but several ongoing projects in Europe [11], through analytical calculations, particle and beam transport simulations and accompanying experiments, have come to the common conclusion that such facilities will be very competitive with existing facilities for beamline applications. Of all the pulsed HiCANS projects, the High Brilliance neutron Source (HBS) project is the most ambitious and advanced. Its conceptual and technical design

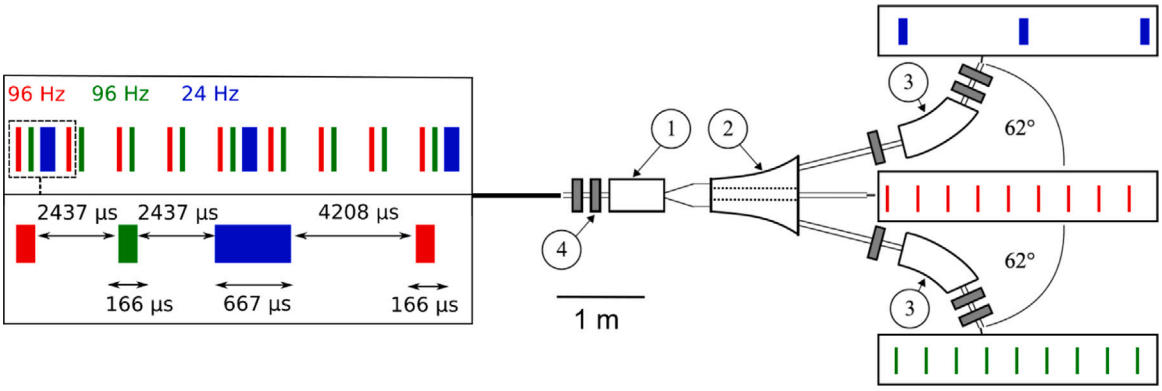

Fig. 7.2. The figure illustrates how an interlaced pulse in LINAC can be used to split the proton beam by a multiplexer unit for delivery to three target stations so that each receives its desired pulse structure. An ExB chopper in the LEBT section of the LINAC is used to generate the imposed interlaced pulse structure in the LINAC. As explained in the text, the encircled numbers in the figure refer to different components of the multiplexer. The figure was inspired by [306].

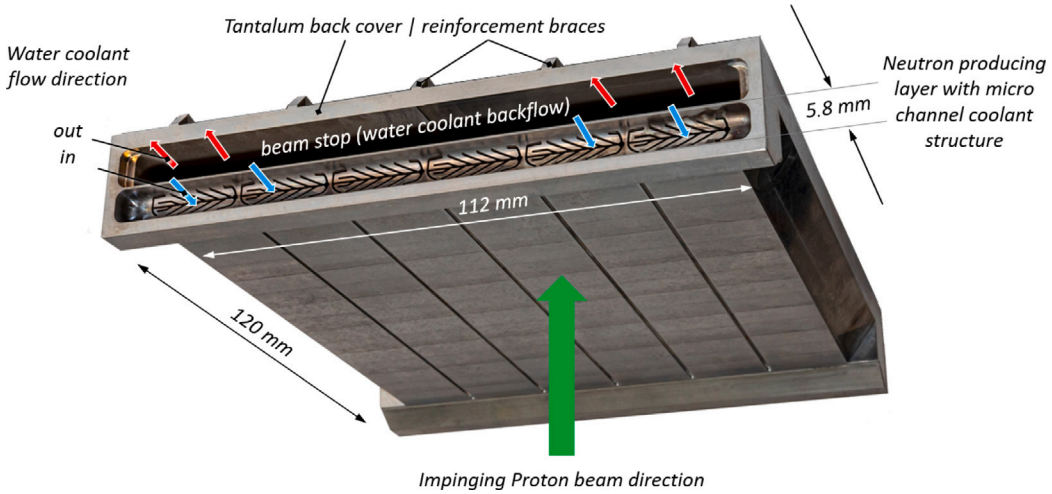

Fig. 7.3. HBS target with internal microchannel cooling structure.
Source: Adapted from [307], under the terms of the Creative Commons Attribution License 4.0.

Fig. 7.4. Moderator plugs for a methane cryogenic moderator with included neutron guide and supply lines.
Source: Copied from [307,308], under the terms of the Creative Commons Attribution License 4.0.

reports (CDR [119] and TDR [281–285]) have been published. The HBS project aims at a facility for neutron scattering, analytics and imaging experiments with a reference suite of 25 instruments at three different target stations. In this section, we follow the approach used for the other types of facilities and select the HBS project as an example to illustrate the main components of a HiCANS. The specifics of the other projects are described in the next Section 7.2.2.

As detailed for the HBS project in the TDR Accelerator [282], Target Station [281], Instrumentation [283] and Infrastructure [284], a HiCANS consists of the following main components:

- Ion source, LEBT and ExB Chopper: In the energy range between 50 and 70 MeV, the neutron yields due to low energy nuclear reactions induced by protons or deuterons are quite similar [86] and from this point of view either particle (p or d) could be chosen. However, a HiCANS with its high current places high demands on the accelerator structure in terms of beam transmission and negligible beam loss due to the high space charge in the charged particle bunches. Therefore, for practical purposes, a proton LINAC is preferred. As for most CANS projects, a continuous ECR source was chosen for the HBS project because of its high reliability, easy availability, low maintenance and high proton fraction. In contrast to a typical CANS, the source provides a high proton current of up to 120 mA, of which 100 mA are used in standard operation. An increase to 200 mA or more is possible. The output energy of the proton is 85 keV entering the LEBT section. The LEBT section matches the beam from the ion source to the RFQ structures, as is also the case for a typical CANS or spallation neutron source. Different beam pulsing schemes will be delivered to the three target stations planned for scattering experiments at the HBS facility. The interlaced pulsing structure will be imposed on the beam in the LEBT section with an ExB chopper [309]. The HBS plans to provide two proton beams with 96 Hz and one with 24 Hz as shown in Fig. 7.2, all with a duty cycle of 1.6%. This corresponds to proton pulse lengths of 166 μs and 667 μs, respectively. The individual bunch trains for the three target stations do not overlap because the frequencies are integer multiples of each other. Each beam delivered to one of the target stations provides a total average beam power of 100 kW.
- LINAC: Like spallation neutron sources and most CANS, the LINAC consists of an RFQ structure and several DTL structures. The RFQ and DTL structures are based on the MYRRHA design [310] which has been successfully tested. This reduces the risk and cost of the HBS project. As for MYRRHA, the radio frequency (RF) for the HBS accelerator is 176.1 MHz. Due to the high proton beam current, the transition energy from the RFQ structure to the DTL section should be between 2 and 3 MeV. At the 176.1 MHz frequency and a chosen transition energy of 2.5 MeV, a single RFQ structure would be very long, making it difficult to produce it with the required precision [311]. It was therefore decided to split the RFQ into two shorter structures of 2.5 m length, each accelerating the protons by about 1.25 MeV. To accelerate the 2.5 MeV proton beam to an energy of 70 MeV, 45 DTL cavities are needed. The second, fifth and eighth sections are rebunchers, resulting in a 66.7 m long DTL section. For reliability reasons, CH-type cavities based on the proven MYRRHA design have been chosen, which are operated at room temperature due to the pulsed high-current proton beam. The choice of normal conducting cavities is based on practicality and arguments for the transition energy from normal conducting to superconducting cavities as a function of duty cycle and beam current. Due to the relatively low operating frequency and high peak power, the accelerator structures are driven by solid-state amplifiers. An additional advantage of these amplifiers is resilience, the possibility of a redundant design and a small footprint. The entire accelerator is designed for a maximum RF duty cycle of 25%, of which only about 8% (3×1.6 + RF overhead) are used for the target stations designed for neutron scattering, analytics and imaging. This allows for future upgrades or other applications such as isotope production or positron source operation.
- Multiplexer and HEBT: The transport of the proton beam from the last DTL to the target stations is performed by the HEBT system using 90° and 45° bending magnets and quadrupole triplets for focusing and defocusing. This section also contains the multiplexer [306], which is used to disentangle the interlaced proton beam and direct it to the different target stations. The schematic principle of the multiplexer is shown in Fig. 7.2. It consists of a small bipolar kicker magnet ① that deflects a specific proton pulse to different field regions of a three-field septum magnet ②. The three fields are an up-field and a down-field at the edges, which further deflect the beam, and a zero-field region in the center, which does not affect the beam. Additional 45° bending magnets ③ further deflect the beam from the outer regions of the septum magnet. Quadrupole magnets ④ in combination with the sector bending dipole magnets serve to realize an achromat for the beamlines. The proton beam can thus be separated into three different directions in a small space of about 5 m.
- Target: To maximize the source strength of a HiCANS operating at 70 MeV, a heavy target material should be selected [86] such as lead, tungsten, or tantalum. Tantalum also has very favorable properties in terms of machinability, thermal conductivity, mechanical stability, etc. An important selection criterion is the response to the high proton current, as it is known that many materials tend to blister [312]. Thus, tantalum was chosen as a target material for HBS because it shows a high blistering threshold with necessary proton fluences above 10^{20} cm^{-2} [313,314] due to its ability to store a high hydrogen fraction (0.79 H/Ta atom) [315]. The lifetime, limited by the damage due to the displacements per atom (DPA) inside the target, can thus be extended to one year [316]. Other solutions for high power targets that are being investigated or have been implemented to prevent blistering and achieve the desired high average power on target, are to operate the target at elevated temperatures to increase the hydrogen diffusion coefficient, as in the ICONE project with a temperature of 550 °C for a beryllium target cooled indirectly by mounting it on a water-cooled copper plate [317], or to use a liquid metal target with a liquid metal cooling circuit, as in the SARAF project with its liquid lithium jet [318].

  As in the case of CANS, and in contrast to spallation neutron sources, the target for a HiCANS is rather thin and thus of small volume. This leads to a high power density in the target which, depending on the operating parameters, cannot be cooled by conventional cooling methods. The HBS project aims to deposit an average power of 100 kW on a surface area of 100 cm^2. The resulting power density of 1 kW/cm^2 is one of the main challenges for a HiCANS with the desired performance level. One method to handle the high power density is the use of microchannel cooling structures with heat removal capacities up to 3.5 kW/cm^2 [319]. The HBS project has developed a target with an internal microchannel cooling structure as shown in Fig. 7.3 with channel widths of 0.35 mm [320]. The resulting high heat transfer coefficient allows a high heat removal capacity, as demonstrated by an electron beam irradiation experiment that achieved deposited power densities of 1.7 kW/cm^2. Since electrons have a small penetration range in tantalum, electron heating occurs only near the surface, in contrast to the volume heating of a proton beam. Thus, a heat removal capacity of 3 kW/cm^2 can be estimated for a proton beam, resulting in a

safety factor of 3 for the reference design.
The final target design is shown in Fig. 7.3. It features a neutron producing layer with the internal microchannel structure and a water beam stop behind it. The proton beam hits the target from below and penetrates the neutron-producing layer with only 4.6% of the protons stopped inside Ta [321], while the remaining 95.4% are stopped in the water beam stop and cannot contribute to blistering effects. Nevertheless, the neutron production is equal to 99% of a thick Ta target. The microchannel and notch structures are designed so that, on average, all protons experience the same stopping power throughout their path in the tantalum layer. This results in homogeneous energy deposition and low temperature induced stresses. This target can be operated for one year at 100 kW average power with a resulting neutron yield of 10^{15} n/s.

- Moderator and reflector: The small size of the target for a HiCANS and the arrangement of the moderator and reflector optimized to cover a large solid angle thus avoiding the loss of neutrons from the target result in a compact Target–Moderator–Reflector (TMR) assembly. The thermal moderator can be placed at a distance of a few centimeters from the target, resulting in a very efficient moderator feeding, which also allows an efficient extraction from the flux maximum. This advantage of a compact TMR unit also requires an efficient and compact confinement of the neutrons inside the TMR unit, which is best realized with hydrogen-rich moderators [322] based on e.g. PE or light water as thermal moderator materials.
  In contrast to CANS with their low operating power, HiCANS as HBS with their high power at the target lead to a not negligible heat deposition in the moderator–reflector structure due to the high radiation fields. For a power deposition of 100 kW at the target, a heat deposition of up to 0.7 W/cm^3 [323] can be expected in the thermal moderator, thus requiring a mechanism for heat removal. Since polyethylene and light water have similar neutronic properties, a simple solution is to use a light water moderator where the water flow acts as a coolant. This also prevents accelerated degradation of a solid thermal moderator due to the high radiation fields in the moderator.
  An efficient reflector increases the thermal neutron flux inside the thermal moderator and thus improves the performance of the instruments. In contrast to the spallation neutron source ESS with its very long proton pulse of 2.86 ms and a full saturation in the TMR unit, which allows to define the neutron pulse length with chopper systems, CANS and HiCANS try to match the proton pulses to the lifetime of the neutrons in the TMR unit in order to realize a high peak flux/resolution ratio and to use the full pulse. The typically used beryllium reflector provides only a small improvement in peak flux under these conditions, with the disadvantage of producing a large neutron pulse tail that significantly increases the background and is undesirable for most instruments. The preferred materials are therefore materials that confine the neutrons more strongly in space and time, such as lead [324].
  The compact TMR unit allows cryogenic moderators to be placed in close proximity to the target within the thermal moderator for efficient feeding of the cold moderator with thermal neutrons. The typical dimensions of the target and the entire TMR unit are similar to the mean free path of cold neutrons in liquid para-hydrogen, which is in the range of 10 cm. This results in a high extractable brightness, especially considering the new development of one dimensional moderators [111,325]. Inside the extraction channels of the TMR unit [323,326] other cryogenic moderators like methane [103], ethane [327] or mesitylene [328] can be placed, which allows a very flexible tailoring of the neutron spectrum to the needs of the instruments [324].
- Target station: The target station consists mainly of (i) a shielding structure to maintain a proper radiation level at the experimental stations, (ii) the TMR unit at its inner core, and (iii) neutron beam extraction ducts [307]. Due to the low energy nuclear reaction of a HiCANS, the neutron energies of about 0.8 MeV for tantalum do not require much shielding. The shielding for the HBS, based on double layers of borated polyethylene for neutron moderation and lead for efficient fast neutron energy reduction due to the Pb$(n, 2n)$ reaction channel, requires a thickness of only about 1.5 m. With the TMR unit included, the target station for the HBS has a diameter of about 4 m, in stark contrast to the dimensions of target stations of spallation neutron sources [329,330]. For the HBS, this allows the placement of instrument components such as choppers or slit systems close to the moderator surface, thus providing more flexibility in instrument design.
  In contrast to CANS, where the proton beam is horizontal, the proton beam at HBS enters the target station vertically from below, similar to SINQ [278]. This leaves a large solid angle available for neutron instrumentation, with each instrument occupying its own neutron beam extraction channel.
- Moderator plug and beam extraction: A paradigm shift took place during the development of HiCANS. Conventionally, a moderator serves many instruments. For HBS, however, the moderators are considered part of the instrument. Thus, they can be optimized together with all instrument components to achieve the best instrument performance. Therefore, the target station and the TMR unit have been designed to accept standard extraction ducts into which the cryogenic moderators can be inserted and pushed from outside the shielding into the thermal moderators. The whole moderator plug as shown in Fig. 7.4 is therefore part of the instrument. It allows replacement of the moderator vessel at its front and the use of different cryogenic moderator materials, e.g. liquid para-hydrogen, methane, mesitylene or any other as desired for the instrument. This enables the vessel dimensions to be optimized for the needs of the instrument, the neutron optics used, and the expected sample size. Neutron guides can be inserted into the moderator plug, extracting a large phase space volume with high divergence, or focusing optics can look directly at the moderator surface without the need for a virtual source further downstream. This offers a unique flexibility that has yet to be fully exploited.
- Instrumentation: In contrast to CANS facilities with only a few neutron scattering instruments [288] or frequent assembly and disassembly of the instruments [286,290], HiCANS, as large scale facilities, aim to provide neutrons for an entire instrument suite with large variety [121]. Due to the possibility to operate multiple target stations, such as two for the ICONE project [301] and three for the HBS project [285], the neutron instruments for scattering, imaging and analytics can be provided with

an optimized proton and thus neutron pulse structure. The optimized pulse structure together with the efficient neutron production, neutron moderation and neutron extraction enables highly competitive instrument performances [121,331–335]. A main advantage of HiCANS is the higher flexibility of the instrument design with specifically optimized instrument moderators for the expected sample size. With new developments in neutron optics such as nested mirrors [132] and Selene optics [336], the emitting moderator surface can be mapped one-to-one to the sample area. This allows the sample size to be reduced and thus the moderator size to benefit from the brightness increase with reduced dimensions [109]. Small sample diameters can be homogeneously illuminated with high flux [337]. Another very important aspect and advantage of HiCANS is the expected improved signal-to-background ratio. While the ability to observe a small signal is proportional to the signal and the inverse of the background level squared, keeping the background low is even more important. This is where HiCANSs excel. Unlike steady-state research reactors, data at pulsed HiCANS are collected when the source is off, eliminating a background source from the environment of the instrument. Compared to spallation sources, the relatively low proton energy of HiCANS means that many background processes have not reached the threshold, and cascades/showers of background introduced by high energy particles are very much suppressed. To achieve a similar low background level for spallation sources a much heavier shielding is required. Thus, HiCANS offers potentially improved conditions to observe small signals due to an excellent signal-to-background ratio.

7.2.2. Existing facilities and projects

A number of projects have been established within the last decade to elucidate the potential of accelerator driven neutron sources driven by high current proton or deuteron accelerators (Table 7.1). The projects can be divided into two main groups: projects using accelerators with high duty cycles up to CW, and projects using pulsed accelerators with comparatively low duty cycles in the single to few percent range. The former are mostly aimed at basic research such as astrophysics, isotope production and non-destructive testing. The latter projects are aimed at neutron scattering experiments and therefore require a pulsed proton beam with low duty cycles to achieve good energy or wavelength resolution. As this review paper mostly aims for neutron sources for large scale user facilities with a strong focus on neutron scattering and analytics, the high duty cycle projects will be described briefly and a larger focus will be given to the other projects with a pulsed proton beam.

At least three projects fall into the first category with high duty cycle accelerators. These projects are the SARAF project [338, 339], the FRANZ project [340] and the SPES project [341]. As the requirements for the neutron beams produced are different, the specific technology choices for accelerators, targets and instrumentation are slightly different from those for neutron scattering projects. The targets must either withstand the very high beam power or produce a well defined energy spectrum. The targets are therefore either based on liquid metal jets, use the microchannel solution described, or have a well defined mixture of target materials. The accelerators for these high duty cycle projects either use a CW cyclotron with currents below 1 mA, have a very low end energy or use a superconducting linear accelerator.

One of the earliest projects is the SARAF project in Israel [338,339]. Here a 5 mA, 40 MeV CW proton/deuteron superconducting linear accelerator will be used for neutron production at a liquid lithium target. The total beam power at SARAF will reach 200 kW thus requiring the liquid target solution and the neutron source strength will be 10^{15} n/s [339]. Phase I of SARAF (SARAF-I, 4 MeV, 2 mA CW protons, 5 MeV 1 mA CW deuterons) is already in operation [342], producing scientific results in astrophysics [343] and exotic radioisotopes. However, because SARAF is designed as a continuous source, it cannot benefit from the higher peak brightness of pulsed sources, limiting its performance for many beamline applications.

The FRANZ project at the Frankfurt University in Germany plans to operate a 2 MeV proton accelerator with a solid lithium target [340] aimed at astrophysical applications. The accelerator is designed to consist of a 200 mA ion source, an RFQ structure for accelerating protons to 0.7 MeV and a single IH cavity DTL structure for reaching the final energy. The RFQ can be operated with up to 50 mA average current. It is planned to impose a very fine pulse structure (maximum repetition rate of 250 kHz and pulse lengths below 1 ns) with an ExB chopper to limit the beam current. The accelerator is in the commissioning phase. The experiments will mainly focus on measurements of differential neutron capture cross sections for the astrophysical s-process in nuclear synthesis.

At INFN-LNL in Legnaro, Italy, the SPES project for a high-current cyclotron with a tunable proton beam energy of 35–70 MeV and 0.20–0.75 mA is under construction [341]. The CW proton beam can be directed to several experimental areas with different objectives. The objective of the SPES Radioactive Ion Beam (RIB) Facility will be to provide high intensity and high quality beams of neutron-rich nuclei for nuclear physics research, and thus has a very different focus from the other projects.

The projects ARGITU, ICONE and HBS, which aim to provide pulsed neutron beams for scattering or analytical instrumentation, have more similarities as the group described above. These projects need to use a linear accelerator with a very high peak current of a few mA up to 100 mA to compensate for the low duty cycle. Because of the pulsed beam, these projects require a room-temperature accelerator. The final energy is different for each of these projects. It can be achieved by choosing the right number of DTL acceleration segments. With a different final energy, different target concepts must be used as described above. Since the goal of these projects is to provide neutron beams to a large user community, they usually have multiple target stations and up to 25 instruments. The layout of the instrument suits depends strongly on the number of target stations and thus on the TMR unit installed. A single target station must provide neutrons for very different instruments to meet the needs of different user communities. Therefore a facility with a single target station requires compromises in pulse structure and TMR design. Either the TMR provides a long neutron pulse and then instruments requiring shorter pulses have to use choppers. Alternatively, different pulse modes could be provided, targeted at specific instruments. To avoid such compromises, multiple target stations can be used. This is economically feasible since the cost of a HiCANS target station is quite low, comparable to the cost of a typical instrument. A second target

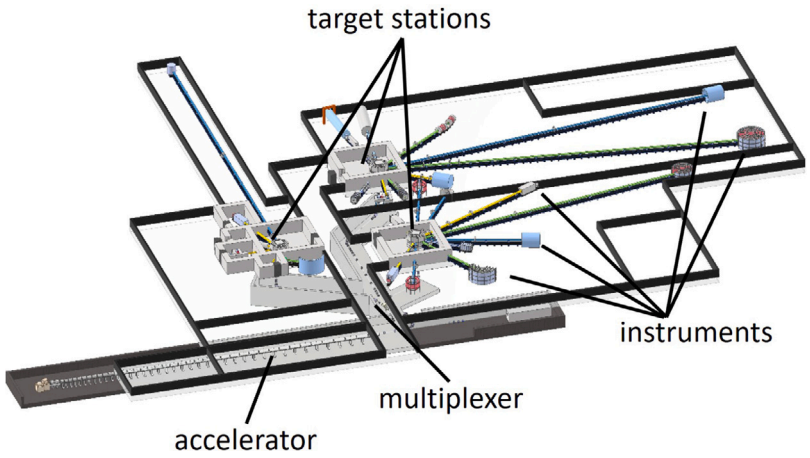

Fig. 7.5. Schematic layout of the HBS facility. The 70 MeV, 100 mA proton accelerator delivers pulsed proton beams via a multiplexer to three target stations around which up to 8 instruments are placed.

station can be used to separate instruments according to their requirements. Instruments that require similar pulse structures can be grouped around target stations so that the target station and TMR unit are optimized for that group of instruments. In this scenario, a medium pulse length target station is best suited to provide thermal neutrons with high temporal resolution. A long pulse length target station, on the other hand, is well suited to provide cold neutrons with low resolution. A third target station can be used for further specialization, e.g. for epithermal and fast neutron instrumentation.

The ARGITU project has undergone many changes from its original concept. The project at ESS Bilbao in Spain originally envisaged a neutron target station providing neutron beams with a source strength of 10^{15} n/s from a Be target using a 75 mA proton beam at 50 MeV [344,345]. The target was designed as a rotating wheel with Be sheets supporting high power operation up to 112 kW. Such a design requires a lot of space and does not offer one of the main advantages of a HiCANS, namely the compact TMR unit. Efficiency is sacrificed. The developments on HiCANS led to design updates [302,346] resulting in a 31.5 MeV proton accelerator with a peak current of 32 mA and a Be target. A single target station with up to 4 instruments is planned. The instrument suite will be decided based on the requirements of the Spanish user community.

The construction of the HiCANS source ICONE is proposed at CEA Saclay in France to support the French community in materials science research [301]. A 25 MeV, 80–100 mA proton accelerator is planned to serve two target stations with a high power Be target and to deliver a thermal neutron flux of the order of 4×10^{12} n/cm^2/s [347]. The target stations are operated at 4% duty cycle and 2% duty cycle for low and high resolution instrumentation, respectively. The Be target must therefore withstand 50 kW or 25 kW, which is done by operating the target at elevated temperatures to allow diffusion of the hydrogen atoms. A total of 10 instruments distributed in groups of 5 is planned, covering the most requested instruments such as SANS, diffraction, reflectometry, radiography and spectroscopy.

The most ambitious project in this context is the High Brilliance neutron Source HBS [303] which features a 70 MeV, 100 mA proton accelerator to feed three target stations with different pulse structures (different pulse length and frequencies). A solid Ta target sustaining a beam power of 100 kW has been developed [307,320]. The reference design includes a full suite of scattering, imaging and analytics instruments distributed among the three target stations. Each individual instrument will compare well with existing leading instruments at present day sources. Major components of the HBS have been realized and tested and their interplay was demonstrated by a test setup [308]. A schematic drawing of the layout of the experimental areas and target stations of the HBS in its reference design is depicted in Fig. 7.5.

Since the relevant components for a HiCANS have been explained using the HBS project as an example, we will not go into further detail. We just want to emphasize that HiCANS can be built in stages and that major upgrades can be planned from the beginning. The accelerator of a HiCANS can be upgraded in terms of its final energy, allowing a large increase in the neutron yield. This would require different target solutions, being developed in the ARGITU, ICONE and HBS projects. A HiCANS can be built with only one or two target stations, and other target stations can be added during its lifetime. This allows more instruments to be added and allows specialization of the target station to specific instrument requirements, further improving efficiency. For example, the HBS can be started with the intended 100 mA ion source, but with only a single target station and a final energy of only 20 MeV by omitting the last DTL segments. The target concept of ICONE could be used or the developed tantalum target could be adapted to the lower proton beam energy. The single target station would provide neutrons for 5 of the most requested instruments, e.g. SANS, diffractometer, reflectometer, imaging and PGNAA. Facility upgrades could bring the first phase to final design. The other projects can be similarly upgraded. The ARGITU project can be further developed, and additional target stations will increase the number of instruments.

7.3. Laser-driven sources

7.3.1. Basics and realization

Laser photons can be used to release neutrons by accelerating particles (electrons, protons, deuterons) and then either utilize hard X-ray from e.g. electron acceleration to create photo-neutrons or nuclear reactions such as deuteron break-up in so-called pitcher-catcher methods [348,349]. In the latter, a thin (100 nm–1 μm) target is hit by the laser beam, heating the target electrons to MeV temperatures and accelerating them via the pondermotive force and other mechanisms towards the rear side of the target. There they build an electron-sheath behind the target which generates an electric field through the charge separation. This electric field is in the range of TeV/m and the field ionizes the ions at the rear surface, which subsequently are accelerated to tens of MeV in the direction normal to the target surface.

7.3.2. Existing facilities and projects

Laser-driven neutron generation was demonstrated at several facilities, typically with pitcher-catcher configurations, and the production of 10^{10} neutrons per pulse with 70 J lasers has therefore been reproduced at different facilities. Those facilities include the TRIDENT laser at Los Alamos National Laboratory [350], the Texas Petawatt Laser at the University of Texas in Austin [351], the PHELIX laser at the Gesellschaft für Schwerionenforschung in Darmstadt [352], the VULCAN laser at AWE in the UK [353], and others. These lasers can produce single pulses and do not operate at repetition rates suitable for data collection for ≈1000 pulses or so. Lasers with repetition rate of 1 Hz or more, such as the DRACO laser in Dresden [354], the BELLA laser at Lawrence Berkeley Laboratory [355], or the ALEPH laser at Colorado State University [356] provide typically at least an order of magnitude less laser energy.

Recently first experiments were performed at the ELI-ALPS laser facility with a repetition rate of up to 10 Hz [357]. However, no laser has been designed specifically for the purpose of ion acceleration to enable neutron and X-ray production for material characterization. The aforementioned laser systems are all designed as multi-purpose laser user facilities, in the United States accessible through LaserNET [358].

8. Summary, conclusion and outlook

The neutron is a magical particle, irreplaceable as a spy in the micro- and nanoworld to probe structure and dynamics of matter, as a source for the production of much needed radioisotopes in medical diagnostic and treatments, and as a research object in its own right. Neutrons have a tremendous impact on materials research, materials and device development, and many of today's technological advances would not exist without research with neutrons. They allow us to produce materials with unique properties, such as extremely homogeneously doped silicon semiconductors, the key component of high-power thyristors urgently needed in the energy transition. High intensity neutron sources are key for the development of materials for fusion reactors. Neutrons have saved millions of lives by enabling the production of much needed radionuclides, the core of radiopharmaceuticals for diagnostics and therapy. They give us a powerful tool for understanding the fundamental laws of nature on the smallest and largest length scales, as they allow us to approach the mysteries of particle physics and the secrets of our universe.

In some areas there are competing approaches from other techniques like synchrotron radiation or electron microscopy that are developing and touching some of the areas of research with neutrons. However, due to its unique properties, the neutron remains unrivaled in many respects, irreplaceable in providing solutions to urgent societal challenges such as environmental protection, the climate crisis, energy transition, sustainable, safe and fast transport, health and information and communication technologies, or uncovering the secrets of our cultural heritage, as well as curiosity-driven research that gives us a better fundamental understanding of the world and universe we live in, to name just a few. It is not surprising, therefore, that many thousands of researchers from academia and industry around the world are flocking to large facilities based on neutron sources.

In this report we have provided an overview over the various methods used at large scale facilities to produce intense fields of free neutrons and bright neutron beams. Different types of sources are best suited to serve certain applications:

- Medium to high flux research reactors based on nuclear fission provide high thermal neutron fluxes within large volumes and continuous bright beams of free neutrons, from ultracold to hot, for a wide variety of applications. They are mostly operated in steady state mode, with the exception of IBR-2 in Dubna. They have been continuously improved since the 50th or 60th of last century and have reached a high level of maturity.
- Spallation neutron sources based on nuclear spallation provide average neutron fluxes comparable to those of medium to high flux research reactors, but in much smaller volumes. They are mostly operated in pulsed mode, with the exception of SINQ at PSI. With the first spallation sources coming online in the late 1970s, they are not yet as mature as research reactors. New facilities, such as the CSNS or ESS, and additional target stations, such as the second target station at the SNS, are currently being ramped up, built or planned, and will offer new opportunities. The strength of spallation sources lies in applications that can take advantage of their high peak brightness, e.g. through time-of-flight techniques. Due to their adaptable pulse structure, spallation neutron sources can exist as short pulse and long pulse sources and offer additional flexibility compared to research reactors for beam applications. Short pulse sources extend the usable neutron spectrum for research to higher energy neutrons beyond the "hot" neutrons of research reactors. The unique advantage of spallation neutron sources, in particular of MW sources, is the peak flux, which can be several tens of times higher than the average flux of research reactors.

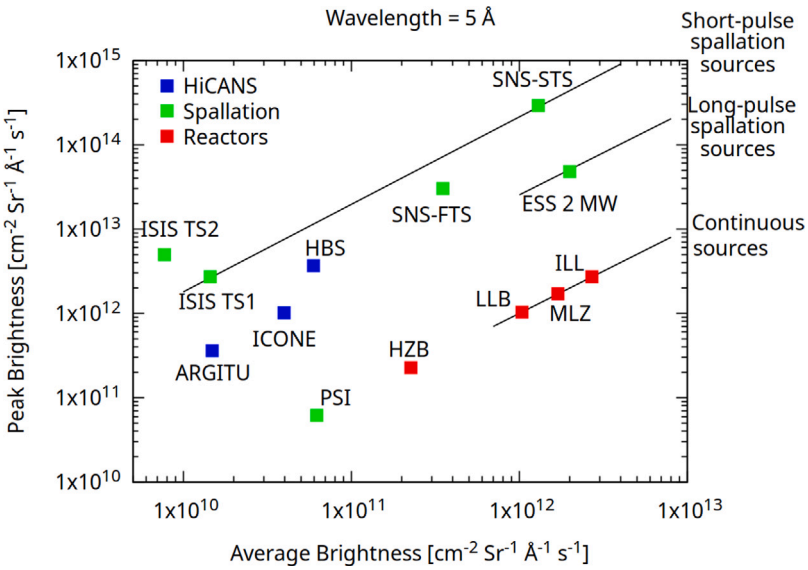

Fig. 8.1. Comparison of peak and average brightness for different neutron sources for neutrons of wavelength 5 Å. The reactor sources at HZB and LLB had an excellent scientific output, but were permanently shut down in 2019. ESS is under construction and the presented data point is scaled down from the 5 MW value presented in [33]. HiCANS exist only as projects and the corresponding data points are based on simulations. Values are based on [359] for HBS and ICONE and based on [346] for ARGITU. The data points for SNS-FTS, ILL and MLZ are from the IAEA report [33]. The data point for SNS-STS has been updated using [360] and the brightness values for ISIS TS1 & TS2 are from a private communication and are yet to be published [361]. The data points for HZB, LLB and PSI have been obtained from McStas simulations using the definitions in the source module [362]. When comparing the performance of different types of facilities, it should be kept in mind that HiCANS are at a very early stage of development and their performance is certainly not yet fully optimized. Further improvements can be expected for these facilities as more experience is gained, similar to the progress that has been made over the years for fission and spallation sources.

- High Current Accelerator-driven Neutron Sources (HiCANS) based on low energy nuclear processes are the most recent development which are mostly at the project stage. Simulations accompanied by experiments at several neutron centers in Europe, partly with complete test setups, demonstrate the potential of such sources. Although the basic process is not as efficient in neutron production as fission or spallation, the extremely compact target–moderator–reflector arrangement, together with the paradigm change to make the source an integral part of each single instrument, makes these facilities highly competitive in terms of brightness and signal-to-noise ratio when operated in pulsed mode. Nevertheless they are not capable to compete with the latest generation of high-brightness MW spallation sources. Additional benefits of HiCANS include their inherent resilience and reliability, flexibility, accessibility, reduced generation of radioactive material and, last but not least, lower installation and operating costs. Since HiCANS are a completely new type of facility, they inherently have a large potential for further performance improvement over current reference designs.
- Finally, smaller neutron sources, such as TRIGA reactors or Compact Accelerator-based Neutron Sources (CANS) exist, which do not serve a large user community and are therefore not large user facilities in the strict sense. In particular CANS are wide spread in JAPAN with a number of existing facilities based at universities and various projects.

Fig. 8.1 provides a comparison of various neutron facilities in only one aspect: source brightness. It demonstrates that research reactors have a high average brightness, which for steady state sources is equal to the peak brightness. Spallation sources have the highest peak brightness, but lower average brightness, with the exception of SNS-STS and ESS, which excel in both. The HBS project, as the most advanced pulsed HiCANS, is somewhere in between, but has a very remarkable performance in terms of peak brightness.

In addition to pure brightness there is a whole value chain important for the scientific performance of a user facility, from the brightness of the source and its reliability, to the mode of beam time distribution, the quality of the staff, the ancillary equipment such as the sample environment, the user community, the data processing packages, and so on.

Currently, in the 2020s, we are in a transition period for research with neutrons. Many of the older research reactors have reached or are reaching the end of their lifetimes and are being decommissioned. Spallation neutron sources have taken over or will take over much of the research that has been done at beamlines of research reactors. The MW spallation sources have made these facilities extremely powerful scientifically, but also very large, complex and expensive. As a result, there are only three such facilities in the world, one in each region of the northern hemisphere. While for beamline instruments such facilities enable entirely new types of science not possible elsewhere, they cannot provide the much needed capacity for the large and very diverse community of researchers simply because of the limited total number of instrument days offered. With the different types of facilities and their associated parameters, a scenario for a future neutron ecosystem based on the different facilities could be as follows:

- Fission-based neutron sources are absolutely essential to provide the high continuous thermal flux in large volumes needed for many very important applications, in particular, but not limited to, the production of neutron-rich radionuclides for radiopharmaceuticals that cannot be produced by cyclotrons. High flux reactors can also provide high brightness continuous beams for materials research. However, given the many regulatory restrictions on operating a fissile material facility and the complex fuel cycle, it is becoming increasingly difficult to license and operate such a source. And while a nuclear reactor is a very reliable source under normal operating conditions, incidents can result in very long downtime, up to several years, as recent examples show. Such a long shutdown is extremely detrimental to the user base.
- Spallation based neutron sources, due to their high peak flux, are excellent for beamline applications requiring the highest beam brightness. For these applications they are likely to be the "flagship" facilities. Due to their high installation and operating costs, it is unlikely that there will be enough of these facilities to meet the full demand from science and industry.
- High Current Accelerator-driven Neutron Sources (HiCANS) are a completely new type of facility. While simulations and experiments indicate their good performance, a demonstrator needs to be realized to prove their usefulness as a user facility. Nevertheless, it is likely that HiCANS can provide much needed capacity for beamline research, which is lacking due to the slowly disappearing network of fission-based sources. The projects show that the peak brightness can be comparable to today's medium- to high-flux sources with an improved signal-to-background ratio, and for a first-of-a-kind facility, there is likely to be a large potential for further improvement. HiCANS have several additional advantages such as intrinsic resilience and reliability, flexibility, accessibility, much reduced generation of nuclear waste, lower cost of installation and operation, all of which are extremely important for a large-scale user facility.
- Smaller sources (TRIGA, CANS) are and can be extremely important for method development, user recruitment and training, and for addressing specific scientific problems relevant to a local or regional community.

Such a wide range of different sources – from quasi-laboratory facilities to high-performance sources – is extremely important for research with neutrons, as a comparison with other methods shows. Thus, for research with X-rays, there are (i) standard laboratory facilities that provide easy access to the method, especially for students and new users, (ii) first- and second-generation synchrotron radiation sources, and for special applications, top-class laboratory sources with comparable performance as workhorses (e.g. for small-angle scattering with metal-jet sources [363]), and (iii) finally highest-brilliance synchrotron radiation sources of the latest generation or X-ray free-electron lasers that allow unique experiments that cannot be performed at the other sources. A neutron ecosystem consisting of CANS, HiCANS, research reactors and finally MW spallation sources could reflect this well-proven structure in the field of research with neutrons and lead to an increasing impact of neutrons in basic research and applications.

Acronyms

- ANSTO: Australian Nuclear Science and Technology Organization, AU
- ARGITU: HiCANS project of ESS-Bilbao, Bilbao, ES
- ATI: Atominstitut with TRIGA reactor, TU Wien, Vienna, AT
- BER II: former "Berliner Experimentier-Reaktor" of Helmholtz-Zentrum Berlin, DE
- BNC: Budapest Neutron Centre with the Budapest Research Reactor, HU
- BNCT: Boron Neutron Capture Therapy
- CANS: Compact Accelerator-based Neutron Sources
- CARR: China Advanced Research Reactor at China Institute of Atomic Energy, CN
- CDR: Conceptual Design Report
- CERN: "Conseil Européen pour la Recherche Nucléaire", Geneva, CH
- CPHS: Compact Pulsed Hadron Source at Tsinghua University, Beijing, CN
- CSNS: China Spallation Neutron Source in Dongguan, Guangdong, CN
- CW: Constant Wavelength mode
- DTL: Drift-Tube Linac
- ECR: Electron Cyclotron Resonance
- ELENA: European Low Energy accelerator-based Neutron facilities Association
- ESS: European Spallation Source, Lund, SE
- FRANZ: "Frankfurt Neutron Source at the Stern-Gerlach-Zentrum" - CANS at Frankfurt University, DE
- FRM II: "Forschungs Reaktor München II" - research neutron source Heinz Maier-Leibnitz, Garching, DE
- GISAS: Grazing Incidence Small Angle Scattering
- HANARO: High Flux Advanced Neutron Application Reactor of Korea Atomic Energy Research Institute, Daejeon, KR
- HBS: High Brilliance neutron Source Project of Jülich Centre for Neutron Science, Jülich, DE
- HEBT: High Energy Beam Transport
- HEP: High Energy Physics
- HFIR: High Flux Isotope Reactor at ORNL, Oak Ridge, US
- HFR: High Flux Reactor of ILL, Grenoble, FR
- HiCANS: High Current Accelerator-driven Neutron Sources
- HUNS: Hokkaido University Neutron Source, Hokkaido, JP
- HZDR: Helmholtz Zentrum Dresden Rossendorf, Dresden, DE

- IAEA: International Atomic Energy Agency
- IBR-2: Fast pulsed reactor of Frank Laboratory of Neutron Physics at JINR, Dubna, RU
- ICANS: International Collaboration on Advanced Neutron Sources
- ICONE: Innovative COmpact NEutron facility project of Laboratoire Léon-Brillouin, Saclay, FR
- ILL: Institut Laue-Langevin, Grenoble, FR
- IPNS: Intense Pulsed Neutron Source, formerly at Argonne National Laboratory, Argonne, US
- ISIS: Neutron and Muon Source at the Rutherford Appleton Laboratory, Didcot, UK
- JCANS: Japan Collaboration on Accelerator-driven Neutron Sources
- JINR: Joint Institute for Nuclear Research, Dubna, RU
- J-PARC: Japan Proton Accelerator Research Complex of Japan Atomic Energy Agency and High Energy Accelerator Research Organization, Tokai, JP
- JRR-3: Japan Research Reactor of Japan Atomic Energy Agency, Tokai, JP
- LEBT: Low Energy Beam Transport
- LENS: League of advanced European Neutron Sources
- LENS: Low Energy Neutron Source at Indiana University, Bloomington, US
- LINAC: Linear accelerator
- MARIA: Reactor at the National Center for Nuclear Research, Swierk, PL
- MCNP: Monte Carlo N-Particle Transport code by Los Alamos National Laboratory, Los Alamos, US
- MEBT: Medium Energy Beam Transport
- MLZ: Heinz Maier-Leibnitz Zentrum, Garching, DE
- MYRRHA: Multi-purpose hYbrid Research Reactor for High-tech Applications project by the Belgian Centre for Nuclear Research, Mol, BE
- NBSR: National Bureau of Standards Reactor at NIST, Gaithersburg, US
- NCNR: Nist Center for Neutron Research at NIST, Gaithersburg, US
- NIST: National Institute of Standards and Technology, Gaithersburg, US
- NNS: project for a new NIST Neutron Source reactor at NIST, Gaithersburg, US
- NPI: Nuclear Physics Institute of the Czech Academy of Sciences, Řež, CZ
- NTD: Neutron Transmutation Doping
- OPAL: Open Pool Australian Lightwater reactor at ANSTO, Lucas Heights, AU
- ORNL: Oak Ridge National Laboratory, Oak Ridge, US
- ORPHEE: former reactor of the Laboratoire Leon-Brilloiun, Saclay, FR
- PDF: Pair Distribution Function
- PGNAA: Prompt Gamma Neutron Activation Analysis (see PGA)
- PGA: Neutron-induced Prompt Gamma-ray Analysis (see PGNAA)
- PIK: Reactor project of Petersburg Nuclear Physics Institute, Gatchina, RU
- PS: Phase Space
- QENS: Quasi Elastic Neutron Scattering
- RANS: RIKEN Accelerator-driven compact Neutron Systems at RIKEN, Wako, JP
- RBE: Relative Biological Effectiveness
- RFQ: Radio Frequency Quadrupole
- RIB: Radioactive Ion Beam
- RID: Reactor Institute Delft at Technical University Delft, Delft, NL
- RIKEN: National Research and Development Institute, Wako, JP
- SANS: Small Angle Neutron Scattering
- SARAF: Soreq Applied Research Accelerator Facility at Soreq Nuclear Research Center, Yavne, IL
- SESAME: Spin-Echo Scattering Angle MEasurement
- SINQ: Swiss Spallation Neutron Source at Paul Scherrer Institut, Villingen, CH
- SNS : Spallation Neutron Source at ORNL, Oak Ridge, US
- TDR: Technical Design Report
- TMR: Target–Moderator–Reflector assembly
- TOF/tof: time-of-flight
- TRIGA: pulsed reactors for “Training, Research, Isotopes, General Atomics”
- UCANS: Union of Compact Accelerator-driven Neutron Sources
- VITESS: Virtual Instrumentation Tool for the ESS for the simulation of neutron scattering experiments

CRediT authorship contribution statement

P. Zakalek: Writing – review & editing, Writing – original draft, Visualization, Software, Methodology, Investigation, Formal analysis, Data curation, Conceptualization. **T. Gutberlet:** Writing – review & editing, Writing – original draft, Project administration,

Methodology, Investigation, Conceptualization. **Th. Brückel:** Writing – review & editing, Writing – original draft, Supervision, Resources, Project administration, Methodology, Investigation, Funding acquisition, Conceptualization.

Declaration of competing interest

The authors declare that they have no known competing financial interests or personal relationships that could have appeared to influence the work reported in this paper.

Acknowledgments

We would like to express our gratitude to Jörg Voigt for proofreading and providing valuable insights, Günter Muhrer for his contributions to our discussions, Eric Mauerhofer, Alexander Schwab and Johannes Baggemann for their assistance in preparing figures, and Jingjing Li, Junyang Chen and Noberto Schmidt for performing simulations. We are indebted to our colleagues from a multitude of neutron research facilities across the globe for their invaluable contributions to numerous joint experiments and exchanges at workshops and conferences. In particular, we would like to express our gratitude to our colleagues from the various CANS and HiCANS projects who have collaborated with us in ELENA. These interactions have been instrumental in our acquisition of knowledge regarding the intricacies of their facilities and experimental methodologies.

Funding provided by Forschungszentrum Jülich GmbH, the Helmholtz Association of German Research Centres, and the German Ministry of Education and Research is gratefully acknowledged.

References

[1] C.G. Shull, 1994, URL https://www.nobelprize.org/prizes/physics/1994/shull/lecture/.
[2] B.N. Brockhouse, 1994, URL https://www.nobelprize.org/prizes/physics/1994/brockhouse/lecture/.
[3] H. Abele, A. Alekou, A. Algora, K. Andersen, S. Baeßler, L. Barron-Pálos, J. Barrow, E. Baussan, P. Bentley, Z. Berezhiani, Y. Beßler, A. Bhattacharyya, A. Bianchi, J. Bijnens, C. Blanco, N.B. Kraljevic, M. Blennow, K. Bodek, M. Bogomilov, C. Bohm, B. Bolling, E. Bouquerel, G. Brooijmans, L. Broussard, O. Buchan, A. Burgman, H. Calén, C. Carlile, J. Cederkall, E. Chanel, P. Christiansen, V. Cirigliano, J. Collar, M. Collins, C. Crawford, E.C. Morales, P. Cupiał, L. D'Alessi, J.M. Damian, H. Danared, D. Dancila, J. de André, J. Delahaye, S. Degenkolb, D. Di Julio, M. Dracos, K. Dunne, I. Efthymiopoulos, T. Ekelöf, L. Eklund, M. Eshraqi, I. Esteban, G. Fanourakis, A. Farricker, E. Fernandez-Martinez, M. Ferreira, M. Fertl, P. Fierlinger, B. Folsom, A. Frank, A. Fratangelo, U. Friman-Gayer, T. Fukuda, H. Fynbo, A.G. Sosa, N. Gazis, B. Gålnander, T. Geralis, M. Ghosh, G. Gokbulut, J. Gomez-Cadenas, M. Gonzalez-Alonso, F. Gonzalez, L. Halić, C. Happe, P. Heil, A. Heinz, H. Herde, M. Holl, T. Jenke, M. Jenssen, E. Jericha, H. Johansson, R. Johansson, T. Johansson, Y. Kamyshkov, A.K. Topaksu, B. Kildetoft, K. Kirch, B. Kliček, E. Klinkby, R. Kolevatov, G. Konrad, M. Kozioł, K. Krhač, A. Kupść, Ł. Łacny, L. Larizgoitia, C. Lewis, M. Lindroos, E. Lychagin, E. Lytken, C. Maiano, P. Marciniewski, G. Markaj, B. Märkisch, C. Marrelli, C. Martins, B. Meirose, M. Mezzetto, N. Milas, D. Milstead, F. Monrabal, G. Muhrer, A. Nepomuceno, V. Nesvizhevsky, T. Nilsson, P. Novella, M. Oglakci, T. Ohlsson, M. Olvegård, A. Oskarsson, T. Ota, J. Park, D. Patrzalek, H. Perrey, M. Persoz, G. Petkov, F. Piegsa, C. Pistillo, P. Poussot, P. Privitera, B. Rataj, D. Ries, N. Rizzi, S. Rosauro-Alcaraz, D. Rozpedzik, D. Saiang, V. Santoro, U. Schmidt, H. Schober, I. Schulthess, S. Silverstein, A. Simón, H. Sina, J. Snamina, W. Snow, T. Soldner, G. Stavropoulos, M. Stipčević, B. Szybiński, A. Takibayev, Z. Tang, R. Tarkeshian, C. Theroine, J. Thorne, F. Terranova, J. Thomas, T. Tolba, P. Torres-Sánchez, E. Trachanas, R. Tsenov, U. Uggerhøj, G. Vankova-Kirilova, N. Vassilopoulos, R. Wagner, X. Wang, E. Wildner, M. Wolke, J. Wurtz, S. Yiu, S. Yoon, A. Young, L. Zanini, J. Zejma, D. Zerzion, O. Zimmer, O. Zormpa, Y. Zou, Phys. Rep. 1023 (2023) 1–84, http://dx.doi.org/10.1016/j.physrep.2023.06.001, URL https://www.sciencedirect.com/science/article/pii/S0370157323001898.
[4] World Nuclear Association, 2024, URL https://world-nuclear.org/information-library/non-power-nuclear-applications/radioisotopes-research/radioisotopes-in-medicine.aspx.
[5] M. Suzuki, Int. J. Clin. Oncol. 25 (2020) 43–50, URL https://doi.org/10.1007/s10147-019-01480-4.
[6] C.D. Siewert, H. Haas, V. Cornet, S.S. Nogueira, T. Nawroth, L. Uebbing, A. Ziller, J. Al-Gousous, A. Radulescu, M.A. Schroer, C.E. Blanchet, D.I. Svergun, M.P. Radsak, U. Sahin, P. Langguth, Cells 9 (9) (2020) http://dx.doi.org/10.3390/cells9092034, URL https://www.mdpi.com/2073-4409/9/9/2034.
[7] C. Siewert, H. Haas, T. Nawroth, A. Ziller, S. Nogueira, M. Schroer, C. Blanchet, D. Svergun, A. Radulescu, F. Bates, Y. Huesemann, M. Radsak, U. Sahin, P. Langguth, Biomaterials 192 (2019) 612–620, http://dx.doi.org/10.1016/j.biomaterials.2018.10.020, URL https://www.sciencedirect.com/science/article/pii/S0142961218307348.
[8] X. Li, H. Gerstenberg, I. Neuhaus, Appl. Radiat. Isot. 67 (2009) 1220–1224, http://dx.doi.org/10.1016/j.apradiso.2009.02.017, URL https://www.sciencedirect.com/science/article/pii/S0969804309001262.
[9] League of Advanced Neutron Sources, 2022, URL https://lens-initiative.org/lens-position-papers/.
[10] T. Brückel, T. Gutberlet, S. Schmidt, C. Alba-Simionesco, F. Ott, A. Menelle, Neutron News 31 (2–4) (2020) 13–18, http://dx.doi.org/10.1080/10448632.2020.1819125.
[11] ELENA Association, URL www.ELENA-neutron.eu.
[12] J.M. Carpenter, C.-K. Loong, Elements of Slow-Neutron Scattering: Basics, Techniques, and Applications, Cambridge University Press, 2015, http://dx.doi.org/10.1017/CBO9781139029315.
[13] D. Filges, F. Goldenbaum, Handbook of Spallation Research: Theory, Experiments and Applications, Wiley-VCH Verlag, 2009, http://dx.doi.org/10.1002/9783527628865, URL https://onlinelibrary.wiley.com/doi/book/10.1002/9783527628865.
[14] D.G. Cacuci (Ed.), Handbook of Nuclear Engineering (Vol.1 to 5.), Springer New York, 2010, http://dx.doi.org/10.1007/978-0-387-98149-9.
[15] E. Rutherford, Proc. R. Soc. Lond. Ser. A Contain. Pap. A Math. Phys. Character 97 (686) (1920) 374–400, http://dx.doi.org/10.1098/rspa.1920.0040, URL https://royalsocietypublishing.org/doi/abs/10.1098/rspa.1920.0040.
[16] W.D. Harkins, Lond. Edinb. Dublin Philos. Mag. J. Sci. 42 (249) (1921) 305–339, http://dx.doi.org/10.1080/14786442108633770.
[17] W. Bothe, H. Becker, Z. Phys. 66 (1930) 289–306, http://dx.doi.org/10.1007/BF01390908.
[18] I. Joliot-Curie, F. Joliot, C. R. 194 (1932) URL https://gallica.bnf.fr/ark:/12148/bpt6k31473/f273.item.
[19] J. Chadwick, Nature 129 (1932) 312, http://dx.doi.org/10.1038/129312a0.
[20] H. Abele, Prog. Part. Nucl. Phys. 60 (1) (2008) 1–81, http://dx.doi.org/10.1016/j.ppnp.2007.05.002, URL https://www.sciencedirect.com/science/article/pii/S0146641007000622.
[21] The NIST Reference on Constants, Units, and Uncertainty, URL https://physics.nist.gov/cgi-bin/cuu/Value?mn.
[22] B. Povh, K. Rith, C. Scholz, F. Zetsche, Particles and Nuclei: An Introduction to the Physical Concepts, Springer-Verlag, 2002, http://dx.doi.org/10.1007/978-3-662-05432-1.

[23] J. Baumann, R. Gähler, J. Kalus, W. Mampe, Phys. Rev. D 37 (1988) 3107–3112, http://dx.doi.org/10.1103/PhysRevD.37.3107, URL https://link.aps.org/doi/10.1103/PhysRevD.37.3107.

[24] J. Beringer, J.F. Arguin, R.M. Barnett, K. Copic, O. Dahl, D.E. Groom, C.J. Lin, J. Lys, H. Murayama, C.G. Wohl, W.M. Yao, P.A. Zyla, C. Amsler, M. Antonelli, D.M. Asner, H. Baer, H.R. Band, T. Basaglia, C.W. Bauer, J.J. Beatty, V.I. Belousov, E. Bergren, G. Bernardi, W. Bertl, S. Bethke, H. Bichsel, O. Biebel, E. Blucher, S. Blusk, G. Brooijmans, O. Buchmueller, R.N. Cahn, M. Carena, A. Ceccucci, D. Chakraborty, M.C. Chen, R.S. Chivukula, G. Cowan, G. D'Ambrosio, T. Damour, D. de Florian, A. de Gouvêa, T. DeGrand, P. de Jong, G. Dissertori, B. Dobrescu, M. Doser, M. Drees, D.A. Edwards, S. Eidelman, J. Erler, V.V. Ezhela, W. Fetscher, B.D. Fields, B. Foster, T.K. Gaisser, L. Garren, H.J. Gerber, G. Gerbier, T. Gherghetta, S. Golwala, M. Goodman, C. Grab, A.V. Gritsan, J.F. Grivaz, M. Grünewald, A. Gurtu, T. Gutsche, H.E. Haber, K. Hagiwara, C. Hagmann, C. Hanhart, S. Hashimoto, K.G. Hayes, M. Heffner, B. Heltsley, J.J. Hernández-Rey, K. Hikasa, A. Höcker, J. Holder, A. Holtkamp, J. Huston, J.D. Jackson, K.F. Johnson, T. Junk, D. Karlen, D. Kirkby, S.R. Klein, E. Klempt, R.V. Kowalewski, F. Krauss, M. Kreps, B. Krusche, Y.V. Kuyanov, Y. Kwon, O. Lahav, J. Laiho, P. Langacker, A. Liddle, Z. Ligeti, T.M. Liss, L. Littenberg, K.S. Lugovsky, S.B. Lugovsky, T. Mannel, A.V. Manohar, W.J. Marciano, A.D. Martin, A. Masoni, J. Matthews, D. Milstead, R. Miquel, K. Mönig, F. Moortgat, K. Nakamura, M. Narain, P. Nason, S. Navas, M. Neubert, P. Nevski, Y. Nir, K.A. Olive, L. Pape, J. Parsons, C. Patrignani, J.A. Peacock, S.T. Petcov, A. Piepke, A. Pomarol, G. Punzi, A. Quadt, S. Raby, G. Raffelt, B.N. Ratcliff, P. Richardson, S. Roesler, S. Rolli, A. Romaniouk, L.J. Rosenberg, J.L. Rosner, C.T. Sachrajda, Y. Sakai, G.P. Salam, S. Sarkar, F. Sauli, O. Schneider, K. Scholberg, D. Scott, W.G. Seligman, M.H. Shaevitz, S.R. Sharpe, M. Silari, T. Sjöstrand, P. Skands, J.G. Smith, G.F. Smoot, S. Spanier, H. Spieler, A. Stahl, T. Stanev, S.L. Stone, T. Sumiyoshi, M.J. Syphers, F. Takahashi, M. Tanabashi, J. Terning, M. Titov, N.P. Tkachenko, N.A. Törnqvist, D. Tovey, G. Valencia, K. van Bibber, G. Venanzoni, M.G. Vincter, P. Vogel, A. Vogt, W. Walkowiak, C.W. Walter, D.R. Ward, T. Watari, G. Weiglein, E.J. Weinberg, L.R. Wiencke, L. Wolfenstein, J. Womersley, C.L. Woody, R.L. Workman, A. Yamamoto, G.P. Zeller, O.V. Zenin, J. Zhang, R.Y. Zhu, G. Harper, V.S. Lugovsky, P. Schaffner, Particle Data Group Collaboration Collaboration, Phys. Rev. D 86 (2012) 010001, http://dx.doi.org/10.1103/PhysRevD.86.010001, URL https://link.aps.org/doi/10.1103/PhysRevD.86.010001.

[25] S. Navas, C. Amsler, T. Gutsche, C. Hanhart, J.J. Hernández-Rey, C. Lourenço, A. Masoni, M. Mikhasenko, R.E. Mitchell, C. Patrignani, C. Schwanda, S. Spanier, G. Venanzoni, C.Z. Yuan, K. Agashe, G. Aielli, B.C. Allanach, J. Alvarez-Muñiz, M. Antonelli, E.C. Aschenauer, D.M. Asner, K. Assamagan, H. Baer, S. Banerjee, R.M. Barnett, L. Baudis, C.W. Bauer, J.J. Beatty, J. Beringer, A. Bettini, O. Biebel, K.M. Black, E. Blucher, R. Bonventre, R.A. Briere, A. Buckley, V.D. Burkert, M.A. Bychkov, R.N. Cahn, Z. Cao, M. Carena, G. Casarosa, A. Ceccucci, A. Cerri, R.S. Chivukula, G. Cowan, K. Cranmer, V. Crede, O. Cremonesi, G. D'Ambrosio, T. Damour, D. de Florian, A. de Gouvêa, T. DeGrand, S. Demers, Z. Demiragli, B.A. Dobrescu, M. D'Onofrio, M. Doser, H.K. Dreiner, P. Eerola, U. Egede, S. Eidelman, A.X. El-Khadra, J. Ellis, S.C. Eno, J. Erler, V.V. Ezhela, A. Fava, W. Fetscher, B.D. Fields, A. Freitas, H. Gallagher, T. Gershon, Y. Gershtein, T. Gherghetta, M.C. Gonzalez-Garcia, M. Goodman, C. Grab, A.V. Gritsan, C. Grojean, D.E. Groom, M. Grünewald, A. Gurtu, H.E. Haber, M. Hamel, S. Hashimoto, Y. Hayato, A. Hebecker, S. Heinemeyer, K. Hikasa, J. Hisano, A. Höcker, J. Holder, L. Hsu, J. Huston, T. Hyodo, A. Ianni, M. Kado, M. Karliner, U.F. Katz, M. Kenzie, V.A. Khoze, S.R. Klein, F. Krauss, M. Kreps, P. Križan, B. Krusche, Y. Kwon, O. Lahav, L.P. Lellouch, J. Lesgourgues, A.R. Liddle, Z. Ligeti, C.-J. Lin, C. Lippmann, T.M. Liss, A. Lister, L. Littenberg, K.S. Lugovsky, S.B. Lugovsky, A. Lusiani, Y. Makida, F. Maltoni, A.V. Manohar, W.J. Marciano, J. Matthews, U.-G. Meißner, I.-A. Melzer-Pellmann, P. Mertsch, D.J. Miller, D. Milstead, K. Mönig, P. Molaro, F. Moortgat, M. Moskovic, N. Nagata, K. Nakamura, M. Narain, P. Nason, A. Nelles, M. Neubert, Y. Nir, H.B. O'Connell, C.A.J. O'Hare, K.A. Olive, J.A. Peacock, E. Pianori, A. Pich, A. Piepke, F. Pietropaolo, A. Pomarol, S. Pordes, S. Profumo, A. Quadt, K. Rabbertz, J. Rademacker, G. Raffelt, M. Ramsey-Musolf, P. Richardson, A. Ringwald, D.J. Robinson, S. Roesler, S. Rolli, A. Romaniouk, L.J. Rosenberg, J.L. Rosner, G. Rybka, M.G. Ryskin, R.A. Ryutin, B. Safdi, Y. Sakai, S. Sarkar, F. Sauli, O. Schneider, S. Schönert, K. Scholberg, A.J. Schwartz, J. Schwiening, D. Scott, F. Sefkow, U. Seljak, V. Sharma, S.R. Sharpe, V. Shiltsev, G. Signorelli, M. Silari, F. Simon, T. Sjöstrand, P. Skands, T. Skwarnicki, G.F. Smoot, A. Soffer, M.S. Sozzi, C. Spiering, A. Stahl, Y. Sumino, F. Takahashi, M. Tanabashi, J. Tanaka, M. Taševský, K. Terao, K. Terashi, J. Terning, U. Thoma, R.S. Thorne, L. Tiator, M. Titov, D.R. Tovey, K. Trabelsi, P. Urquijo, G. Valencia, R. Van de Water, N. Varelas, L. Verde, I. Vivarelli, P. Vogel, W. Vogelsang, V. Vorobyev, S.P. Wakely, W. Walkowiak, C.W. Walter, D. Wands, D.H. Weinberg, E.J. Weinberg, N. Wermes, M. White, L.R. Wiencke, S. Willocq, C.L. Woody, R.L. Workman, W.-M. Yao, M. Yokoyama, R. Yoshida, G. Zanderighi, G.P. Zeller, R.-Y. Zhu, S.-L. Zhu, F. Zimmermann, P.A. Zyla, J. Anderson, M. Kramer, P. Schaffner, W. Zheng, Particle Data Group Collaboration Collaboration Collaboration, Phys. Rev. D 110 (2024) 030001, http://dx.doi.org/10.1103/PhysRevD.110.030001, URL https://link.aps.org/doi/10.1103/PhysRevD.110.030001.

[26] A. Furrer, J. Mesot, T. Strässle, Neutron Scattering in Condensed Matter Physics, World Scientific, 2009, http://dx.doi.org/10.1142/4870, arXiv:https://www.worldscientific.com/doi/pdf/10.1142/4870. URL https://www.worldscientific.com/doi/abs/10.1142/4870.

[27] C.R. Gould, E.I. Sharapov, Eur. Phys. J. H 47 (1) (2022) 10, URL https://doi.org/10.1140/epjh/s13129-022-00042-z.

[28] B. Allen, I. Bergqvist, R. Chrien, D. Gardner, W. Poenitz (Eds.), Neutron Radiative Capture, Pergamon, 1984, pp. 1–270, http://dx.doi.org/10.1016/B978-0-08-029330-1.50007-9, URL https://www.sciencedirect.com/science/article/pii/B9780080293301500079.

[29] H.T. Motz, Annu. Rev. Nucl. Part. Sci. 20 (1970) 1–38, http://dx.doi.org/10.1146/annurev.ns.20.120170.000245, URL https://www.annualreviews.org/content/journals/10.1146/annurev.ns.20.120170.000245.

[30] J. Schweizer, Polarized neutrons and polarization analysis, Neutron Scattering from Magnetic Materials, Elsevier Science, Amsterdam, 2006, pp. 153–213, http://dx.doi.org/10.1016/B978-044451050-1/50005-7, URL https://www.sciencedirect.com/science/article/pii/B9780444510501500057,

[31] K. Coulter, T. Chupp, A. McDonald, C. Bowman, J. Bowman, J. Szymanski, V. Yuan, G. Cates, D. Benton, E. Earle, Nucl. Instrum. Methods Phys. Res. Sect. A: Accel. Spectrometers Detect. Assoc. Equip. 288 (2) (1990) 463–466, http://dx.doi.org/10.1016/0168-9002(90)90139-W, URL https://www.sciencedirect.com/science/article/pii/016890029090139W.

[32] H. Börner, J. Brown, C. Carlile, R. Cubitt, R. Currat, A. Dianoux, B. Farago, A. Hewat, J. Kulda, E. Lelièvre-Berna, et al., Neutron Data Booklet, ILL, Grenoble, France, 2003, URL https://www.ill.eu/fileadmin/user_upload/ILL/1_About_ILL/Documentation/NeutronDataBooklet.pdf.

[33] Y. Beßler, R. Bewley, M. Bullavin, J. de Jong, S. Gallimore, R. Granada, T. Grosz, T. Gutberlet, D. Jenkins, M. Kickulies, R. Kumar, K.-H. Lee, S. Lilley, W. Lu, H. Mavric, R. Mazzi, A. Moleg, V. Mityukhlyaev, K. Mukhin, S. Panyam, N. Pessoa Barradas, G. Škoro, K. Sun, I. Swainson, K. Thomsen, K. Ünlü, Cold Neutron Sources: Practical Considerations And Modern Research, in: TECDOC Series, International Atomic Energy Agency, 2023, https://www.iaea.org/publications/15409/cold-neutron-sources-practical-considerations-and-modern-research.

[34] F. Mezei, C. R. Phys. 8 (7–8) (2007) 909–920, http://dx.doi.org/10.1016/j.crhy.2007.10.003.

[35] U. Rücker, T. Cronert, J. Voigt, J.P. Dabruck, P.E. Doege, J. Ulrich, R. Nabbi, Y. Beßler, M. Butzek, M. Büscher, C. Lange, M. Klaus, T. Gutberlet, T. Brückel, Eur. Phys. J. Plus 131 (1) (2016) 19, http://dx.doi.org/10.1140/epjp/i2016-16019-5.

[36] A. Taylor, M. Dunne, S. Bennington, S. Ansell, I. Gardner, P. Norreys, T. Broome, D. Findlay, R. Nelmes, Science 315 (5815) (2007) 1092–1095, http://dx.doi.org/10.1126/science.1127185, arXiv:https://www.science.org/doi/pdf/10.1126/science.1127185. URL https://www.science.org/doi/abs/10.1126/science.1127185.

[37] D. Habs, M. Gross, P.G. Thirolf, P. Böni, Appl. Phys. B 103 (2) (2011) 485–499, http://dx.doi.org/10.1007/s00340-010-4276-3.

[38] R. Martin, J. Knauer, P. Balo, Appl. Radiat. Isot. 53 (4) (2000) 785–792, http://dx.doi.org/10.1016/S0969-8043(00)00214-1, URL https://www.sciencedirect.com/science/article/pii/S0969804300002141.

[39] D.L. Chichester, J.D. Simpson, Ind. Phys. 9 (6) (2003) 22–25, URL https://web.archive.org/web/20071117191652/http://www.aip.org/tip/INPHFA/vol-9/iss-6/p22.html.

[40] A. Vertes, S. Nagy, Z. Klencsar, Handbook of Nuclear Chemistry: Basics of Nuclear Science; Elements and Isotopes: Formation, Transformation, Distribution; Chemical Applications of Nuclear Reactions and Radiations; Radiochemistry and Radiopharmaceutical Chemistry in Life Sciences; Instrumentation, Separation Techniques, Environmental Issues, Springer US, Boston, MA, 2004, pp. 1186–1209, http://dx.doi.org/10.1007/0-387-30682-X_27.

[41] Z. Wei, C. Han, S.H. Peng, X.H. Bai, C.Q. Liu, Z.W. Ma, Z.W. Huang, S.J. Zhang, W.M. Li, Y. Yang, Z.E. Yao, W.S. Wu, Y. Zhang, X.L. Lu, J.R. Wang, X.D. Su, D.P. Xu, Eur. Phys. J. A 55 (9) (2019) 162, http://dx.doi.org/10.1140/epja/i2019-12848-5.

[42] Z. Huang, J. Wang, Z. Ma, X. Lu, Z. Wei, S. Zhang, Y. Liu, Z. Zhang, Y. Zhang, Z. Yao, Nucl. Instrum. Methods Phys. Res. Sect. A: Accel. Spectrometers Detect. Assoc. Equip. 904 (2018) 107–112, http://dx.doi.org/10.1016/j.nima.2018.07.005, URL https://www.sciencedirect.com/science/article/pii/S0168900218308283.

[43] B.K. Das, A. Shyam, Rev. Sci. Instrum. 79 (12) (2008) 123305, http://dx.doi.org/10.1063/1.3054268, arXiv:https://pubs.aip.org/aip/rsi/article-pdf/doi/10.1063/1.3054268/9921254/123305_1_online.pdf.

[44] J.M. Verbeke, K.N. Leung, J. Vujic, Appl. Radiat. Isot. 53 (4) (2000) 801–809, http://dx.doi.org/10.1016/S0969-8043(00)00262-1, URL https://www.sciencedirect.com/science/article/pii/S0969804300002621.

[45] F.R. O'Donnell, H.L. Adair, Nucl. Instrum. Methods 102 (3) (1972) 501–512, http://dx.doi.org/10.1016/0029-554X(72)90640-4, URL https://www.sciencedirect.com/science/article/pii/0029554X72906404.

[46] J.E. Jobst, Z.G. Burson, F.F. Haywood, Self-Replenishing Tritium Target, Tech. Rep., EG and G, Inc., Las Vegas, Nev., 1972, http://dx.doi.org/10.2172/4641194, URL https://www.osti.gov/biblio/4641194.

[47] F.F. Haywood, Z.G. Burson, H.E. Banta, Self-Replenishing Tritium Target for Neutron Generators, Tech. Rep., Oak Ridge National Lab.(ORNL), Oak Ridge, TN (United States), 1972, URL https://inis.iaea.org/search/search.aspx?orig_q=RN:4040625.

[48] O. Hahn, F. Strassmann, Naturwissenschaften 26 (46) (1938) 755–756, http://dx.doi.org/10.1007/BF01774197.

[49] O. Hahn, F. Strassmann, Naturwissenschaften 27 (1) (1939) 11–15, http://dx.doi.org/10.1007/BF01488241.

[50] L. Meitner, O.R. Frisch, Nature 143 (3615) (1939) 239–240, http://dx.doi.org/10.1038/143239a0.

[51] C.G. Shull, J.S. Smart, Phys. Rev. 76 (1949) 1256–1257, http://dx.doi.org/10.1103/PhysRev.76.1256.2, URL https://link.aps.org/doi/10.1103/PhysRev.76.1256.2.

[52] T. Brückel, T. Gutberlet, P. Zakalek, Phys.- J. 22 (2023) 7, URL https://pro-physik.de/zeitschriften/physik-journal/2023-5/.

[53] IAEA Nuclear Data Services, 2016, URL https://www-nds.iaea.org/amdc/.

[54] W. Huang, G. Audi, W. Meng, F.G. Kondev, S. Naimi, X. Xing, Chin. Phys. C 41 (3) (2017) 030002, http://dx.doi.org/10.1088/1674-1137/41/3/030002.

[55] M. Wang, W. Huang, F. Kondev, G. Audi, S. Naimi, Chin. Phys. C 45 (3) (2021) 030003, http://dx.doi.org/10.1088/1674-1137/abddaf.

[56] N. Bohr, J.A. Wheeler, Phys. Rev. 56 (1939) 426–450, http://dx.doi.org/10.1103/PhysRev.56.426, URL https://link.aps.org/doi/10.1103/PhysRev.56.426.

[57] A.N. Andreyev, K. Nishio, K.-H. Schmidt, Rep. Progr. Phys. 81 (1) (2017) 016301, http://dx.doi.org/10.1088/1361-6633/aa82eb.

[58] N. Schunck, D. Regnier, Prog. Part. Nucl. Phys. 125 (2022) 103963, http://dx.doi.org/10.1016/j.ppnp.2022.103963, URL https://www.sciencedirect.com/science/article/pii/S0146641022000242.

[59] K.-H. Schmidt, B. Jurado, Rep. Progr. Phys. 81 (10) (2018) 106301, http://dx.doi.org/10.1088/1361-6633/aacfa7.

[60] S. Okumura, T. Kawano, P. Jaffke, P. Talou, S. Chiba, J. Nucl. Sci. Technol. 55 (9) (2018) 1009–1023, http://dx.doi.org/10.1080/00223131.2018.1467288, arXiv:https://doi.org/10.1080/00223131.2018.1467288.

[61] C. Liu, K. Tao, L. Huang, D. E., X. Bai, Z. Ma, Nucl. Eng. Technol. (2023) http://dx.doi.org/10.1016/j.net.2023.12.052, URL https://www.sciencedirect.com/science/article/pii/S1738573323006046.

[62] R. Capote, Y.-J. Chen, F.-J. Hambsch, N. Kornilov, J. Lestone, O. Litaize, B. Morillon, D. Neudecker, S. Oberstedt, T. Ohsawa, N. Otuka, V. Pronyaev, A. Saxena, O. Serot, O. Shcherbakov, N.-C. Shu, D. Smith, P. Talou, A. Trkov, A. Tudora, R. Vogt, A. Vorobyev, Nucl. Data Sheets 131 (2016) 1–106, http://dx.doi.org/10.1016/j.nds.2015.12.002, URL https://www.sciencedirect.com/science/article/pii/S0090375215000678. Special Issue on Nuclear Reaction Data.

[63] A. Carlson, V. Pronyaev, R. Capote, G. Hale, Z.-P. Chen, I. Duran, F.-J. Hambsch, S. Kunieda, W. Mannhart, B. Marcinkevicius, R. Nelson, D. Neudecker, G. Noguere, M. Paris, S. Simakov, P. Schillebeeckx, D. Smith, X. Tao, A. Trkov, A. Wallner, W. Wang, Nucl. Data Sheets 148 (2018) 143–188, http://dx.doi.org/10.1016/j.nds.2018.02.002, URL https://www.sciencedirect.com/science/article/pii/S0090375218300218. Special Issue on Nuclear Reaction Data.

[64] A. Carlson, V. Pronyaev, R. Capote, G. Hale, Z.-P. Chen, I. Duran, F.-J. Hambsch, S. Kunieda, W. Mannhart, B. Marcinkevicius, R. Nelson, D. Neudecker, G. Noguere, M. Paris, S. Simakov, P. Schillebeeckx, D. Smith, X. Tao, A. Trkov, A. Wallner, W. Wang, Nucl. Data Sheets 163 (2020) 280–281, http://dx.doi.org/10.1016/j.nds.2019.12.008, URL https://www.sciencedirect.com/science/article/pii/S0090375219300754.

[65] M. Mastromarco, S. Amaducci, N. Colonna, P. Finocchiaro, L. Cosentino, M. Barbagallo, O. Aberle, J. Andrzejewski, L. Audouin, M. Bacak, J. Balibrea, F. Bečvář, E. Berthoumieux, J. Billowes, D. Bosnar, A. Brown, M. Caamaño, F. Calviño, M. Calviani, D. Cano-Ott, R. Cardella, A. Casanovas, F. Cerutti, Y.H. Chen, E. Chiaveri, G. Cortés, M.A. Cortés-Giraldo, L.A. Damone, M. Diakaki, C. Domingo-Pardo, D. Diacono, R. Dressler, E. Dupont, I. Durán, B. Fernández-Domínguez, A. Ferrari, P. Ferreira, V. Furman, K. Göbel, A.R. García, A. Gawlik, S. Gilardoni, T. Glodariu, I.F. Gonçalves, E. González-Romero, E. Griesmayer, C. Guerrero, F. Gunsing, H. Harada, S. Heinitz, J. Heyse, D.G. Jenkins, E. Jericha, F. Käppeler, Y. Kadi, A. Kalamara, P. Kavrigin, A. Kimura, N. Kivel, I. Knapova, M. Kokkoris, M. Krtička, D. Kurtulgil, E. Leal-Cidoncha, C. Lederer, H. Leeb, J. Lerendegui-Marco, S.L. Meo, S.J. Lonsdale, D. Macina, A. Manna, J. Marganiec, T. Martínez, A. Masi, C. Massimi, P. Mastinu, E.A. Maugeri, A. Mazzone, E. Mendoza, A. Mengoni, P.M. Milazzo, F. Mingrone, A. Musumarra, A. Negret, R. Nolte, A. Oprea, N. Patronis, A. Pavlik, J. Perkowski, I. Porras, J. Praena, J.M. Quesada, D. Radeck, T. Rauscher, R. Reifarth, C. Rubbia, J.A. Ryan, M. Sabaté-Gilarte, A. Saxena, P. Schillebeeckx, et al., Eur. Phys. J. A 58 (8) (2022) 147, http://dx.doi.org/10.1140/epja/s10050-022-00779-7.

[66] R. Serber, Phys. Rev. 72 (1947) 1114–1115, http://dx.doi.org/10.1103/PhysRev.72.1114, URL https://link.aps.org/doi/10.1103/PhysRev.72.1114.

[67] B.G. Harvey, in: O. Frisch (Ed.), Progress in Nuclear Physics, Vol. 7, Pergamon Press, London, 1959, pp. 90–120.

[68] G. Lander, Physica B+C 120 (1) (1983) 15–24, http://dx.doi.org/10.1016/0378-4363(83)90333-9, URL https://www.sciencedirect.com/science/article/pii/0378436383903339.

[69] N. Watanabe, Rep. Progr. Phys. 66 (3) (2003) 339, http://dx.doi.org/10.1088/0034-4885/66/3/202.

[70] G. Bauer, Nucl. Instrum. Methods Phys. Res. Sect. A: Accel. Spectrometers Detect. Assoc. Equip. 463 (3) (2001) 505–543, http://dx.doi.org/10.1016/S0168-9002(01)00167-X, URL https://www.sciencedirect.com/science/article/pii/S016890020100167X. Accelerator driven systems.

[71] G. Russell, Proceedings of the Eleventh Meeting of the International Collaboration on Advanced Neutron Sources, ICANS-XI, Tsukuba, 1991, pp. 291–299, URL http://inis.iaea.org/search/search.aspx?orig_q=RN:23015552.

[72] J. Fraser, R. Green, J. Hilborn, J. Milton, W.G.E. Gross, A. Zucker, Phys. Can. 21 (Volume 2, 1965) (1965) 17–18, URL https://pic-pac.cap.ca/index.php/Issues/view_issue/49.

[73] J.M. Carpenter, W.B. Yelon, in: K. Sköld, D.L. Price (Eds.), Methods of Experimental Physics Volume 23: Neutron Scattering, Academic Press, Inc., 1986, pp. 99–196, URL https://www.sciencedirect.com/bookseries/methods-in-experimental-physics/vol/23/part/PA.

[74] M. Danos, E.G. Fuller, Annu. Rev. Nucl. Part. Sci. 15 (Volume 15, 1965) (1965) 29–66, http://dx.doi.org/10.1146/annurev.ns.15.120165.000333, URL https://www.annualreviews.org/content/journals/10.1146/annurev.ns.15.120165.000333.

[75] M. Schumacher, J. Phys. G: Nucl. Phys. 14 (S) (1988) S235, http://dx.doi.org/10.1088/0305-4616/14/S/026.

[76] A. Zilges, D. Balabanski, J. Isaak, N. Pietralla, Prog. Part. Nucl. Phys. 122 (2022) 103903, http://dx.doi.org/10.1016/j.ppnp.2021.103903, URL https://www.sciencedirect.com/science/article/pii/S0146641021000624.

[77] B.S. Ishkhanov, I.M. Kapitonov, Phys.-Usp. 64 (2) (2021) 141, http://dx.doi.org/10.3367/UFNe.2020.02.038725.

[78] D. Measday, A. Clegg, P. Fisher, Nucl. Phys. 61 (2) (1965) 269–281, http://dx.doi.org/10.1016/0029-5582(65)90900-4, URL https://www.sciencedirect.com/science/article/pii/0029558265909004.

[79] G. Baur, D. Trautmann, Phys. Rep. 25 (4) (1976) 293–358, http://dx.doi.org/10.1016/0370-1573(76)90038-7, URL https://www.sciencedirect.com/science/article/pii/0370157376900387.

[80] Z. Wei, J.-R. Wang, Y.-L. Zhang, Z.-W. Huang, Z.-W. Ma, J. Zhang, Y.-Y. Ding, L. Xia, J.-Y. Li, X.-L. Lu, Y. Zhang, D.-P. Xu, L. Yang, Z.-E. Yao, Chin. Phys. C 43 (5) (2019) 054001, http://dx.doi.org/10.1088/1674-1137/43/5/054001.

[81] Z. Wei, Y. Yan, Z.E. Yao, C.L. Lan, J. Wang, Phys. Rev. C 87 (2013) 054605, http://dx.doi.org/10.1103/PhysRevC.87.054605, URL https://link.aps.org/doi/10.1103/PhysRevC.87.054605.

[82] A. Toth, G. Gyürky, E. Papp, T. Szücs, Nucl. Phys. A 1041 (2024) 122778, http://dx.doi.org/10.1016/j.nuclphysa.2023.122778, URL https://www.sciencedirect.com/science/article/pii/S0375947423001811.

[83] M.S. Herrera, G.A. Moreno, A.J. Kreiner, Appl. Radiat. Isot. 88 (2014) 243–246, http://dx.doi.org/10.1016/j.apradiso.2013.11.042, URL https://www.sciencedirect.com/science/article/pii/S0969804313004880. 15th International Congress on Neutron Capture Therapy Impact of a new radiotherapy against cancer.

[84] Y.-N. Zhu, Z.-K. Lin, H.-Y. Yu, Y. Dai, Z.-M. Dai, X.-H. Yu, Nucl. Sci. Tech. 35 (3) (2024) 60, http://dx.doi.org/10.1007/s41365-024-01420-6.

[85] G. Martín-Hernández, P. Mastinu, M. Maggiore, L. Pranovi, G. Prete, J. Praena, R. Capote-Noy, F. Gramegna, A. Lombardi, L. Maran, C. Scian, E. Munaron, Phys. Rev. C 94 (2016) 034620, http://dx.doi.org/10.1103/PhysRevC.94.034620, URL https://link.aps.org/doi/10.1103/PhysRevC.94.034620.

[86] P. Zakalek, P.-E. Doege, J. Baggemann, E. Mauerhofer, T. Brückel, EPJ Web Conf. 231 (2020) 03006, http://dx.doi.org/10.1051/epjconf/202023103006.

[87] M. Rimmler, J. Baggemann, S. Böhm, P.-E. Doege, O. Felden, N.-O. Fröhlich, R. Gebel, J. Li, J. Li, E. Mauerhofer, U. Rücker, M. Strothmann, Y. Valdau, P. Zakalek, T. Gutberlet, T. Brückel, Nucl. Instrum. Methods Phys. Res. Sect. A: Accel. Spectrometers Detect. Assoc. Equip. 990 (2021) 164989, http://dx.doi.org/10.1016/j.nima.2020.164989, URL https://www.sciencedirect.com/science/article/pii/S0168900220313863.

[88] G. Mank, G. Bauer, F. Mulhauser, Rev. Accel. Sci. Technol. 04 (01) (2011) 219–233, http://dx.doi.org/10.1142/S1793626811000549, arXiv:https://doi.org/10.1142/S1793626811000549.

[89] A. Kreisel, I. Eliyahu, S. Vintraub, M. Tessler, I. Horin, N. Goldberger, P. Zakalek, E. Mauerhofer, T. Gutberlet, O. Felden, M. Rimmler, Y. Valdau, Eur. Phys. J. A 59 (8) (2023) 185, URL https://doi.org/10.1140/epja/s10050-023-01056-x.

[90] H. Sato, T. Kamiyama, H. Nagakura, K.-i. Sato, M. Ohnuma, M. Furusaka, EPJ Web Conf. 298 (2024) 05006, http://dx.doi.org/10.1051/epjconf/202429805006.

[91] Y. Otake, J. Neutron Res. 23 (2021) 119–125, http://dx.doi.org/10.3233/JNR-210018, URL https://content.iospress.com/articles/journal-of-neutron-research/jnr210018.

[92] K. Sköld, D.L. Price (Eds.), Neutron Scattering, in: Methods of Experimental Physics, Academic Press, 1986, URL https://www.sciencedirect.com/bookseries/methods-in-experimental-physics/vol/23/part/PA.

[93] T. Brückel, W. Schweika, Polarized Neutron Scattering: Lectures of the 1st Summer School Held at the Forschungszentrum Jülich from 10 to 14 September 2002, in: Schriften des Forschungszentrums Jülich / Materie und Material: Materie und Material, Forschungszentrum Jülich, Central Library, 2002, URL https://books.google.de/books?id=WTaoAAAACAAJ.

[94] A.T. Boothroyd, Principles of Neutron Scattering from Condensed Matter, Oxford University Press, 2020, http://dx.doi.org/10.1093/oso/9780198862314.001.0001.

[95] T. Brückel, S. Förster, M. Kruteva, M. Zobel, R. Zorn, Laboratory Course Neutron Scattering: Lectures, in: Schlüsseltechnologien, vol. 255, Forschungszentrum Jülich GmbH Zentralbibliothek, Verlag, Jülich, 2022, p. 300, URL https://juser.fz-juelich.de/record/909557.

[96] K.H. Beckurts, in: K. Wirtz (Ed.), Neutron Physics [E-Book], Springer, Berlin, Heidelberg, 1964, p. 444, URL http://dx.doi.org/10.1007/978-3-642-87614-1.

[97] The MCNP® Code, URL https://mcnp.lanl.gov/index.html.

[98] T. Sato, Y. Iwamoto, S. Hashimoto, T. Ogawa, T. Furuta, S. Abe, T. Kai, Y. Matsuya, N. Matsuda, Y. Hirata, T. Sekikawa, L. Yao, P.E. Tsai, H.N. Ratliff, H. Iwase, Y. Sakaki, K. Sugihara, N. Shigyo, L. Sihver, K. Niita, J. Nucl. Sci. Technol. 61 (1) (2024) 127–135, http://dx.doi.org/10.1080/00223131.2023.2275736.

[99] A. Ferrari, P.R. Sala, A. Fassò, J. Ranft, FLUKA: A Multi-Particle Transport Code (Program Version 2005), in: CERN Yellow Reports: Monographs, CERN, Geneva, 2005, http://dx.doi.org/10.5170/CERN-2005-010, URL https://cds.cern.ch/record/898301.

[100] T. Böhlen, F. Cerutti, M. Chin, A. Fassò, A. Ferrari, P. Ortega, A. Mairani, P. Sala, G. Smirnov, V. Vlachoudis, Nucl. Data Sheets 120 (2014) 211–214, http://dx.doi.org/10.1016/j.nds.2014.07.049, URL https://www.sciencedirect.com/science/article/pii/S0090375214005018.

[101] J. Allison, K. Amako, J. Apostolakis, P. Arce, M. Asai, T. Aso, E. Bagli, A. Bagulya, S. Banerjee, G. Barrand, B. Beck, A. Bogdanov, D. Brandt, J. Brown, H. Burkhardt, P. Canal, D. Cano-Ott, S. Chauvie, K. Cho, G. Cirrone, G. Cooperman, M. Cortés-Giraldo, G. Cosmo, G. Cuttone, G. Depaola, L. Desorgher, X. Dong, A. Dotti, V. Elvira, G. Folger, Z. Francis, A. Galoyan, L. Garnier, M. Gayer, K. Genser, V. Grichine, S. Guatelli, P. Guèye, P. Gumplinger, A. Howard, I. Hřivnáčová, S. Hwang, S. Incerti, A. Ivanchenko, V. Ivanchenko, F. Jones, S. Jun, P. Kaitaniemi, N. Karakatsanis, M. Karamitros, M. Kelsey, A. Kimura, T. Koi, H. Kurashige, A. Lechner, S. Lee, F. Longo, M. Maire, D. Mancusi, A. Mantero, E. Mendoza, B. Morgan, K. Murakami, T. Nikitina, L. Pandola, P. Paprocki, J. Perl, I. Petrović, M. Pia, W. Pokorski, J. Quesada, M. Raine, M. Reis, A. Ribon, A. Ristić Fira, F. Romano, G. Russo, G. Santin, T. Sasaki, D. Sawkey, J. Shin, I. Strakovsky, A. Taborda, S. Tanaka, B. Tomé, T. Toshito, H. Tran, P. Truscott, L. Urban, V. Uzhinsky, J. Verbeke, M. Verderi, B. Wendt, H. Wenzel, D. Wright, D. Wright, T. Yamashita, J. Yarba, H. Yoshida, Nucl. Instrum. Methods Phys. Res. Sect. A: Accel. Spectrometers Detect. Assoc. Equip. 835 (2016) 186–225, http://dx.doi.org/10.1016/j.nima.2016.06.125, URL https://www.sciencedirect.com/science/article/pii/S0168900216306957.

[102] Neutron scattering lengths and cross sections, URL https://www.ncnr.nist.gov/resources/n-lengths/.

[103] A. Schwab, Design and Manufacturing of a Cryostat for a Compact Cryogenic Neutron Moderator for Operation at Temperatures below 10 K (Ph.D. thesis), RWTH Aachen University, 2024, http://dx.doi.org/10.18154/RWTH-2024-09021, URL https://www.isf.rwth-aachen.de/go/id/jdjp/lidx/1/file/993864.

[104] M.H. Parajon, E. Abad, F. Bermejo, Phys. Procedia 60 (2014) 74–82, http://dx.doi.org/10.1016/j.phpro.2014.11.012, URL https://www.sciencedirect.com/science/article/pii/S1875389214005598.

[105] F. Cantargi, J. Granada, Nucl. Instrum. Methods Phys. Res. Sect. B: Beam Interact. Mater. Atoms 268 (16) (2010) 2487–2491, http://dx.doi.org/10.1016/j.nimb.2010.04.030, URL https://www.sciencedirect.com/science/article/pii/S0168583X10004209.

[106] R. Granada, F. Cantargi, AIP Conf. Proc. 1202 (2010) 8–13, http://dx.doi.org/10.1063/1.3295617.

[107] P. Ageron, Nucl. Instrum. Methods Phys. Res. Sect. A: Accel. Spectrometers Detect. Assoc. Equip. 284 (1) (1989) 197–199, http://dx.doi.org/10.1016/0168-9002(89)90281-7, URL https://www.sciencedirect.com/science/article/pii/0168900289902817.

[108] J.C. Cook, C.F. Majkrzak, H.E. King, Pre-Conceptual Design Activities of the NIST Neutron Source; Simulations of Neutron Beam Characteristics of the Proposed NIST Neutron Source, Tech. Rep., NIST Center for Neutron Research, 2024, URL https://doi.org/10.6028/NIST.TN.2284.

[109] F. Mezei, L. Zanini, A. Takibayev, K. Batkov, E. Klinkby, E. Pitcher, T. Schönfeldt, J. Neutron Res. 17 (2014) 101–105, http://dx.doi.org/10.3233/JNR-140013, URL https://content.iospress.com/articles/journal-of-neutron-research/jnr013.

[110] L. Zanini, K. Andersen, K. Batkov, E. Klinkby, F. Mezei, T. Schönfeldt, A. Takibayev, Nucl. Instrum. Methods Phys. Res. Sect. A: Accel. Spectrometers Detect. Assoc. Equip. 925 (2019) 33–52, http://dx.doi.org/10.1016/j.nima.2019.01.003, URL https://www.sciencedirect.com/science/article/pii/S0168900219300087.

[111] S. Eisenhut, M. Klaus, J. Baggemann, U. Rücker, Y. Beßler, A. Schwab, C. Haberstroh, T. Cronert, T. Gutberlet, T. Brückel, C. Lange, EPJ Web Conf. 231 (2020) 04001, http://dx.doi.org/10.1051/epjconf/202023104001.

[112] Experimental Facilities; Heinz Maier-Leibnitz Zentrum (MLZ), Tech. Rep., MLZ Heinz Maier-Leibnitz Zentrum, 2015, URL https://mlz-garching.de/aktuelles-und-presse/broschueren-und-filme/broschueren/experimental-facilities.html.

[113] C.H. Westcott, Effective Cross Section Values for Well-Moderated Thermal Reactor Spectra. (3rd Edition Corrected), Tech. Rep., Atomic Energy of Canada Ltd., Chalk River, Ontario (Canada), 1960, URL https://www.osti.gov/biblio/4118414.

[114] K.H. Andersen, M. Bertelsen, L. Zanini, E.B. Klinkby, T. Schönfeldt, P.M. Bentley, J. Saroun, J. Appl. Crystallogr. 51 (2) (2018) 264–281, http://dx.doi.org/10.1107/S1600576718002406.

[115] J.R.D. Copley, J. Neutron Res. 1 (1993) 21–36, http://dx.doi.org/10.1080/10238169308200242, URL https://content.iospress.com/articles/journal-of-neutron-research/jnr1-2-01.

[116] F.X. Gallmeier, I. Remec, Rev. Sci. Instrum. 93 (8) (2022) 083301, http://dx.doi.org/10.1063/5.0095900, arXiv:https://pubs.aip.org/aip/rsi/article-pdf/doi/10.1063/5.0095900/16612735/083301_1_online.pdf.

[117] A. Arakengy, Am. J. Phys. 25 (8) (1957) 519–525, http://dx.doi.org/10.1119/1.1934540, arXiv:https://pubs.aip.org/aapt/ajp/article-pdf/25/8/519/11766048/519_1_online.pdf.

[118] J. Voigt, N. Violini, T. Brückel, Nucl. Instrum. Methods Phys. Res. Sect. A: Accel. Spectrometers Detect. Assoc. Equip. 741 (2014) 26–32, http://dx.doi.org/10.1016/j.nima.2013.12.036, URL https://www.sciencedirect.com/science/article/pii/S0168900213017270.

[119] T. Brückel, T. Gutberlet, J. Baggemann, S. Böhm, P. Doege, J. Frenske, M. Feygenson, A. Glavic, O. Holderer, S. Jaksch, M. Jentschel, S. Kleefisch, H. Kleines, J. Li, K. Lieutenant, P. Mastinu, E. Mauerhofer, O. Meusel, S. Pasini, H. Podlech, M. Rimmler, U. Rücker, T. Schrader, W. Schweika, M. Strobl, E. Vezhlev, J. Voigt, P. Zakalek, O. Zimmer, in: T. Brückel, T. Gutberlet (Eds.), Conceptual Design Report Jülich High Brilliance Neutron Source (HBS), Forschungszentrum Jülich GmbH, 2020, URL https://juser.fz-juelich.de/record/884799.

[120] K. Andersen, D. Argyriou, A. Jackson, J. Houston, P. Henry, P. Deen, R. Toft-Petersen, P. Beran, M. Strobl, T. Arnold, H. Wacklin-Knecht, N. Tsapatsaris, E. Oksanen, R. Woracek, W. Schweika, D. Mannix, A. Hiess, S. Kennedy, O. Kirstein, S. Petersson Årsköld, J. Taylor, M. Hagen, G. Laszlo, K. Kanaki, F. Piscitelli, A. Khaplanov, I. Stefanescu, T. Kittelmann, D. Pfeiffer, R. Hall-Wilton, C. Lopez, G. Aprigliano, L. Whitelegg, F. Moreira, M. Olsson, H. Bordallo, D. Martín-Rodríguez, H. Schneider, M. Sharp, M. Hartl, G. Nagy, S. Ansell, S. Pullen, A. Vickery, A. Fedrigo, F. Mezei, M. Arai, R. Heenan, W. Halcrow, D. Turner, D. Raspino, A. Orszulik, J. Cooper, N. Webb, P. Galsworthy, J. Nightingale, S. Langridge, J. Elmer, H. Frielinghaus, R. Hanslik, A. Gussen, S. Jaksch, R. Engels, T. Kozielewski, S. Butterweck, M. Feygenson, P. Harbott, A. Poqué, A. Schwaab, K. Lieutenant, N. Violini, J. Voigt, T. Brückel, M. Koenen, H. Kämmerling, E. Babcock, Z. Salhi, A. Wischnewski, A. Heynen, S. Désert, J. Jestin, F. Porcher, X. Fabrèges, G. Fabrèges, B. Annighöfer, S. Klimko, T. Dupont, T. Robillard, A. Goukassov, S. Longeville, C. Alba-Simionesco, P. Bourges, J. Guyon Le Bouffy, P. Lavie, S. Rodrigues, E. Calzada, M. Lerche, B. Schillinger, P. Schmakat, M. Schulz, M. Seifert, W. Lohstroh, W. Petry, J. Neuhaus, L. Loaiza, A. Tartaglione, A. Glavic, S. Schütz, J. Stahn, E. Lehmann, M. Morgano, J. Schefer, U. Filges, C. Klauser, C. Niedermayer, J. Fenske, G. Nowak, M. Rouijaa, D. Siemers, R. Kiehn, M. Müller, H. Carlsen, L. Udby, K. Lefmann, J. Birk, S. Holm-Dahlin, M. Bertelsen, U.B. Hansen, M. Olsen, M. Christensen, K. Iversen, N. Christensen, H. Rønnow, P. Freeman, B. Hauback, R. Kolevatov, I. Llamas-Jansa, A. Orecchini, F. Sacchetti, C. Petrillo, A. Paciaroni, P. Tozzi, M. Zanatta, P. Luna, I. Herranz, O. del Moral, M. Huerta, M. Magán, M. Mosconi, E. Abad, J. Aguilar, S. Stepanyan, G. Bakedano, R. Vivanco, I. Bustinduy, F. Sordo, J. Martínez, R. Lechner, F. Villacorta, J. Šaroun, P. Lukáš, M. Markó, M. Zanetti, S. Bellissima, L. del Rosso, F. Masi, C. Bovo, M. Chowdhury, A. De Bonis, L. Di Fresco, C. Scatigno, S. Parker, F. Fernandez-Alonso, D. Colognesi, R. Senesi, C. Andreani, G. Gorini, G. Scionti, A. Schreyer, Nucl. Instrum. Methods Phys. Res. Sect. A: Accel. Spectrometers Detect. Assoc. Equip. 957 (2020) 163402, http://dx.doi.org/10.1016/j.nima.2020.163402, URL https://www.sciencedirect.com/science/article/pii/S0168900220300097.

[121] J. Voigt, K. Lieutenant, EPJ Web Conf. 298 (2024) 01004, http://dx.doi.org/10.1051/epjconf/202429801004.

[122] M. Russina, F. Mezei, Nucl. Instrum. Methods Phys. Res. Sect. A: Accel. Spectrometers Detect. Assoc. Equip. 604 (3) (2009) 624–631, http://dx.doi.org/10.1016/j.nima.2009.03.010, URL https://www.sciencedirect.com/science/article/pii/S0168900209004252.

[123] F. Mezei, M. Russina, in: I.S. Anderson, B. Guérard (Eds.), Advances in Neutron Scattering Instrumentation, Vol. 4785, International Society for Optics and Photonics, SPIE, 2002, pp. 24–33, http://dx.doi.org/10.1117/12.451687.

[124] M. Russina, G. Káli, Z. Sánta, F. Mezei, Nucl. Instrum. Methods Phys. Res. Sect. A: Accel. Spectrometers Detect. Assoc. Equip. 654 (1) (2011) 383–389, http://dx.doi.org/10.1016/j.nima.2011.05.077, URL https://www.sciencedirect.com/science/article/pii/S0168900211011673.

[125] M. Harada, N. Watanabe, M. Teshigawara, T. Kai, Y. Ikeda, Nucl. Instrum. Methods Phys. Res. Sect. A: Accel. Spectrometers Detect. Assoc. Equip. 539 (1) (2005) 345–362, http://dx.doi.org/10.1016/j.nima.2004.10.013, URL https://www.sciencedirect.com/science/article/pii/S0168900204022739.

[126] M. Harada, N. Watanabe, M. Teshigawara, T. Kai, T. Kato, Y. Ikeda, Nucl. Instrum. Methods Phys. Res. Sect. A: Accel. Spectrometers Detect. Assoc. Equip. 574 (3) (2007) 407–419, http://dx.doi.org/10.1016/j.nima.2007.01.184, URL https://www.sciencedirect.com/science/article/pii/S0168900207003105.

[127] G.J. Russell, E.J. Pitcher, P.D. Ferguson, B.W. Patton, J. Neutron Res. 6 (1997) 33–62, http://dx.doi.org/10.1080/10238169708200096, URL https://content.iospress.com/articles/journal-of-neutron-research/jnr6-1-3-03.

[128] H. Abele, D. Dubbers, H. Häse, M. Klein, A. Knöpfler, M. Kreuz, T. Lauer, B. Märkisch, D. Mund, V. Nesvizhevsky, A. Petoukhov, C. Schmidt, M. Schumann, T. Soldner, Nucl. Instrum. Methods Phys. Res. Sect. A: Accel. Spectrometers Detect. Assoc. Equip. 562 (1) (2006) 407–417, http://dx.doi.org/10.1016/j.nima.2006.03.020, URL https://www.sciencedirect.com/science/article/pii/S0168900206005328.

[129] P. Böni, Nucl. Instrum. Methods Phys. Res. Sect. A: Accel. Spectrometers Detect. Assoc. Equip. 586 (1) (2008) 1–8, http://dx.doi.org/10.1016/j.nima.2007.11.059, URL https://www.sciencedirect.com/science/article/pii/S0168900207023790. Proceedings of the European Workshop on Neutron Optics.

[130] J. Stahn, U. Filges, T. Panzner, Eur. Phys. J. Appl. Phys. 58 (1) (2012) 11001, http://dx.doi.org/10.1051/epjap/2012110295.

[131] J. Stahn, A. Glavic, Nucl. Instrum. Methods Phys. Res. Sect. A: Accel. Spectrometers Detect. Assoc. Equip. 821 (2016) 44–54, http://dx.doi.org/10.1016/j.nima.2016.03.007, URL https://www.sciencedirect.com/science/article/pii/S0168900216300250.

[132] C. Herb, O. Zimmer, R. Georgii, P. Böni, Nucl. Instrum. Methods Phys. Res. Sect. A: Accel. Spectrometers Detect. Assoc. Equip. 1040 (2022) 167154, http://dx.doi.org/10.1016/j.nima.2022.167154, URL https://www.sciencedirect.com/science/article/pii/S0168900222005290.

[133] A. Houben, W. Schweika, T. Brückel, R. Dronskowski, Nucl. Instrum. Methods Phys. Res. Sect. A: Accel. Spectrometers Detect. Assoc. Equip. 680 (2012) 124–133, http://dx.doi.org/10.1016/j.nima.2012.03.015, URL https://www.sciencedirect.com/science/article/pii/S0168900212002872.

[134] B.V. Kuteev, P.R. Goncharov, V.Y. Sergeev, V.I. Khripunov, Plasma Phys. Rep. 36 (4) (2010) 281–317, http://dx.doi.org/10.1134/S1063780X1004001X.

[135] Komitee Forschung mit Neutronen, 2011, URL https://www.sni-portal.de/en/user-committees/committee-research-with-neutrons.

[136] H.-G. Brokmeier, Procedia Eng. 10 (2011) 1657–1662, http://dx.doi.org/10.1016/j.proeng.2011.04.277, URL https://www.sciencedirect.com/science/article/pii/S1877705811004656. 11th International Conference on the Mechanical Behavior of Materials (ICM11).

[137] H.-G. Brokmeier, W. Gan, C. Randau, M. Völler, J. Rebelo-Kornmeier, M. Hofmann, Nucl. Instrum. Methods Phys. Res. Sect. A: Accel. Spectrometers Detect. Assoc. Equip. 642 (1) (2011) 87–92, http://dx.doi.org/10.1016/j.nima.2011.04.008, URL https://www.sciencedirect.com/science/article/pii/S0168900211007352.

[138] A. Filabozzi, C. Andreani, M. de Pascale, G. Gorini, A. Pietropaolo, E. Perelli Cippo, R. Senesi, M. Tardocchi, W. Kockelmann, J. Neutron Res. 14 (2006) 55, http://dx.doi.org/10.1080/10238160600673128, URL https://content.iospress.com/articles/journal-of-neutron-research/jnr14-1-05.

[139] S. Harjo, T. Kawasaki, F. Grazzi, T. Shinohara, M. Tanaka, AMI Mater. (2019)) http://dx.doi.org/10.2139/ssrn.3391539, URL https://ssrn.com/abstract=3391539.

[140] W. Schäfer, Eur. J. Mineral. 14 (2) (2002) 263–289, http://dx.doi.org/10.1127/0935?1221/2002/0014?0263.

[141] W.B. O'Dell, A.M. Bodenheimer, F. Meilleur, Arch. Biochem. Biophys. 602 (2016) 48–60, http://dx.doi.org/10.1016/j.abb.2015.11.033, URL https://www.sciencedirect.com/science/article/pii/S0003986115301041. Protein Crystallography.

[142] F. Kono, K. Kurihara, T. Tamada, Biophys. Physicobiol. 19 (2022) e190009, http://dx.doi.org/10.2142/biophysico.bppb-v19.0009.
[143] A.V. Feoktystov, H. Frielinghaus, Z. Di, S. Jaksch, V. Pipich, M.-S. Appavou, E. Babcock, R. Hanslik, R. Engels, G. Kemmerling, H. Kleines, A. Ioffe, D. Richter, T. Brückel, J. Appl. Crystallogr. 48 (1) (2015) 61–70, http://dx.doi.org/10.1107/S1600576714025977, arXiv:https://onlinelibrary.wiley.com/doi/pdf/10.1107/S1600576714025977. URL https://onlinelibrary.wiley.com/doi/abs/10.1107/S1600576714025977.
[144] A. Radulescu, V. Pipich, H. Frielinghaus, M.S. Appavou, J. Phys.: Conf. Ser. 351 (1) (2012) 012026, http://dx.doi.org/10.1088/1742-6596/351/1/012026.
[145] S. Mühlbauer, A. Heinemann, A. Wilhelm, L. Karge, A. Ostermann, I. Defendi, A. Schreyer, W. Petry, R. Gilles, Nucl. Instrum. Methods Phys. Res. Sect. A: Accel. Spectrometers Detect. Assoc. Equip. 832 (2016) 297–305, http://dx.doi.org/10.1016/j.nima.2016.06.105, URL https://www.sciencedirect.com/science/article/pii/S0168900216306714.
[146] P. Müller-Buschbaum, E. Metwalli, J.-F. Moulin, V. Kudryashov, M. Haese-Seiller, R. Kampmann, Eur. Phys. J. Spec. Top. 167 (2009) 107–112, http://dx.doi.org/10.1140/epjst/e2009-00944-5.
[147] H. Frielinghaus, M. Gvaramia, G. Mangiapia, S. Jaksch, M. Ganeva, A. Koutsioubas, S. Mattauch, M. Ohl, M. Monkenbusch, O. Holderer, Nucl. Instrum. Methods Phys. Res. Sect. A: Accel. Spectrometers Detect. Assoc. Equip. 871 (2017) 72–76, http://dx.doi.org/10.1016/j.nima.2017.07.064, URL https://www.sciencedirect.com/science/article/pii/S0168900217308392.
[148] M. Stamm, Polymer Surfaces and Interfaces: Characterization, Modification and Applications, in: Springer Ebook Collection / Chemistry and Materials Science 2005-2008, Springer Berlin Heidelberg, 2008, URL https://books.google.de/books?id=nKQ1KVVFmFMC.
[149] A. Ramirez-Cuesta, M. Jones, W. David, Mater. Today 12 (11) (2009) 54–61, http://dx.doi.org/10.1016/S1369-7021(09)70299-8, URL https://www.sciencedirect.com/science/article/pii/S1369702109702998.
[150] Y. Luo, X. Gao, M. Dong, T. Zeng, Z. Chen, M. Yang, Z. Huang, R. Wang, F. Pan, Y. Xiao, Chin. J. Struct. Chem. 42 (5) (2023) 100032, http://dx.doi.org/10.1016/j.cjsc.2023.100032, URL https://www.sciencedirect.com/science/article/pii/S0254586123000259. Special Issue for Neutron Scattering.
[151] M. Abitonze, X. Yu, C.S. Diko, Y. Zhu, Y. Yang, Batteries 8 (12) (2022) http://dx.doi.org/10.3390/batteries8120255, URL https://www.mdpi.com/2313-0105/8/12/255.
[152] O. Holderer, M. Carmo, M. Shviro, W. Lehnert, Y. Noda, S. Koizumi, M.-S. Appavou, M. Appel, H. Frielinghaus, Materials 13 (2020) 1474, http://dx.doi.org/10.3390/ma13061474.
[153] A.T. Boothroyd, Magnetic Diffraction, Oxford University Press, 2020, http://dx.doi.org/10.1093/oso/9780198862314.003.0007, arXiv:https://academic.oup.com/book/0/chapter/367128503/chapter-pdf/45120426/oso-9780198862314-chapter-7.pdf.
[154] S. Mühlbauer, D. Honecker, É.A. Périgo, F. Bergner, S. Disch, A. Heinemann, S. Erokhin, D. Berkov, C. Leighton, M.R. Eskildsen, A. Michels, Rev. Modern Phys. 91 (2019) 015004, http://dx.doi.org/10.1103/RevModPhys.91.015004, URL https://link.aps.org/doi/10.1103/RevModPhys.91.015004.
[155] F. Cousin, G. Fadda, EPJ Web Conf. 236 (2020) 04001, http://dx.doi.org/10.1051/epjconf/202023604001.
[156] C.F. Majkrzak, Nanoscale 15 (2023) 4725–4737, http://dx.doi.org/10.1039/D2NR06756K.
[157] A. Devishvili, K. Zhernenkov, A.J.C. Dennison, B.P. Toperverg, M. Wolff, B. Hjörvarsson, H. Zabel, Rev. Sci. Instrum. 84 (2) (2013) 025112, http://dx.doi.org/10.1063/1.4790717, arXiv:https://pubs.aip.org/aip/rsi/article-pdf/doi/10.1063/1.4790717/16153707/025112_1_online.pdf.
[158] T. Saerbeck, R. Cubitt, A. Wildes, G. Manzin, K.H. Andersen, P. Gutfreund, J. Appl. Crystallogr. 51 (2) (2018) 249–256, http://dx.doi.org/10.1107/S160057671800239X.
[159] R. Campbell, H. Wacklin, I. Sutton, R. Cubitt, G. Fragneto, Eur. Phys. J. Plus 126 (2011) 1–22, http://dx.doi.org/10.1140/epjp/i2011-11107-8.
[160] C.F. Majkrzak, J. Penfold, Neutron News 21 (1) (2010) 46–50, http://dx.doi.org/10.1080/10448630903409483, arXiv:https://doi.org/10.1080/10448630903409483.
[161] Institut Laue Langevin (ILL), URL https://www.ill.eu/neutrons-for-society/neutron-techniques/neutron-diffraction.
[162] ISIS, URL https://www.isis.stfc.ac.uk/Pages/Neutron-diffraction.aspx.
[163] R. Dronskowski, T. Brückel, H. Kohlmann, M. Avdeev, A. Houben, M. Meven, M. Hofmann, T. Kamiyama, M. Zobel, W. Schweika, R.P. Hermann, A. Sano-Furukawa, Z. Krist. - Cryst. Mater. (2024) http://dx.doi.org/10.1515/zkri-2024-0001.
[164] NIMROD@ISIS, URL https://www.isis.stfc.ac.uk/Pages/Nimrod.aspx.
[165] M.T. Dove, G. Li, Nucl. Anal. 1 (4) (2022) 100037, http://dx.doi.org/10.1016/j.nucana.2022.100037, URL https://www.sciencedirect.com/science/article/pii/S2773183922000374.
[166] A.S. Ivanov, P.A. Alekseev, Crystallogr. Rep. 67 (2022) 18–35, http://dx.doi.org/10.1134/S1063774522010072.
[167] M. Kruteva, Adsorption 27 (2021) 875–889, http://dx.doi.org/10.1007/s10450-020-00295-4.
[168] J.S. Gardner, G. Ehlers, A. Faraone, V. García Sakai, Nat. Rev. Phys. 2 (2020) 103–116, http://dx.doi.org/10.1038/s42254-019-0128-1.
[169] N. Kardjilov, I. Manke, A. Hilger, M. Strobl, J. Banhart, Mater. Today 14 (6) (2011) 248–256, http://dx.doi.org/10.1016/S1369-7021(11)70139-0, URL https://www.sciencedirect.com/science/article/pii/S1369702111701390.
[170] D.K. Aswal, P.S. Sarkar, Y.S. Kashyap, Neutron Imaging: Basics, Techniques and Applications, Springer, 2022, http://dx.doi.org/10.1007/978-981-16-6273-7, URL https://link.springer.com/book/10.1007/978-981-16-6273-7.
[171] P. Vontobel, E.H. Lehmann, R. Hassanein, G. Frei, Phys. B 385–386 (2006) 475–480, http://dx.doi.org/10.1016/j.physb.2006.05.252, URL https://www.sciencedirect.com/science/article/pii/S0921452606011161.
[172] R. Woracek, J. Santisteban, A. Fedrigo, M. Strobl, Nucl. Instrum. Methods Phys. Res. Sect. A: Accel. Spectrometers Detect. Assoc. Equip. 878 (2018) 141–158, http://dx.doi.org/10.1016/j.nima.2017.07.040, URL https://www.sciencedirect.com/science/article/pii/S0168900217307817. Radiation Imaging Techniques and Applications.
[173] I.S. Anderson, R.L. McGreevy, H.Z. Bilheux, Neutron Imaging and Applications, vol. 200, Springer Science+ Business Media, 2009, 341 pages. URL https://link.springer.com/book/10.1007/978-0-387-78693-3.
[174] E. Lehmann, D. Mannes, A. Kaestner, C. Grünzweig, Phys. Procedia 88 (2017) 5–12, http://dx.doi.org/10.1016/j.phpro.2017.06.055, URL https://www.sciencedirect.com/science/article/pii/S1875389217301050. Neutron Imaging for Applications in Industry and Science Proceedings of the 8th International Topical Meeting on Neutron Radiography (ITMNR-8) Beijing, China, September 4-8, 2016.
[175] P. Boillat, G. Frei, E.H. Lehmann, G.G. Scherer, A. Wokaun, Electrochem. Solid- State Lett. 13 (3) (2010) B25, http://dx.doi.org/10.1149/1.3279636.
[176] R.F. Ziesche, N. Kardjilov, W. Kockelmann, D.J. Brett, P.R. Shearing, Joule 6 (1) (2022) 35–52, http://dx.doi.org/10.1016/j.joule.2021.12.007, URL https://www.sciencedirect.com/science/article/pii/S2542435121005766.
[177] S. Soria, X. Li, M. Schulz, M. Boin, M. Hofmann, Mater. Charact. 166 (2020) 110453, http://dx.doi.org/10.1016/j.matchar.2020.110453, URL https://www.sciencedirect.com/science/article/pii/S1044580320319240.
[178] M. Strobl, H. Heimonen, S. Schmidt, M. Sales, N. Kardjilov, A. Hilger, I. Manke, T. Shinohara, J. Valsecchi, J. Phys. D: Appl. Phys. 52 (12) (2019) 123001, http://dx.doi.org/10.1088/1361-6463/aafa5e.
[179] C. Tötzke, N. Kardjilov, N. Lenoir, I. Manke, S.E. Oswald, A. Tengattini, Opt. Express 27 (20) (2019) 28640–28648, http://dx.doi.org/10.1364/OE.27.028640, URL https://opg.optica.org/oe/abstract.cfm?URI=oe-27-20-28640.
[180] M. Strobl, Phys. Procedia 69 (2015) 18–26, http://dx.doi.org/10.1016/j.phpro.2015.07.002, URL https://www.sciencedirect.com/science/article/pii/S1875389215006124. Proceedings of the 10th World Conference on Neutron Radiography (WCNR-10) Grindelwald, Switzerland October 5–10, 2014.
[181] E. Lehmann, P. Trtik, D. Ridikas, Phys. Procedia 88 (2017) 140–147, http://dx.doi.org/10.1016/j.phpro.2017.06.019, URL https://www.sciencedirect.com/science/article/pii/S187538921730069X. Neutron Imaging for Applications in Industry and Science Proceedings of the 8th International Topical Meeting on Neutron Radiography (ITMNR-8) Beijing, China, September 4-8, 2016.

[182] D. Dubbers, Prog. Part. Nucl. Phys. 26 (1991) 173–252, http://dx.doi.org/10.1016/0146-6410(91)90011-C, URL https://www.sciencedirect.com/science/article/pii/014664109190011C.

[183] Y. Kuno, G. Pignol, C. R. Phys. 21 (1) (2020) 121–134, http://dx.doi.org/10.5802/crphys.13, URL https://comptes-rendus.academie-sciences.fr/physique/articles/10.5802/crphys.13/.

[184] D. Dubbers, M.G. Schmidt, Rev. Modern Phys. 83 (2011) 1111–1171, http://dx.doi.org/10.1103/RevModPhys.83.1111, URL https://link.aps.org/doi/10.1103/RevModPhys.83.1111.

[185] Particle Data Group, P.A. Zyla, R.M. Barnett, J. Beringer, O. Dahl, D.A. Dwyer, D.E. Groom, C.J. Lin, K.S. Lugovsky, E. Pianori, D.J. Robinson, C.G. Wohl, W.M. Yao, K. Agashe, G. Aielli, B.C. Allanach, C. Amsler, M. Antonelli, E.C. Aschenauer, D.M. Asner, H. Baer, S. Banerjee, L. Baudis, C.W. Bauer, J.J. Beatty, V.I. Belousov, S. Bethke, A. Bettini, O. Biebel, K.M. Black, E. Blucher, O. Buchmuller, V. Burkert, M.A. Bychkov, R.N. Cahn, M. Carena, A. Ceccucci, A. Cerri, D. Chakraborty, R.S. Chivukula, G. Cowan, G. D'Ambrosio, T. Damour, D. de Florian, A. de Gouvêa, T. DeGrand, P. de Jong, G. Dissertori, B.A. Dobrescu, M. D'Onofrio, M. Doser, M. Drees, H.K. Dreiner, P. Eerola, U. Egede, S. Eidelman, J. Ellis, J. Erler, V.V. Ezhela, W. Fetscher, B.D. Fields, B. Foster, A. Freitas, H. Gallagher, L. Garren, H.J. Gerber, G. Gerbier, T. Gershon, Y. Gershtein, T. Gherghetta, A.A. Godizov, M.C. Gonzalez-Garcia, M. Goodman, C. Grab, A.V. Gritsan, C. Grojean, M. Grünewald, A. Gurtu, T. Gutsche, H.E. Haber, C. Hanhart, S. Hashimoto, Y. Hayato, A. Hebecker, S. Heinemeyer, B. Heltsley, J.J. Hernández-Rey, K. Hikasa, J. Hisano, A. Höcker, J. Holder, A. Holtkamp, J. Huston, T. Hyodo, K.F. Johnson, M. Kado, M. Karliner, U.F. Katz, M. Kenzie, V.A. Khoze, S.R. Klein, E. Klempt, R.V. Kowalewski, F. Krauss, M. Kreps, B. Krusche, Y. Kwon, O. Lahav, J. Laiho, L.P. Lellouch, J. Lesgourgues, A.R. Liddle, Z. Ligeti, C. Lippmann, T.M. Liss, L. Littenberg, C. Lourengo, S.B. Lugovsky, A. Lusiani, Y. Makida, F. Maltoni, T. Mannel, A.V. Manohar, W.J. Marciano, A. Masoni, J. Matthews, U.G. Meißner, M. Mikhasenko, D.J. Miller, D. Milstead, R.E. Mitchell, K. Mönig, P. Molaro, F. Moortgat, M. Moskovic, K. Nakamura, M. Narain, P. Nason, S. Navas, M. Neubert, P. Nevski, Y. Nir, K.A. Olive, C. Patrignani, J.A. Peacock, S.T. Petcov, V.A. Petrov, A. Pich, A. Piepke, A. Pomarol, S. Profumo, A. Quadt, K. Rabbertz, J. Rademacker, G. Raffelt, H. Ramani, M. Ramsey-Musolf, B.N. Ratcliff, P. Richardson, A. Ringwald, S. Roesler, S. Rolli, A. Romaniouk, L.J. Rosenberg, J.L. Rosner, G. Rybka, M. Ryskin, R.A. Ryutin, Y. Sakai, G.P. Salam, S. Sarkar, F. Sauli, O. Schneider, K. Scholberg, A.J. Schwartz, J. Schwiening, D. Scott, V. Sharma, S.R. Sharpe, T. Shutt, M. Silari, T. Sjöstrand, P. Skands, T. Skwarnicki, G.F. Smoot, A. Soffer, M.S. Sozzi, S. Spanier, C. Spiering, A. Stahl, S.L. Stone, Y. Sumino, T. Sumiyoshi, M.J. Syphers, F. Takahashi, M. Tanabashi, J. Tanaka, M. Taševský, K. Terashi, J. Terning, U. Thoma, R.S. Thorne, L. Tiator, M. Titov, N.P. Tkachenko, D.R. Tovey, K. Trabelsi, P. Urquijo, G. Valencia, R. Van de Water, N. Varelas, G. Venanzoni, L. Verde, M.G. Vincter, P. Vogel, W. Vogelsang, A. Vogt, V. Vorobyev, S.P. Wakely, W. Walkowiak, C.W. Walter, D. Wands, M.O. Wascko, D.H. Weinberg, E.J. Weinberg, M. White, L.R. Wiencke, S. Willocq, C.L. Woody, R.L. Workman, M. Yokoyama, R. Yoshida, G. Zanderighi, G.P. Zeller, O.V. Zenin, R.Y. Zhu, S.L. Zhu, F. Zimmermann, J. Anderson, T. Basaglia, V.S. Lugovsky, P. Schaffner, W. Zheng, Prog. Theor. Exp. Phys. 2020 (8) (2020) 083C01, http://dx.doi.org/10.1093/ptep/ptaa104, arXiv:https://academic.oup.com/ptep/article-pdf/2020/8/083C01/34673722/ptaa104.pdf.

[186] European Strategy for Particle Physics Preparatory Group, 2020, arXiv:1910.11775. URL https://doi.org/10.48550/arXiv.1910.11775.

[187] C. Abel, S. Afach, N.J. Ayres, C.A. Baker, G. Ban, G. Bison, K. Bodek, V. Bondar, M. Burghoff, E. Chanel, Z. Chowdhuri, P.-J. Chiu, B. Clement, C.B. Crawford, M. Daum, S. Emmenegger, L. Ferraris-Bouchez, M. Fertl, P. Flaux, B. Franke, A. Fratangelo, P. Geltenbort, K. Green, W.C. Griffith, M. van der Grinten, Z.D. Grujić, P.G. Harris, L. Hayen, W. Heil, R. Henneck, V. Hélaine, N. Hild, Z. Hodge, M. Horras, P. Iaydjiev, S.N. Ivanov, M. Kasprzak, Y. Kermaidic, K. Kirch, A. Knecht, P. Knowles, H.-C. Koch, P.A. Koss, S. Komposch, A. Kozela, A. Kraft, J. Krempel, M. Kuźniak, B. Lauss, T. Lefort, Y. Lemière, A. Leredde, P. Mohanmurthy, A. Mtchedlishvili, M. Musgrave, O. Naviliat-Cuncic, D. Pais, F.M. Piegsa, E. Pierre, G. Pignol, C. Plonka-Spehr, P.N. Prashanth, G. Quéméner, M. Rawlik, D. Rebreyend, I. Rienäcker, D. Ries, S. Roccia, G. Rogel, D. Rozpedzik, A. Schnabel, P. Schmidt-Wellenburg, N. Severijns, D. Shiers, R. Tavakoli Dinani, J.A. Thorne, R. Virot, J. Voigt, A. Weis, E. Wursten, G. Wyszynski, J. Zejma, J. Zenner, G. Zsigmond, Phys. Rev. Lett. 124 (2020) 081803, http://dx.doi.org/10.1103/PhysRevLett.124.081803, URL https://link.aps.org/doi/10.1103/PhysRevLett.124.081803.

[188] A. Falkowski, M. González-Alonso, O. Naviliat-Cuncic, J. High Energy Phys. 2021 (4) (2021) 126, http://dx.doi.org/10.1007/JHEP04(2021)126.

[189] S. Sponar, R.I.P. Sedmik, M. Pitschmann, H. Abele, Y. Hasegawa, Nat. Rev. Phys. 3 (5) (2021) 309–327, http://dx.doi.org/10.1038/s42254-021-00298-2.

[190] OECD and Nuclear Energy Agency, 2005, p. 64, http://dx.doi.org/10.1787/9789264008823-en, URL https://www.oecd-ilibrary.org/content/publication/9789264008823-en.

[191] Manual for Reactor Produced Radioisotopes, in: Technical Reports Series, no. 1340, International Atomic Energy Agency, Vienna, 2003, URL https://www.iaea.org/publications/6407/manual-for-reactor-produced-radioisotopes.

[192] Cyclotron Produced Radionuclides: Physical Characteristics and Production Methods, in: Technical Reports Series, no. 468, International Atomic Energy Agency, Vienna, 2009, URL https://www.iaea.org/publications/7892/cyclotron-produced-radionuclides-physical-characteristics-and-production-methods.

[193] Y. Nagai, K. Hashimoto, Y. Hatsukawa, H. Saeki, S. Motoishi, N. Sato, M. Kawabata, H. Harada, T. Kin, K. Tsukada, T.K. Sato, F. Minato, O. Iwamoto, N. Iwamoto, Y. Seki, K. Yokoyama, T. Shiina, A. Ohta, N. Takeuchi, T. Igarashi, J. Phys. Soc. Japan 83 (2013) http://dx.doi.org/10.7566/JPSJ.82.064201, JPSJ.82.064201. URL https://journals.jps.jp/doi/10.7566/JPSJ.82.064201.

[194] The Supply of Medical Radioisotopes: 2019 Medical Isotope Demand and Capacity Projection for the 2019–2024 Period, OECD Publishing, Paris, 2019, URL https://www.oecd-nea.org/med-radio/docs/sen-hlgmr2019-1.pdf.

[195] R. Seviour, IPAC 16, 2016, URL http://eprints.hud.ac.uk/id/eprint/28570/.

[196] Y. Nagai, Phys. Procedia 66 (2015) 370–375, http://dx.doi.org/10.1016/j.phpro.2015.05.046, URL http://www.sciencedirect.com/science/article/pii/S1875389215001996. The 23rd International Conference on the Application of Accelerators in Research and Industry - CAARI 2014.

[197] R.D. Schrimpf, D.M. Fleetwood, Radiation Effects and Soft Errors in Integrated Circuits and Electronic Devices, World Scientific, 2004, http://dx.doi.org/10.1142/5607, arXiv:https://www.worldscientific.com/doi/pdf/10.1142/5607. URL https://www.worldscientific.com/doi/abs/10.1142/5607.

[198] M. Durante, F.A. Cucinotta, Rev. Modern Phys. 83 (2011) 1245–1281, http://dx.doi.org/10.1103/RevModPhys.83.1245, URL https://link.aps.org/doi/10.1103/RevModPhys.83.1245.

[199] A.C.M. Prado, C.A. Federico, E.C.F. Pereira Junior, O.L. Goncalez, Effects of Cosmic Radiation on Devices and Embedded Systems in Aircrafts, Brazil, 2013, URL http://inis.iaea.org/search/search.aspx?orig_q=RN:45087489.

[200] J. Troska, F. Vasey, A. Weidberg, Nucl. Instrum. Methods Phys. Res. Sect. A: Accel. Spectrometers Detect. Assoc. Equip. 1052 (2023) 168208, http://dx.doi.org/10.1016/j.nima.2023.168208, URL https://www.sciencedirect.com/science/article/pii/S0168900223001985.

[201] Q. Huang, J. Jiang, Prog. Nucl. Energy 114 (2019) 105–120, http://dx.doi.org/10.1016/j.pnucene.2019.02.008, URL https://www.sciencedirect.com/science/article/pii/S0149197019300563.

[202] C.-J. Tsai, K.-W. Chang, B.-H. Yang, P.-H. Wu, K.-H. Lin, C.Y.O. Wong, H.-L. Lee, W.-S. Huang, Life 12 (6) (2022) http://dx.doi.org/10.3390/life12060912, URL https://www.mdpi.com/2075-1729/12/6/912.

[203] C. Andreani, R. Senesi, A. Paccagnella, M. Bagatin, S. Gerardin, C. Cazzaniga, C.D. Frost, P. Picozza, G. Gorini, R. Mancini, M. Sarno, AIP Adv. 8 (2) (2018) 025013, http://dx.doi.org/10.1063/1.5017945, arXiv:https://pubs.aip.org/aip/adv/article-pdf/doi/10.1063/1.5017945/12995529/025013_1_online.pdf.

[204] W. Dörr, Ann. ICRP 44 (1_suppl) (2015) 58–68, http://dx.doi.org/10.1177/0146645314560686, arXiv:https://doi.org/10.1177/0146645314560686. PMID: 25816259.

[205] G. Figueroa-González, C. Pérez-Plasencia, Oncol. Lett. 13 (6) (2017) 3982–3988, http://dx.doi.org/10.3892/ol.2017.6002.

[206] W.W. Kuhne, B.B. Gersey, R. Wilkins, H. Wu, S.A. Wender, V. George, W.S. Dynan, Radiat. Res. 172 (4) (2009) 473–480, http://dx.doi.org/10.1667/RR1556.1, arXiv:https://meridian.allenpress.com/radiation-research/article-pdf/172/4/473/2147787/rr1556_1.pdf.

[207] M. Pedrosa-Rivera, M. Ruiz-Magaña, I. Porras, J. Praena, P. Torres-Sánchez, M. Sabariego, U. Köster, T. Forsyth, T. Soldner, M. Haertlein, C. Ruiz-Ruiz, Nucl. Instrum. Methods Phys. Res. Sect. B: Beam Interact. Mater. Atoms 462 (2020) 24–31, http://dx.doi.org/10.1016/j.nimb.2019.10.027, URL https://www.sciencedirect.com/science/article/pii/S0168583X19307396.

[208] M. Hatsuda, H. Kawasaki, A. Shigenaga, A. Taketani, T. Takanashi, Y. Wakabayashi, Y. Otake, Y. Kamata, A. Ichinose, H. Nishioka, H. Kimura, Y. Koganei, S. Komoriya, M. Sakai, Y. Hamano, M. Yoshida, F. Yamakura, Sci. Rep. 13 (1) (2023) 12479.

[209] S. Albright, R. Seviour, Appl. Radiat. Isot. 110 (2016) 224–229, http://dx.doi.org/10.1016/j.apradiso.2015.12.032, URL https://www.sciencedirect.com/science/article/pii/S0969804315303729.

[210] S. Albright, R. Seviour, J. Radiol. Prot. 35 (3) (2015) 507, http://dx.doi.org/10.1088/0952-4746/35/3/507.

[211] D. Bisello, A. Candelori, N. Dzysiuk, J. Esposito, P. Mastinu, S. Mattiazzo, G. Prete, L. Silvestrin, J. Wyss, Phys. Procedia 26 (2012) 284–293, http://dx.doi.org/10.1016/j.phpro.2012.03.036, URL https://www.sciencedirect.com/science/article/pii/S187538921200452X. Proceedings of the first two meetings of the Union of Compact Accelerator-Driven Neutron Sources.

[212] C. Claeys, E.S.E. Division, Electrochemical Society: Proceedings, Electrochemical Society, 1998, URL https://books.google.de/books?id=jD7ZGk12fsgC.

[213] Neutron Transmutation Doping of Silicon at Research Reactors, in: TECDOC Series, no. 1681, International Atomic Eenergy Agency, Vienna, 2012, URL https://www.iaea.org/publications/8739/neutron-transmutation-doping-of-silicon-at-research-reactors.

[214] W.A.G. Sauerwein, L. Sancey, E. Hey-Hawkins, M. Kellert, L. Panza, D. Imperio, M. Balcerzyk, G. Rizzo, E. Scalco, K. Herrmann, P. Mauri, A. De Palma, A. Wittig, Life 11 (4) (2021) http://dx.doi.org/10.3390/life11040330, URL https://www.mdpi.com/2075-1729/11/4/330.

[215] L. Porra, T. Seppälä, L. Wendland, H. Revitzer, H. Joensuu, P. Eide, H. Koivunoro, N. Smick, T. Smick, M. Tenhunen, Acta Oncol. 61 (2) (2022) 269–273, http://dx.doi.org/10.1080/0284186X.2021.1979646, arXiv:https://doi.org/10.1080/0284186X.2021.1979646. PMID: 34569418.

[216] Y. Kiyanagi, Y. Sakurai, H. Kumada, H. Tanaka, AIP Conf. Proc. 2160 (1) (2019) 050012, http://dx.doi.org/10.1063/1.5127704, arXiv:https://pubs.aip.org/aip/acp/article-pdf/doi/10.1063/1.5127704/14196577/050012_1_online.pdf.

[217] H. Kumada, A. Matsumura, H. Sakurai, T. Sakae, M. Yoshioka, H. Kobayashi, H. Matsumoto, Y. Kiyanagi, T. Shibata, H. Nakashima, Appl. Radiat. Isot. 88 (2014) 211–215, http://dx.doi.org/10.1016/j.apradiso.2014.02.018, URL https://www.sciencedirect.com/science/article/pii/S0969804314000700. 15th International Congress on Neutron Capture Therapy Impact of a new radiotherapy against cancer.

[218] Y.-S. Bae, D.-S. Kim, H.J. Seo, J.-U. Han, H.J. Yoon, J.J. Hwang, J.J. Kim, B.H. Woo, H.J. Kim, Y.S. Jang, S.C. Han, W.H. Kim, D.G. Kang, H.J. Seo, S.Y. Lee, S.J. Jeon, J. Yi, J. Lee, I.H. Seo, S.H. Kim, W.H. Kim, N.H. Park, M.H. Lee, S.J. Bae, S.H. Lee, G.H. Cho, S.H. Kim, S.H. Moon, M.K. Lee, J.W. Choi, K.Y. Lee, D.S. Huh, D.W. Kim, K.J. Min, H.M. Yoon, H. Kyung, J. Yang, D. Na, S. Lee, J. Han, Y. Kwak, S.-Y. Lee, J.Y. Nam, B.-H. Choi, Y.-K. Moon, W. Do, M. Yoo, S.-S. Park, AAPPS Bull. 32 (2022) http://dx.doi.org/10.1007/s43673-022-00063-2.

[219] R.L. Paul, R.M. Lindstrom, J. Radioanal. Nucl. Chem. 243 (1) (2000) 181–189, http://dx.doi.org/10.1023/A:1006796003933.

[220] G. Molnar, Handbook of Prompt Gamma Activation Analysis: with Neutron Beams, Springer Science & Business Media, 2010, http://dx.doi.org/10.1007/978-0-387-23359-8, URL https://link.springer.com/book/10.1007/978-0-387-23359-8.

[221] Forschungs-Neutronenquelle Heinz Maier-Leibnitz (FRM II), Technische Universität München, Research Neutron Source Heinz Maier-Leibnitz (FRM II), URL https://www.frm2.tum.de/en/frm2/home/.

[222] A. Axmann, K. Böning, M. Rottmann, Nucl. Eng. Des. 178 (1) (1997) 127–133, http://dx.doi.org/10.1016/S0029-5493(97)00215-X, URL https://www.sciencedirect.com/science/article/pii/S002954939700215X.

[223] C. Reiter, H. Breitkreutz, A. Röhrmoser, A. Seubert, W. Petry, Ann. Nucl. Energy 131 (2019) 1–8, http://dx.doi.org/10.1016/j.anucene.2019.03.010, URL https://www.sciencedirect.com/science/article/pii/S0306454919301355.

[224] A. Röhrmoser, Nucl. Eng. Des. 240 (6) (2010) 1417–1432, http://dx.doi.org/10.1016/j.nucengdes.2010.02.011, URL https://www.sciencedirect.com/science/article/pii/S0029549310001214.

[225] W. Gaubatz, K. Gobrecht, Phys. B 276–278 (2000) 104–105, http://dx.doi.org/10.1016/S0921-4526(99)01260-0, URL https://www.sciencedirect.com/science/article/pii/S0921452699012600.

[226] K. Gobrecht, E. Gutsmiedl, A. Scheuer, Phys. B 311 (1) (2002) 148–151, http://dx.doi.org/10.1016/S0921-4526(01)01130-9, URL https://www.sciencedirect.com/science/article/pii/S0921452601011309. Proceedings of the International Symposium on Advanced Utilizatio n of Research Reactors - Neutron Sources and Neutron Beam Devices.

[227] International Atomic Energy Agency, Research Reactor Database (RRDB), URL https://www.iaea.org/resources/databases/research-reactor-database-rrdb.

[228] General Atomics, TRIGA Nuclear Reactors, URL https://www.ga.com/triga/.

[229] IBR-2, URL https://flnp.jinr.int/en-us/main/facilities/materials/ibr-2-reactor-parameters.

[230] J. Womersley, A. Schreyer, Neutron Users in Europe: Facility-Based Insights and Scientific Trends, European Spallation Source ERIC, 2018, https://europeanspallationsource.se/sites/default/files/files/document/2018-06/NEUTRONUSERSINEUROPE-Facility-BasedInsightsandScientificTrends.pdf.

[231] JRR-3, URL https://www.issp.u-tokyo.ac.jp/labs/neutron/jrr3/.

[232] G.L. Flanagan, 1995, URL https://www.igorr.com/_media/proceedings:1995_igorr4:36023821.pdf.

[233] D. Sahin, O. Celikten, R. Williams, J. Cook, A. Weiss, T. Newton, D. Diamond, C.F. Majkrzak, H. King, J. Shen, A. Gurgen, E. Nahmani, I. Baroukh, L.-Y. Cheng, RERTR 2022 – 42nd International Meeting on Reduced Enrichment for Research and Test Reactors, Vienna, AT, 2022, URL https://tsapps.nist.gov/publication/get_pdf.cfm?pub_id=935600.

[234] CARR, URL https://neutronsources.org/neutron-centres/africa-asia-and-oceania/carr/.

[235] S. Kim, Nucl. Eng. Technol. 38 (2006) 443–448, URL https://koreascience.kr/article/JAKO200633242397743.page.

[236] J.O.J. Lowell A. Charlton, T.A. Gabriel, 2000, pp. 94–102, http://dx.doi.org/10.13182/NT00-A3131, arXiv:https://doi.org/10.13182/NT00-A3131.

[237] F. Maekawa, M. Harada, K. Oikawa, M. Teshigawara, T. Kai, S. ichiro Meigo, M. Ooi, S. Sakamoto, H. Takada, M. Futakawa, T. Kato, Y. Ikeda, N. Watanabe, T. Kamiyama, S. Torii, R. Kajimoto, M. Nakamura, Nucl. Instrum. Methods Phys. Res. Sect. A: Accel. Spectrometers Detect. Assoc. Equip. 620 (2) (2010) 159–165, http://dx.doi.org/10.1016/j.nima.2010.04.020, URL https://www.sciencedirect.com/science/article/pii/S0168900210008223.

[238] W. Jie, F. Shi-Nian, T. Jing-Yu, T. Ju-Zhou, W. Ding-Sheng, W. Fang-Wei, W. Sheng, Chin. Phys. C 33 (11) (2009) 1033, http://dx.doi.org/10.1088/1674-1137/33/11/021.

[239] S. Peggs, R. Kreier, C. Carlile, R. Miyamoto, A. Pahlsson, M. Trojer, J. Weisnd II, ESS Technical Design Report, European Spallation Source ERIC, 2013, URL https://europeanspallationsource.se/sites/default/files/downloads/2017/09/TDR_online_ver_all.pdf.

[240] C. Carlile, Phys. B 385–386 (2006) 961–965, http://dx.doi.org/10.1016/j.physb.2006.05.283, URL https://www.sciencedirect.com/science/article/pii/S0921452606011793.

[241] J.L.M. Andrew Harrison, R. Wagner, Neutron News 21 (2) (2010) 11–14, http://dx.doi.org/10.1080/10448631003697977, arXiv:https://doi.org/10.1080/10448631003697977.

[242] W. Gläser, Appl. Phys. A 74 (2002) s23–s29, http://dx.doi.org/10.1007/s003390201901.

[243] L. Rosta, R. Baranyai, Neutron News 22 (3) (2011) 31–36, http://dx.doi.org/10.1080/10448632.2011.598805, arXiv:https://doi.org/10.1080/10448632.2011.598805.

[244] P. Mikula, P. Strunz, Proceedings of the International Conference on Research Reactors: Safe Management and Effective Utilization, Vienna, Austria, January 16-20, 2015, URL https://conferences.iaea.org/event/75/contributions/10765/attachments/5252/6406/Mikula_IAEA_Paper.pdf.

[245] G. Krzysztoszek, A. Golob, J. Jaroszewicz, 2003, URL https://inis.iaea.org/collection/NCLCollectionStore/_Public/36/036/36036720.pdf?r=1.

[246] K. Eberhardt, C. Geppert, Radiochim. Acta 107 (7) (2019) 535–546, http://dx.doi.org/10.1515/ract-2019-3127, [cited 14 May 2024].

[247] M. Villa, H. Boeck, A. Musilek, Utilization of a Typical 250 kW TRIGA Mark II Reactor at a University, Nuclear Society of Slovenia, Slovenia, 2007, p. 831, URL http://inis.iaea.org/search/search.aspx?orig_q=RN:39095677.

[248] A. Persic, T. Nemec, Ljubljana TRIGA Mark II, 40 Years of Successful Operation, International Atomic Energy Agency, 2008, URL https://inis.iaea.org/search/search.aspx?orig_q=RN:39043156.

[249] D. Chandler, C.D. Bryan, Encycl. Nucl. Energy (2021) 64–73, http://dx.doi.org/10.1016/B978-0-12-819725-7.00051-9, URL https://www.sciencedirect.com/science/article/pii/B9780128197257000519.

[250] H. Prask, J. Rowe, J. Rush, I. Schroeder, J. Res. Natl. Inst. Stand. Technol. 98 (1) (1993) 1, http://dx.doi.org/10.6028/jres.098.001.

[251] F. Sakurai, Y. Horiguchi, S. Kobayashi, M. Takayanagi, Phys. B 311 (1) (2002) 7–13, http://dx.doi.org/10.1016/S0921-4526(01)01048-1, URL https://www.sciencedirect.com/science/article/pii/S0921452601010481. Proceedings of the International Symposium on Advanced Utilization of Research Reactors - Neutron Sources and Neutron Beam Devices.

[252] C.-O. Choi, H.-R. Kim, K.-H. Lee, C.-S. Lee, J.-M. Sohn, Phys. B 311 (1) (2002) 34–39, http://dx.doi.org/10.1016/S0921-4526(01)01052-3, URL https://www.sciencedirect.com/science/article/pii/S0921452601010523. Proceedings of the International Symposium on Advanced Utilization of Research Reactors - Neutron Sources and Neutron Beam Devices.

[253] D. Chen, Y. Liu, C. Gou, C. Ye, Phys. B 385–386 (2006) 966–967, http://dx.doi.org/10.1016/j.physb.2006.05.284, URL https://www.sciencedirect.com/science/article/pii/S092145260601180X.

[254] C. Ye, Phys. B 241–243 (1997) 48–49, http://dx.doi.org/10.1016/S0921-4526(97)00509-7, URL https://www.sciencedirect.com/science/article/pii/S0921452697005097. Proceedings of the International Conference on Neutron Scattering.

[255] G. Sun, C. Zhang, B. Chen, J. Gong, S. Peng, Neutron News 27 (4) (2016) 21–26, http://dx.doi.org/10.1080/10448632.2016.1233018, arXiv:https://doi.org/10.1080/10448632.2016.1233018.

[256] R.A. Robinson, S.J. Kennedy, Neutron News 14 (4) (2003) 14–18, http://dx.doi.org/10.1080/10448630308217652, arXiv:https://doi.org/10.1080/10448630308217652.

[257] A.V. Belushkin, Neutron News 2 (2) (1991) 14–18, http://dx.doi.org/10.1080/10448639108218724, arXiv:https://doi.org/10.1080/10448639108218724.

[258] Y. Dragunov, I. Tretiyakov, A. Lopatkin, N. Romanova, I. Lukasevich, V. Ananyev, A. Vinogradov, A. Dolgikh, L. Yedunov, Y. Pepelyshev, A.D. Rogov, E.P. Shabalin, A.A. Zaikin, I.S. Golovnin, At. Energy 113 (1) (2012) 29–38, http://dx.doi.org/10.1007/s10512-012-9591-9.

[259] A. Serebrov, A. Okorokov, Neutron News 11 (2) (2000) 18–27, http://dx.doi.org/10.1080/10448630008233729, arXiv:https://doi.org/10.1080/10448630008233729.

[260] A.Y. Rumiantsev, V.A. Somenkov, Neutron News 8 (1) (1997) 13–20, http://dx.doi.org/10.1080/10448639708231958, arXiv:https://doi.org/10.1080/10448639708231958.

[261] F. Sánchez, A. Cintas, H. Blaumann, Neutron News 25 (4) (2014) 6–8, http://dx.doi.org/10.1080/10448632.2014.955416, arXiv:https://doi.org/10.1080/10448632.2014.955416.

[262] T. Mason, D. Abernathy, I. Anderson, J. Ankner, T. Egami, G. Ehlers, A. Ekkebus, G. Granroth, M. Hagen, K. Herwig, J. Hodges, C. Hoffmann, C. Horak, L. Horton, F. Klose, J. Larese, A. Mesecar, D. Myles, J. Neuefeind, M. Ohl, C. Tulk, X.-L. Wang, J. Zhao, Phys. B 385–386 (2006) 955–960, http://dx.doi.org/10.1016/j.physb.2006.05.281, URL https://www.sciencedirect.com/science/article/pii/S092145260601177X.

[263] R.K. Crawford, R. Dean, P. Ferguson, J. Galambos, F. Gallmeier, T. McManamy, M. Rennich, J. Phys.: Conf. Ser. 251 (1) (2010) 012054, http://dx.doi.org/10.1088/1742-6596/251/1/012054.

[264] M. Arai, F. Maekawa, Nucl. Phys. News 19 (4) (2009) 34–39, http://dx.doi.org/10.1080/10506890903405316.

[265] M. Futakawa, F. Maekawa, S. Sakamoto, Neutron News 22 (1) (2011) 15–19, http://dx.doi.org/10.1080/10448632.2011.546307.

[266] R. Garoby, A. Vergara, H. Danared, I. Alonso, E. Bargallo, B. Cheymol, C. Darve, M. Eshraqi, H. Hassanzadegan, A. Jansson, I. Kittelmann, Y. Levinsen, M. Lindroos, C. Martins, Ø. Midttun, R. Miyamoto, S. Molloy, D. Phan, A. Ponton, E. Sargsyan, T. Shea, A. Sunesson, L. Tchelidze, C. Thomas, M. Jensen, W. Hees, P. Arnold, M. Juni-Ferreira, F. Jensen, A. Lundmark, D. McGinnis, N. Gazis, J.W. II, M. Anthony, E. Pitcher, L. Coney, M. Gohran, J. Haines, R. Linander, D. Lyngh, U. Oden, H. Carling, R. Andersson, S. Birch, J. Cereijo, T. Friedrich, T. Korhonen, E. Laface, M. Mansouri-Sharifabad, A. Monera-Martinez, A. Nordt, D. Paulic, D. Piso, S. Regnell, M. Zaera-Sanz, M. Aberg, K. Breimer, K. Batkov, Y. Lee, L. Zanini, M. Kickulies, Y. Bessler, J. Ringnér, J. Jurns, A. Sadeghzadeh, P. Nilsson, M. Olsson, J.-E. Presteng, H. Carlsson, A. Polato, J. Harborn, K. Sjögreen, G. Muhrer, F. Sordo, Phys. Scr. 93 (1) (2017) 014001, http://dx.doi.org/10.1088/1402-4896/aa9bff.

[267] J. Galambos, Technical Design Report Second Target Station, Tech. Rep., Oak Ridge National Laboratory, 2015, URL https://neutrons.ornl.gov/sts/documents.

[268] J. Haines, T. McManamy, T. Gabriel, R. Battle, K. Chipley, J. Crabtree, L. Jacobs, D. Lousteau, M. Rennich, B. Riemer, Nucl. Instrum. Methods Phys. Res. Sect. A: Accel. Spectrometers Detect. Assoc. Equip. 764 (2014) 94–115, http://dx.doi.org/10.1016/j.nima.2014.03.068, URL https://www.sciencedirect.com/science/article/pii/S0168900214003829.

[269] S. Sakamoto, Technical Design Report of Spallation Neutron Source Facility in J-PARC, Tech. Rep., Japan Atomic Energy Agency (JAEA), 2012, URL https://doi.org/10.11484/jaea-technology-2011-035.

[270] A. Aguilar, F. Sordo, T. Mora, L. Mena, M. Mancisidor, J. Aguilar, G. Bakedano, I. Herranz, P. Luna, M. Magan, R. Vivanco, F. Jimenez-Villacorta, K. Sjogreen, U. Oden, J. Perlado, J. Martinez, F. Bermejo, Nucl. Instrum. Methods Phys. Res. Sect. A: Accel. Spectrometers Detect. Assoc. Equip. 856 (2017) 99–108, http://dx.doi.org/10.1016/j.nima.2017.03.003, URL https://www.sciencedirect.com/science/article/pii/S0168900217303194.

[271] W. Lu, P. Ferguson, E. Iverson, F. Gallmeier, I. Popova, J. Nucl. Mater. 377 (1) (2008) 268–274, http://dx.doi.org/10.1016/j.jnucmat.2008.02.087, URL https://www.sciencedirect.com/science/article/pii/S0022311508001530. Spallation Materials Technology.

[272] Y. Beßler, M. Klaus, C. Henkes, G. Natour, J. Ringnér, J. Phys.: Conf. Ser. 1021 (1) (2018) 012080, http://dx.doi.org/10.1088/1742-6596/1021/1/012080.

[273] H. Schober, E. Farhi, F. Mezei, P. Allenspach, K. Andersen, P. Bentley, P. Christiansen, B. Cubitt, R. Heenan, J. Kulda, P. Langan, K. Lefmann, K. Lieutenant, M. Monkenbusch, P. Willendrup, J. Šaroun, P. Tindemans, G. Zsigmond, Nucl. Instrum. Methods Phys. Res. Sect. A: Accel. Spectrometers Detect. Assoc. Equip. 589 (1) (2008) 34–46, http://dx.doi.org/10.1016/j.nima.2008.01.102, URL https://www.sciencedirect.com/science/article/pii/S0168900208001551.

[274] K. Crawford, Neutron News 1 (3) (1990) 9–15, http://dx.doi.org/10.1080/10448639008202037, arXiv:https://doi.org/10.1080/10448639008202037.

[275] Y. Ishikawa, N. Watanabe, 1978, URL http://inis.iaea.org/search/search.aspx?orig_q=RN:11497096.

[276] J. Thomason, Nucl. Instrum. Methods Phys. Res. Sect. A: Accel. Spectrometers Detect. Assoc. Equip. 917 (2019) 61–67, http://dx.doi.org/10.1016/j.nima.2018.11.129, URL https://www.sciencedirect.com/science/article/pii/S0168900218317820.

[277] W. Fischer, Phys. B 234–236 (1997) 1202–1208, http://dx.doi.org/10.1016/S0921-4526(97)00260-3, URL https://www.sciencedirect.com/science/article/pii/S0921452697002603. Proceedings of the First European Conference on Neutron Scattering.

[278] B. Blau, K.N. Clausen, S. Gvasaliya, M. Janoschek, S. Janssen, L. Keller, B. Roessli, J. Schefer, P. Tregenna-Piggott, W. Wagner, O. Zaharko, Neutron News 20 (3) (2009) 5–8, http://dx.doi.org/10.1080/10448630903120387, arXiv:https://doi.org/10.1080/10448630903120387.

[279] H. Chen, Y. Chen, F. Wang, T. Liang, X. Jia, Q. Ji, C. Hu, W. He, W. Yin, K. He, B. Zhang, L. Wang, Neutron News 29 (2) (2018) 2–6, http://dx.doi.org/10.1080/10448632.2018.1514186, arXiv:https://doi.org/10.1080/10448632.2018.1514186.

[280] R. Garoby, in: N. Saito (Ed.), JPS Conf. Proc. 33 (2021) 011003, http://dx.doi.org/10.7566/JPSCP.33.011003, URL https://journals.jps.jp/doi/10.7566/JPSCP.33.011003.

[281] T. Brückel, T. Gutberlet, J. Baggemann, E. Mauerhofer, U. Rücker, P. Zakalek, R. Achten, Y. Bessler, R. Hanslik, H. Kleines, J. Li, K. Lieutenant, F. Löchte, I. Pechenizkiy, E. Vezhlev, J. Voigt, J. Wolters, in: J. Baggemann, E. Mauerhofer, U. Rücker, P. Zakalek, T. Brückel, T. Gutberlet (Eds.), Target Stations and Moderators, in: Technical Design Report High Brilliance neutron Source (HBS), vol. 2, Forschungszentrum Jülich GmbH, 2023, http://dx.doi.org/10.34734/FZJ-2023-03723.

[282] T. Brückel, T. Gutberlet, R. Gebel, A. Lehrach, H. Podlech, J. Baggemann, M. Droba, O. Felden, H. Kleines, K. Kümpel, S. Lamprecht, E. Mauerhofer, O. Meusel, I. Pechenizkiy, N. Petry, S. Reimann, U. Rücker, M. Schwarz, P. Zakalek, C. Zhang, Accelerator, Technical Design Report High Brilliance Neutron Source (HBS), vol. 1, Forschungszentrum Jülich GmbH, 2023, http://dx.doi.org/10.34734/FZJ-2023-03722,

[283] T. Brückel, T. Gutberlet, K. Lieutenant, J. Voigt, R. Bewley, J. Fenske, M. Feygenson, C. Franz, H. Frielinghaus, M. Ganeva, A. Glavic, A. Houben, S. Jaksch, N. Kardjilov, G. Kemmerling, H. Kleines, I. Krasnov, Z. Ma, S. Mattauch, E. Mauerhofer, Y. Meinerzhagen, S. Pasini, U. Rücker, K. Schmalzl, N. Schmidt, T. Schrader, W. Schweika, M. Strobl, E. Vezhlev, N. Violini, R. Zorn, in: K. Lieutenant, J. Voigt, T. Brückel, T. Gutberlet (Eds.), Instrumentation, in: Technical Design Report High Brilliance neutron Source (HBS), vol. 3, Forschungszentrum Jülich GmbH, 2023, http://dx.doi.org/10.34734/FZJ-2023-03724.

[284] T. Brückel, T. Gutberlet, T.C. Weber, F. Galeazzi, D. Haar, N. Krause, B. Kreft, O. Krieger, E. Mauerhofer, J. Ottersbach, M. Pauli, A. Schreyer, J. Womersley, in: T. Gutberlet, T. Brückel (Eds.), Infrastructure and Sustainability, in: Technical Design Report High Brilliance neutron Source (HBS), vol. 4, Forschungszentrum Jülich GmbH, 2023, http://dx.doi.org/10.34734/FZJ-2023-03725.

[285] T. Brückel, T. Gutberlet, in: T. Brückel, T. Gutberlet (Eds.), Opportunities for Research with Neutrons at the Next Generation Facility HBS Overview of the High Brilliance Neutron Source (HBS), in: Technical Design Report High Brilliance neutron Source (HBS), vol. 5, Forschungszentrum Jülich GmbH, 2023, http://dx.doi.org/10.34734/FZJ-2023-03726.

[286] M. Furusaka, H. Sato, T. Kamiyama, M. Ohnuma, Y. Kiyanagi, Phys. Procedia 60 (2014) 167–174, http://dx.doi.org/10.1016/j.phpro.2014.11.024, URL https://www.sciencedirect.com/science/article/pii/S1875389214005719. 3rd International Meeting of the Union for Compact Accelerator-driven Neutron Sources, UCANS III, 31 July–3 August 2012, Bilbao, Spain & the 4th International Meeting of the Union for Compact Accelerator-driven Neutron Sources, UCANS IV, 23-27 September 2013, Sapporo, Hokkaido, Japan.

[287] Y. Otake, Plasma Fusion Res. 13 (2018) http://dx.doi.org/10.1585/pfr.13.2401017, 2401017–2401017.

[288] D.V. Baxter, S. Aldaihan, S. Parnell, R. Pynn, P. Sokol, W. Snow, T. Rinckel, Phys. Procedia 60 (2014) 175–180, http://dx.doi.org/10.1016/j.phpro.2014.11.025, URL https://www.sciencedirect.com/science/article/pii/S1875389214005720. 3rd International Meeting of the Union for Compact Accelerator-driven Neutron Sources, UCANS III, 31 July–3 August 2012, Bilbao, Spain & the 4th International Meeting of the Union for Compact Accelerator-driven Neutron Sources, UCANS IV, 23-27 September 2013, Sapporo, Hokkaido, Japan.

[289] E. Mauerhofer, U. Rücker, T. Cronert, P. Zakalek, J. Baggemann, P.-E. Doege, J. Li, S. Böhm, H. Kleines, T. Gutberlet, T. Brückel, Conceptual Design Report - NOVA ERA (Neutrons Obtained Via Accelerator for Education and Research Activities) - A Jülich High Brilliance Neutron Source Project, in: Schriften des Forschungszentrums Jülich Reihe Allgemeines / General, vol. 7, Forschungszentrum Jülich GmbH Zentralbibliothek, Verlag, Jülich, 2017, p. 68, URL https://juser.fz-juelich.de/record/840313?ln=de.

[290] Y. Otake, EPJ Web Conf. 231 (2020) 01009, http://dx.doi.org/10.1051/epjconf/202023101009.

[291] Y. Ikeda, A. Taketani, M. Takamura, H. Sunaga, M. Kumagai, Y. Oba, Y. Otake, H. Suzuki, Nucl. Instrum. Methods Phys. Res. Sect. A: Accel. Spectrometers Detect. Assoc. Equip. 833 (2016) 61–67, http://dx.doi.org/10.1016/j.nima.2016.06.127, URL https://www.sciencedirect.com/science/article/pii/S0168900216306994.

[292] I. Anderson, C. Andreani, J. Carpenter, G. Festa, G. Gorini, C.-K. Loong, R. Senesi, Phys. Rep. 654 (2016) 1–58, http://dx.doi.org/10.1016/j.physrep.2016.07.007, URL https://www.sciencedirect.com/science/article/pii/S0370157316301958. Research opportunities with compact accelerator-driven neutron sources.

[293] Y. Yamagata, K. Hirota, J. Ju, S. Wang, S.-Y. Morita, J.-I. Kato, Y. Otake, A. Taketani, Y. Seki, M. Yamada, H. Ota, U. Bautista, Q. Jia, J. Radioanal. Nucl. Chem. 305 (2015) http://dx.doi.org/10.1007/s10967-015-4059-8.

[294] Y. Kiyanagi, J. Nucl. Sci. Technol. 22 (11) (1985) 934–938, http://dx.doi.org/10.1080/18811248.1985.9735745.

[295] R.J.W. Frost, M. Elfman, K. Fissum, P. Kristiansson, N. Mauritzson, J. Pallon, G. Pédehontaa-Hiaa, H. Perrey, K.E. Stenström, A. Sjöland, EPJ Tech. Instrum. 10 (1) (2023) 14, http://dx.doi.org/10.1140/epjti/s40485-023-00101-9, URL https://link.springer.com/article/10.1140/epjti/s40485-023-00101-9.

[296] D.V. Baxter, Eur. Phys. J. Plus 131 (4) (2016) 83, http://dx.doi.org/10.1140/epjp/i2016-16083-9.

[297] D.V. Baxter, J. Cameron, M. Leuschner, H. Meyer, H. Nann, W. Snow, Nucl. Instrum. Methods Phys. Res. Sect. A: Accel. Spectrometers Detect. Assoc. Equip. 542 (1) (2005) 28–31, http://dx.doi.org/10.1016/j.nima.2005.01.007, URL https://www.sciencedirect.com/science/article/pii/S0168900205001166. Proceedings of the Fifth International Topical Meeting on Neutron Radiography.

[298] X. Wang, Q. Xing, S. Zheng, Y. Yang, H. Gong, Y. Xiao, H. Wu, Z. Wang, Z. Fang, Z. Jiang, X. Guan, J. Phys.: Conf. Ser. 1021 (1) (2018) 012006, http://dx.doi.org/10.1088/1742-6596/1021/1/012006.

[299] B. Zhong, T. Liang, Q. Feng, G. Yu, K. Wang, C.-K. Loong, Phys. Procedia 26 (2012) 25–30, http://dx.doi.org/10.1016/j.phpro.2012.03.004, URL https://www.sciencedirect.com/science/article/pii/S1875389212004208. Proceedings of the first two meetings of the Union of Compact Accelerator-Driven Neutron Sources.

[300] I. Mardor, H. Wilsenach, T. Dickel, I. Eliyahu, M. Friedman, T.Y. Hirsh, A. Kreisel, O. Sharon, M. Tessler, S. Vaintraub, F.V. Uhlemann, Front. Phys. 11 (2023) http://dx.doi.org/10.3389/fphy.2023.1248191, URL https://www.frontiersin.org/journals/physics/articles/10.3389/fphy.2023.1248191.

[301] F. Ott, J. Darpentigny, B. Annighöfer, M.A. Paulin, J.-L. Meuriot, A. Menelle, N. Sellami, J. Schwindling, EPJ Web Conf. 286 (2023) 02001, http://dx.doi.org/10.1051/epjconf/202328602001.

[302] M. Pérez, F. Sordo, I. Bustinduy, J.L. Muñoz, F.J. Villacorta, Neutron News 31 (2–4) (2020) 19–25, http://dx.doi.org/10.1080/10448632.2020.1819140.

[303] T. Brückel, T. Gutberlet, J. Baggemann, J. Chen, T. Claudio-Weber, Q. Ding, M. El-Barbari, J. Li, K. Lieutenant, E. Mauerhofer, U. Rücker, N. Schmidt, A. Schwab, J. Voigt, P. Zakalek, Y. Bessler, R. Hanslik, R. Achten, F. Löchte, M. Strothmann, O. Felden, R. Gebel, A. Lehrach, M. Rimmler, H. Podlech, O. Meusel, F. Ott, A. Menelle, M.A. Paulin, EPJ Web Conf. 286 (2023) 02003, http://dx.doi.org/10.1051/epjconf/202328602003.

[304] J.R. Granada, R.E. Mayer, J. Dawidowski, J.R. Santisteban, F. Cantargi, J.J. Blostein, L.A. Rodríguez Palomino, A. Tartaglione, Eur. Phys. J. Plus 131 (2016) http://dx.doi.org/10.1140/epjp/i2016-16216-2.

[305] Union for Compact Accelerator-driven Neutron Sources (UCANS), URL https://www.ucans.org/.

[306] M. Rimmler, O. Felden, U. Rücker, H. Soltner, P. Zakalek, R. Gebel, T. Gutberlet, T. Brückel, J. Neutron Res. 23 (2021) 143–156, http://dx.doi.org/10.3233/JNR-210009, URL https://content.iospress.com/articles/journal-of-neutron-research/jnr210009.

[307] P. Zakalek, R. Achten, J. Baggemann, Y. Beßler, F. Beule, T. Brückel, J. Chen, Q. Ding, M. El-Barbari, R. Engels, O. Felden, R. Gebel, K. Grigoryev, T. Gutberlet, R. Hanslik, V. Kamerdzhiev, P. Kämmerling, H. Kleines, J. Li, K. Lieutenant, F. Löchte, E. Mauerhofer, M.A. Paulin, I. Pechenizkiy, U. Rücker, N. Schmidt, A. Schwab, A. Steffens, F. Ott, Y. Valdau, E. Vezhlev, J. Voigt, EPJ Web Conf. 286 (2023) 02004, http://dx.doi.org/10.1051/epjconf/202328602004.

[308] P. Zakalek, J. Baggemann, J. Li, U. Rücker, T. Gutberlet, T. Brückel, EPJ Web Conf. 298 (2024) 05003, http://dx.doi.org/10.1051/epjconf/202429805003.

[309] C. Wiesner, L.P. Chau, H. Dinter, M. Droba, N. Joshi, O. Meusel, I. Müller, U. Ratzinger, 25th International Linear Accelerator Conference, 2011, THP071, URL https://inspirehep.net/literature/1363940.

[310] H. Abderrahim, P. Kupschus, E. Malambu, P. Benoit, K. Van Tichelen, B. Arien, F. Vermeersch, P. D'hondt, Y. Jongen, S. Ternier, D. Vandeplassche, Nucl. Instrum. Methods Phys. Res. Sect. A: Accel. Spectrometers Detect. Assoc. Equip. 463 (3) (2001) 487–494, http://dx.doi.org/10.1016/S0168-9002(01)00164-4.

[311] H. Podlech, J. Baggemann, S. Böhm, T. Brückel, T. Cronert, P.-E. Doege, M. Droba, T. Gutberlet, J. Li, K. Kümpel, S. Lamprecht, E. Mauerhofer, O. Meusel, N. Petry, U. Rücker, P. Schneider, M. Schwarz, P. Zakalek, C. Zhang, 2019, http://dx.doi.org/10.18429/JACoW-IPAC2019-MOPTS027.

[312] V. Astrelin, A. Burdakov, P. Bykov, I. Ivanov, A. Ivanov, Y. Jongen, S. Konstantinov, A. Kudryavtsev, K. Kuklin, K. Mekler, S. Polosatkin, V. Postupaev, A. Rovenskikh, S. Sinitskiy, E. Zubairov, J. Nucl. Mater. 396 (1) (2010) 43–48, http://dx.doi.org/10.1016/j.jnucmat.2009.10.051.

[313] A. Badrutdinov, T. Bykov, S. Gromilov, Y. Higashi, D. Kasatov, I. Kolesnikov, A. Koshkarev, A. Makarov, T. Miyazawa, I. Shchudlo, E. Sokolova, H. Sugawara, S. Taskaev, Metals 7 (12) (2017) http://dx.doi.org/10.3390/met7120558, URL https://www.mdpi.com/2075-4701/7/12/558.

[314] T. Zaharoni, D. Yunger, N. Mishra, I.G. Segev, A. Kraisel, E. Yahel, G. Makov, J. Nucl. Mater. 553 (2021) 153058, http://dx.doi.org/10.1016/j.jnucmat.2021.153058, URL https://www.sciencedirect.com/science/article/pii/S0022311521002816.

[315] S.M. Hosseini, Z. Fuer Met. 67 (2) (1976) 123–127, URL http://inis.iaea.org/search/search.aspx?orig_q=RN:07257182.

[316] N. Ophoven, E. Mauerhofer, J. Li, U. Rücker, P. Zakalek, J. Baggemann, T. Gutberlet, T. Brückel, C. Langer, Appl. Phys. A 127 (8) (2021) 576, http://dx.doi.org/10.1007/s00339-021-04713-4.

[317] J. Schwindling, B. Annighöfer, N. Chauvin, J.-L. Meuriot, B. Mom, F. Ott, N. Sellami, L. Thulliez, J. Neutron Res. 24 (2022) 289–298, http://dx.doi.org/10.3233/JNR-220024.

[318] I. Silverman, A. Arenshtam, D. Berkovits, I. Eliyahu, I. Gavish, A. Grin, S. Halfon, M. Hass, T.Y. Hirsh, B. Kaizer, D. Kijel, A. Kreisel, I. Mardor, Y. Mishnayot, T. Palchan, A. Perry, M. Paul, G. Ron, G. Shimel, A. Shor, N. Tamim, M. Tessler, S. Vaintraub, L. Weissman, AIP Conf. Proc. 1962 (1) (2018) 020002, http://dx.doi.org/10.1063/1.5035515, arXiv:https://pubs.aip.org/aip/acp/article-pdf/doi/10.1063/1.5035515/13317356/020002_1_online.pdf.

[319] P. Mastinu, J. Praena, G. Martìn-Hernàndez, N. Dzysiuk, G. Prete, R. Capote, M. Pignatari, A. Ventura, Phys. Procedia 26 (2012) 261–273, http://dx.doi.org/10.1016/j.phpro.2012.03.034, URL https://www.sciencedirect.com/science/article/pii/S1875389212004506. Proceedings of the first two meetings of the Union of Compact Accelerator-Driven Neutron Sources.

[320] J. Baggemann, T. Gutberlet, P. Zakalek, J. Wolters, U. Rücker, E. Mauerhofer, J. Li, Q. Ding, T. Loewenhoff, D. Dorow-Gerspach, Y. Bessler, T. Brückel, Nucl. Instrum. Methods Phys. Res. / Sect. A 1069 (2024) 169912, http://dx.doi.org/10.1016/j.nima.2024.169912, URL https://juser.fz-juelich.de/record/1031484.

[321] Q. Ding, U. Rücker, P. Zakalek, J. Baggemann, J. Wolters, J. Li, Y. Beßler, T. Gutberlet, T. Brückel, G. Natour, Nucl. Instrum. Methods Phys. Res. Sect. A: Accel. Spectrometers Detect. Assoc. Equip. 1045 (2023) 167508, http://dx.doi.org/10.1016/j.nima.2022.167508, URL https://www.sciencedirect.com/science/article/pii/S0168900222008002.

[322] J. Chen, U. Rücker, J. Voigt, P. Zakalek, E. Vezhlev, J. Li, T. Gutberlet, T. Brückel, EPJ Web Conf. 286 (2023) 02005, http://dx.doi.org/10.1051/epjconf/202328602005.

[323] U. Rücker, I. Pechenizkiy, J. Li, E. Vezhlev, P. Zakalek, J. Voigt, T. Gutberlet, T. Brückel, EPJ Web Conf. 298 (2024) 05008, http://dx.doi.org/10.1051/epjconf/202429805008.

[324] P. Zakalek, J. Li, S. Böhm, U. Rücker, J. Voigt, E. Mauerhofer, T. Gutberlet, T. Brückel, J. Neutron Res. 23 (2021) 185–200, http://dx.doi.org/10.3233/JNR-210016.

[325] T. Cronert, J.P. Dabruck, P.E. Doege, Y. Bessler, M. Klaus, M. Hofmann, P. Zakalek, U. Rücker, C. Lange, M. Butzek, W. Hansen, R. Nabbi, T. Brückel, J. Phys.: Conf. Ser. 746 (2016) 012036, http://dx.doi.org/10.1088/1742-6596/746/1/012036.

[326] D. Shabani, U. Rücker, C. Langer, J. Li, P. Zakalek, N. Schmidt, T. Gutberlet, T. Brückel, EPJ Web Conf. 298 (2024) 03002, http://dx.doi.org/10.1051/epjconf/202429803002.

[327] M.E. Barbari, U. Rücker, A. Schwab, J. Chen, P. Zakalek, J. Li, T. Gutberlet, T. Brückel, EPJ Web Conf. 298 (2024) 01003, http://dx.doi.org/10.1051/epjconf/202429801003.

[328] T. Cronert, J.P. Dabruck, M. Klaus, C. Lange, P. Zakalek, P.E. Doege, J. Baggemann, Y. Beßler, M. Butzek, U. Rücker, T. Gutberlet, R. Nabbi, T. Brückel, Phys. B 551 (2018) 377–380, http://dx.doi.org/10.1016/j.physb.2018.01.016, URL http://www.sciencedirect.com/science/article/pii/S0921452618300255. The 11th International Conference on Neutron Scattering (ICNS 2017).

[329] U. Odén, J. Neutron Res. 24 (2022) 229–237, http://dx.doi.org/10.3233/JNR-220014, URL https://ip.ios.semcs.net/articles/journal-of-neutron-research/jnr220014.

[330] F. Gallmeier, P. Ferguson, E. Iverson, Proc. of the 16th Meeting of the Int. Collaboration on Advanced Neutron Sources ICANS-XVI May 12–15, Düsseldorf Germany, Vol. 3, 2003, pp. 1023–1032.

[331] J. Voigt, S. Böhm, J. Dabruck, U. Rücker, T. Gutberlet, T. Brückel, Nucl. Instrum. Methods Phys. Res. Sect. A: Accel. Spectrometers Detect. Assoc. Equip. 884 (2018) 59–63, http://dx.doi.org/10.1016/j.nima.2017.11.085, URL https://www.sciencedirect.com/science/article/pii/S0168900217313414.

[332] T. Gutberlet, J. Voigt, Neutron News 33 (4) (2022) 2–3, http://dx.doi.org/10.1080/10448632.2022.2108664, arXiv:https://doi.org/10.1080/10448632.2022.2108664.

[333] S. Jaksch, K. Lieutenant, E. Babcock, H. Frielinghaus, Nucl. Instrum. Methods Phys. Res. Sect. A: Accel. Spectrometers Detect. Assoc. Equip. 1048 (2023) 167919, http://dx.doi.org/10.1016/j.nima.2022.167919, URL https://www.sciencedirect.com/science/article/pii/S0168900222012116.

[334] M.A. Paulin, I. Pechenizkiy, P. Zakalek, K. Lieutenant, P. Kämmerling, A. Steffens, H. Kleines, U. Rücker, T. Gutberlet, S. Gautrot, A. Menelle, F. Ott, EPJ Web Conf. 298 (2024) 01001, http://dx.doi.org/10.1051/epjconf/202429801001.

[335] Z. Ma, K. Lieutenant, J. Voigt, T.E. Schrader, T. Gutberlet, Rev. Sci. Instrum. 95 (6) (2024) 065104, http://dx.doi.org/10.1063/5.0203509, arXiv:https://pubs.aip.org/aip/rsi/article-pdf/doi/10.1063/5.0203509/19975648/065104_1_5.0203509.pdf.

[336] J. Stahn, T. Panzner, U. Filges, C. Marcelot, P. Böni, Nucl. Instrum. Methods Phys. Res. Sect. A: Accel. Spectrometers Detect. Assoc. Equip. 634 (1, Supplement) (2011) S12–S16, http://dx.doi.org/10.1016/j.nima.2010.06.221, URL https://www.sciencedirect.com/science/article/pii/S0168900210014117. Proceedings of the International Workshop on Neutron Optics NOP2010.

[337] Z. Ma, K. Lieutenant, J. Voigt, T. Gutberlet, M. Feygenson, T. Brückel, Nucl. Instrum. Methods Phys. Res. Sect. A: Accel. Spectrometers Detect. Assoc. Equip. 1009 (2021) 165479, http://dx.doi.org/10.1016/j.nima.2021.165479, URL https://www.sciencedirect.com/science/article/pii/S0168900221004642.

[338] A. Nagler, I. Mardor, D. Berkovits, K. Dunkel, M. Pekeler, C. Piel, P. vom Stein, H. Vogel, Proc. LINAC 2006, 2006, MOP054, URL https://accelconf.web.cern.ch/l06/PAPERS/MOP054.PDF.

[339] I. Mardor, O. Aviv, M. Avrigeanu, D. Berkovits, A. Dahan, T. Dickel, I. Eliyahu, M. Gai, I. Gavish-Segev, S. Halfon, M. Hass, T. Hirsh, B. Kaiser, D. Kijel, A. Kreisel, Y. Mishnayot, I. Mukul, B. Ohayon, M. Paul, A. Perry, H. Rahangdale, J. Rodnizki, G. Ron, R. Sasson-Zukran, A. Shor, I. Silverman, M. Tessler, S. Vaintraub, L. Weissman, Eur. Phys. J. A 54 (5) (2018) 91, http://dx.doi.org/10.1140/epja/i2018-12526-2.

[340] S. Alzubaidi, U. Bartz, M. Basten, A. Bechtold, L.P. Chau, C. Claessens, H. Dinter, M. Droba, C. Fix, H. Hähnel, M. Heilmann, O. Hinrichs, S. Huneck, B. Klump, M. Lotz, D. Mäder, O. Meusel, D. Noll, T. Nowottnick, M. Obermayer, O. Payir, N. Petry, H. Podlech, U. Ratzinger, A. Schempp, S. Schmidt, P. Schneider, A. Seibel, M. Schwarz, W. Schweizer, K. Volk, C. Wagner, C. Wiesner, Eur. Phys. J. Plus 131 (5) (2016) 124, http://dx.doi.org/10.1140/epjp/i2016-16124-5.

[341] L. Silvestrin, D. Bisello, J. Esposito, P. Mastinu, G. Prete, J. Wyss, Eur. Phys. J. Plus 131 (3) (2016) 72, http://dx.doi.org/10.1140/epjp/i2016-16072-0.

[342] M. Paul, I. Silverman, S. Halfon, S. Sukoriansky, B. Mikhailovich, T. Palchan, A. Kapusta, A. Shoihet, D. Kijel, A. Arenshtam, E. Barami, EPJ Web Conf. 231 (2020) 03004, http://dx.doi.org/10.1051/epjconf/202023103004.

[343] M. Paul, M. Tessler, T. Palchan, S. Halfon, L. Weissman, N. Hazenshprung, A. Kreisel, T. Makmal, A. Shor, I. Silverman, M. Avila Coronado, S. Almaraz-Calderon, W. Jiang, Z.-T. Lu, P. Müller, R. Pardo, K. Ernst Rehm, R. Scott, R. Talwar, C. Ugalde, R. Vondrasek, J. Zappala, D. Santiago-Gonzalez, P. Collon, Y. Kashiv, M. Weigand, T. Heftrich, R. Reifarth, D. Veltum, R. Purtschert, C. Guerrero, J. Lerendegui Marco, J. Manuel Quesada, U. Köster, D. Schumann, R. Dressler, S. Heinitz, N. Kivel, E. Andrea Maugeri, PoS INPC2016 (2017) 139, http://dx.doi.org/10.22323/1.281.0139.

[344] E. Abad, I. Arredondo, I. Badillo, D. Belver, F.J. Bermejo, I. Bustinduy, D. Cano, D. Cortazar, D. de Cos, S. Djekic, S. Domingo, P. Echevarria, M. Eguiraun, V. Etxebarria, D. Fernandez, F.J. Fernandez, J. Feuchtwanger, N. Garmendia, G. Harper, H. Hassanzadegan, J. Jugo, F. Legarda, M. Magan, R. Martinez, A. Megia, L. Muguira, G. Mujika, J.L. Muñoz, A. Ortega, J. Ortega, M. Perlado, J. Portilla, I. Rueda, F. Sordo, V. Toyos, A. Vizcaino, J. Phys.: Conf. Ser. 325 (1) (2011) 012003, http://dx.doi.org/10.1088/1742-6596/325/1/012003.

[345] F. Sordo, F. Fernandez-Alonso, M.A. Gonzalez, A. Ghiglino, M. Magán, S. Terrón, F. Martínez, J.P. de Vicente, R. Vivanco, F.J. Bermejo, J.M. Perlado, J. Phys.: Conf. Ser. 549 (1) (2014) 012001, http://dx.doi.org/10.1088/1742-6596/549/1/012001.
[346] O.G. del Moral, M. Magán, F. Sordo, F.J. Villacorta, M. Pérez, EPJ Web Conf. 286 (2023) 02002, http://dx.doi.org/10.1051/epjconf/202328602002.
[347] H.N. Tran, F. Ott, J. Darpentigny, A. Marchix, A. Letourneau, N. Chauvin, F. Prunes, B. Homatter, B. Annighöfer, A. Menelle, J. Schwindling, EPJ Web Conf. 231 (2020) 01007, http://dx.doi.org/10.1051/epjconf/202023101007.
[348] S.P. Hatchett, C.G. Brown, T.E. Cowan, E.A. Henry, J.S. Johnson, M.H. Key, J.A. Koch, A.B. Langdon, B.F. Lasinski, R.W. Lee, A.J. Mackinnon, D.M. Pennington, M.D. Perry, T.W. Phillips, M. Roth, T.C. Sangster, M.S. Singh, R.A. Snavely, M.A. Stoyer, S.C. Wilks, K. Yasuike, Phys. Plasmas 7 (5) (2000) 2076–2082, http://dx.doi.org/10.1063/1.874030, arXiv:https://pubs.aip.org/aip/pop/article-pdf/7/5/2076/12332262/2076_1_online.pdf.
[349] S.C. Wilks, A.B. Langdon, T.E. Cowan, M. Roth, M. Singh, S. Hatchett, M.H. Key, D. Pennington, A. MacKinnon, R.A. Snavely, Phys. Plasmas 8 (2) (2001) 542–549, http://dx.doi.org/10.1063/1.1333697, arXiv:https://pubs.aip.org/aip/pop/article-pdf/8/2/542/12669088/542_1_online.pdf.
[350] S.H. Batha, R. Aragonez, F.L. Archuleta, T.N. Archuleta, J.F. Benage, J.A. Cobble, J.S. Cowan, V.E. Fatherley, K.A. Flippo, D.C. Gautier, R.P. Gonzales, S.R. Greenfield, B.M. Hegelich, T.R. Hurry, R.P. Johnson, J.L. Kline, S.A. Letzring, E.N. Loomis, F.E. Lopez, S.N. Luo, D.S. Montgomery, J.A. Oertel, D.L. Paisley, S.M. Reid, P.G. Sanchez, A. Seifter, T. Shimada, J.B. Workman, Rev. Sci. Instrum. 79 (10) (2008) 10F305, http://dx.doi.org/10.1063/1.2972020, arXiv:https://pubs.aip.org/aip/rsi/article-pdf/doi/10.1063/1.2972020/15668025/10f305_1_online.pdf.
[351] M. Martinez, W. Bang, G. Dyer, X. Wang, E. Gaul, T. Borger, M. Ringuette, M. Spinks, H. Quevedo, A. Bernstein, M. Donovan, T. Ditmire, AIP Conf. Proc. 1507 (1) (2012) 874–878, http://dx.doi.org/10.1063/1.4773814, arXiv:https://pubs.aip.org/aip/acp/article-pdf/1507/1/874/11481700/874_1_online.pdf.
[352] V. Bagnoud, B. Aurand, A. Blazevic, S. Borneis, C. Bruske, B. Ecker, U. Eisenbarth, J. Fils, A. Frank, E. Gaul, S. Goette, C. Haefner, T. Hahn, K. Harres, H.-M. Heuck, D. Hochhaus, D.H.H. Hoffmann, D. Javorková, H.-J. Kluge, T. Kuehl, S. Kunzer, M. Kreutz, T. Merz-Mantwill, P. Neumayer, E. Onkels, D. Reemts, O. Rosmej, M. Roth, T. Stoehlker, A. Tauschwitz, B. Zielbauer, D. Zimmer, K. Witte, Appl. Phys. B 100 (1) (2010) 137–150, http://dx.doi.org/10.1007/s00340-009-3855-7.
[353] C. Hernandez-Gomez, P. Brummitt, D. Canny, R. Clarke, J. Collier, C. Danson, A. Dunne, B. Fell, A. Frackiewicz, S. Hancock, et al., Journal de Physique IV (Proceedings), Vol. 133, EDP sciences, 2006, pp. 555–559, http://dx.doi.org/10.1051/jp4:2006133114.
[354] U. Schramm, M. Bussmann, A. Irman, M. Siebold, K. Zeil, D. Albach, C. Bernert, S. Bock, F. Brack, J. Branco, J. Couperus, T. Cowan, A. Debus, C. Eisenmann, M. Garten, R. Gebhardt, S. Grams, U. Helbig, A. Huebl, T. Kluge, A. Köhler, J. Krämer, S. Kraft, F. Kroll, M. Kuntzsch, U. Lehnert, M. Loeser, J. Metzkes, P. Michel, L. Obst, R. Pausch, M. Rehwald, R. Sauerbrey, H. Schlenvoigt, K. Steiniger, O. Zarini, J. Phys.: Conf. Ser. 874 (1) (2017) 012028, http://dx.doi.org/10.1088/1742-6596/874/1/012028.
[355] W.P. Leemans, R. Duarte, E. Esarey, S. Fournier, C.G.R. Geddes, D. Lockhart, C.B. Schroeder, C. Toth, J.-L. Vay, S. Zimmermann, AIP Conf. Proc. 1299 (1) (2010) 3–11, http://dx.doi.org/10.1063/1.3520352, arXiv:https://pubs.aip.org/aip/acp/article-pdf/1299/1/3/11927656/3_1_online.pdf.
[356] Y. Wang, S. Wang, A. Rockwood, B.M. Luther, R. Hollinger, A. Curtis, C. Calvi, C.S. Menoni, J.J. Rocca, Opt. Lett. 42 (19) (2017) 3828–3831, http://dx.doi.org/10.1364/OL.42.003828, URL https://opg.optica.org/ol/abstract.cfm?URI=ol-42-19-3828.
[357] K. Osvay, L. Stuhl, P. Varmazyar, T. Gilinger, Z. Elekes, A. Fenyvesi, K. Hideghethy, R.E. Szabo, M. Füle, B. Biró, Z. Halász, Z. Korkulu, I. Kuti, R. Molnár, A. Ébert, R. Polanek, E. Buzás, B. Nagy, P.K. Singh, S. Hussain, A. Börzsönyi, Z. Fülöp, T. Tajima, G. Mourou, G. Szabo, Eur. Phys. J. Plus 139 (2024) 574, http://dx.doi.org/10.1140/epjp/s13360-024-05338-1.
[358] U.S. Department of Energy's Office of Fusion Energy Sciences (FES), 2023, URL https://lasernetus.org/.
[359] F. Sordo, F. Villacorta, I. Bustinduy, P. Mastinu, G. Prete, L. Silvestrin, J. Wyss, P. King, R. McGreevy, M. Jentschel, Y. Calzavara, K. Thomsen, J. Schwindling, H. Podlech, H. Ronnow, E. Mauerhofer, U. Rücker, J. Voigt, P. Zakalek, 2021, URL https://lens-initiative.org/wp-content/uploads/2021/02/LENS-Report-on-Low-Energy-Accelerator-driven-Neutron-Sources.pdf.
[360] L. Zavorka, K. Ghoos, J. Risner, I. Remec, Nucl. Instrum. Methods Phys. Res. Sect. A: Accel. Spectrometers Detect. Assoc. Equip. 1052 (2023) 168252, http://dx.doi.org/10.1016/j.nima.2023.168252, URL https://www.sciencedirect.com/science/article/pii/S0168900223002425.
[361] G. Skoro, 2024. private communication.
[362] McStas module: Source_gen, URL https://www.mcstas.org/download/components/2.7.2/sources/Source_gen.comp.
[363] E. Kentzinger, M. Krutyeva, U. Rücker, J. Large- Scale Res. Facil. 2 (2016) A61, http://dx.doi.org/10.17815/jlsrf-2-109.